EXHIBIT A

BEST AVAILABLE COPY

PAGE 15/77 * RCVD AT 8/29/2005 7:17:05 PM [Eastern Daylight Time] * SVR:USPTO-EFXRF-6/26 * DNIS:2738300 * CSID:6504936811 * DURATION (mm-ss):60-28

JOURNAL OF VIROLOGY, Mar. 1996, p. 1845–1854
0022-538X/96/$04.00+0
Copyright © 1996, American Society for Microbiology
Vol. 70, No. 3

Recruitment of Wild-Type and Recombinant Adeno-Associated Virus into Adenovirus Replication Centers

MATTHEW D. WEITZMAN, KRISHNA J. FISHER, AND JAMES M. WILSON*

Institute for Human Gene Therapy and Department of Molecular and Cellular Engineering, University of Pennsylvania Medical Center and the Wistar Institute, Philadelphia, Pennsylvania

Received 25 September 1995/Accepted 28 November 1995

Replication of a human parvovirus, adeno-associated virus (AAV), is facilitated by coinfection with adenovirus to provide essential helper functions. We have used the techniques of in situ hybridization and immunocytochemistry to characterize the localization of AAV replication within infected cells. Previous studies have shown that adenovirus establishes foci called replication centers within the nucleus, where adenoviral replication and transcription occur. Our studies indicate that AAV is colocalized with the adenovirus replication centers, where it may utilize adenovirus and cellular proteins for its own replication. Expression of the AAV Rep protein inhibits the normal maturation of the adenovirus centers. Similar experiments were performed with recombinant AAV (rAAV) to establish a relationship between intranuclear localization and rAAV transduction. rAAV efficiently entered the cell, and its genome was faintly detectable in a perinuclear distribution and was mobilized to replication centers when the cell was infected with adenovirus. The recruitment of the replication-defective genome into the intranuclear adenovirus domains resulted in enhanced transduction. These studies illustrate the importance of intracellular compartmentalization for such complex interactions as the relationship between AAV and adenovirus.

Studies of viral infections in cell cultures have provided important clues about the fundamental mechanisms that regulate DNA replication, transcription and RNA metabolism, and cell cycle control. Importantly, many of the lessons learned have implications for the development of eukaryotic viruses for gene therapy. DNA vectors based on adenovirus and adeno-associated virus (AAV) are currently among the most useful for in vivo gene therapy because of their ability to target nondividing cells following systemic delivery. Although the life cycle of both viruses has been well characterized, it is difficult to predict the behavior of recombinants that have had critical open reading frames (ORFs) deleted. Understanding the biology of replication-defective forms, and their mechanism for transduction, is important for their continued development for gene therapy.

AAV is a nonpathogenic, defective human parvovirus that requires coinfection with a second virus, adenovirus or herpesvirus, to provide essential helper functions for its replication (10). The AAV genome is a single-stranded linear DNA molecule with inverted terminal repeats (ITRs) at both ends that serve as the origin and primer for DNA replication. The genome contains two ORFs encoding the nonstructural (Rep) and structural (Cap) viral proteins. In the absence of helper virus, the AAV genome integrates stably into the host genome at high frequency to establish a latent infection. The latent provirus can be rescued and replicated by superinfection with helper virus. There has been increasing interest in AAV as a potential gene delivery vector for human gene therapy (11, 28). AAV vectors are derived from plasmids that carry the ITRs flanking the foreign gene of interest. Vectors are packaged into AAV particles by cotransfection into adenovirus-infected cells along with a second packaging plasmid containing the *rep* and *cap* genes; recombinant AAV (rAAV) is harvested in cell lysates, and the helper virus is removed. rAAV is an attractive vector for gene therapy because it is easily purified, all viral ORFs are eliminated, and transduction can occur in nondividing cells. In addition, the viral genome can efficiently integrate, although the site specificity of integration that characterizes wild-type AAV appears to be lost in the absence of *rep*.

A greater understanding of the interaction between AAV and its helper viruses, adenovirus and herpesvirus, will be useful in its further development as a gene therapy vector. Previous studies regarding DNA replication and RNA transcription of adenovirus form an important foundation on which to assess further its role as a helper virus in AAV replication. The infectious cycle of adenovirus is approximately 36 h in duration and is divided into early and late stages that are separated by the onset of viral DNA replication at 8 h postinfection (31). Upon cell entry, infecting adenovirus undergoes multiple sequential uncoating steps as it migrates to the nuclear membrane, where the viral DNA is released into the nucleus (19). The double-stranded linear DNA genome of adenovirus is 35 kb long, with ITRs at each end that contain the origin of replication and the packaging sequences are located next to the 5′ ITR. The 5′ end of each strand is covalently attached to the virus-encoded terminal protein, which appears to mediate association of the viral genome with the nuclear matrix (42).

The life cycle of adenovirus is associated with dramatic reorganization of nuclear structure. The earliest virus-induced ultrastructural changes observed in adenovirus-infected cells are small discrete nuclear inclusions composed of cellular factors, viral nucleic acids, and proteins, which increase in size as DNA synthesis proceeds (32). Both replication and transcription are active in these centers early in infection; however, resolution into subdomains of the centers occurs as replication proceeds. The viral single-stranded DNA (ssDNA) colocalizes with the E2a gene product (an ssDNA-binding protein [DBP]) and forms nuclear inclusions that are variable in size and appear in shapes of crescents, rings, and spheres (31). Surrounding the sites of ssDNA accumulation is a granular network containing the viral double-stranded DNA (dsDNA).

* Corresponding author. Mailing address: 204 Wistar Institute, 3601 Spruce St., Philadelphia, PA 19104-4268. Phone: (215) 898-3000. Fax: (215) 898-6588.

PAGE 16/77 * RCVD AT 8/29/2005 7:17:05 PM [Eastern Daylight Time] * SVR:USPTO-EFXRF-6/26 * DNIS:2738300 * CSID:6504936811 * DURATION (mm-ss):60-28

6504936811 8/29/2005 4:17 PM PAGE 17/077 Fax Server

This compartment is active for both transcription and replication and has been termed the peripheral replicative zone. Infection with both adenovirus and herpesvirus results in some proteins involved in cellular DNA replication being recruited to the discrete subnuclear sites of viral DNA synthesis (6, 50), and there is a dynamic nuclear organization of host splicing factors in infected cells which may reflect the changes in gene expression as the infection proceeds (8). Compartmentalization of AAV within the cell during a lytic infection has not been studied in any detail, although the Rep proteins have been localized to intranuclear domains (22, 44).

We are interested in the behavior of adenovirus and AAV within cells and their effects upon each other as either wild-type replicating viruses or replication-deficient recombinant vectors. We recently analyzed the effect of adenovirus on rAAV vectors and showed that various adenovirus gene products can be used to enhance the transduction by AAV vectors (16a). Using a series of mutant viruses, we have demonstrated that the E1 and E4 gene products are necessary for the augmentation of expression from rAAV. In this report, we have extended our studies of the interaction between these viruses. Techniques of in situ hybridization and immunocytochemistry were used to demonstrate the localization of wild-type AAV DNA and Rep protein within the replication centers established by wild-type adenovirus. In the absence of helper virus, rAAV is localized in a perinuclear pattern and is recruited to the intranuclear domains when cells are infected with adenoviruses that are capable of enhancing transduction.

MATERIALS AND METHODS

Cells and viruses. HeLa and 293 cells were maintained as monolayers in Dulbecco modified Eagle's minimal essential medium supplemented with 10% fetal bovine serum and 100 U of penicillin-streptomycin per ml. All cultures were maintained at 37°C in a humidified atmosphere containing 5% CO_2.

The E1b mutant H5*dl*110 carries a lesion which disrupts only the 55-kDa product of E1b (2). Recombinant adenovirus AdCBALP from which E1 has been deleted contains the gene for human placental alkaline phosphatase in place of coding sequences for E1a and b (16a). The E4 mutant H4*dl*1004 has had all E4 coding regions except ORF1 deleted (7). E2a mutant virus H5*dl*802 contains a deletion in the gene for the 72K DBP (34). The E4 mutant virus was propagated in Vero-derived, E4-complementing cell line W162, and its titers were determined by plaque assay (47). The E2a mutant virus was propagated in HeLa-derived, E2a-complementing cell line gmDBP6, and its titers were determined by plaque assay (9). All other adenoviruses were propagated in 293 cells, and their titers were determined (18). Adenoviruses were purified by two sequential rounds of ultracentrifugation in CsCl gradients.

rAAV vector which expresses the *Escherichia coli lacZ* gene under the control of a cytomegalovirus promoter was used, and its construction, production, and purification have recently been described (16a). A crude lysate of wild-type AAV was obtained by transfection of plasmid pNTC244 into 293 cells infected with Ad5 (15). After 48 h, the cultures were harvested, resuspended in 10 mM Tris-HCl (pH 8), and frozen and thawed three times. Lysates were treated with DNase I (100 U/ml) at 37°C for 30 min and then heated at 60°C for 30 min to inactivate the enzyme and adenovirus helper. The extract was centrifuged at 10,000 × *g* for 20 min at 4°C, and the supernatant was used for infections.

Subconfluent cell monolayers were infected with adenovirus at a multiplicity of infection (MOI) of 10 to 100 PFU per cell. Infections with wild-type and rAAV used 5 μl and 1 to 2 μl, respectively. Cells were inoculated with virus in serum-free medium or medium containing 3% FBS. After incubation at 37°C for 2 to 3 h, the medium was replaced with fresh medium supplemented with 10% FBS until the time of fixation.

Expression of Rep protein in transfected cells. Plasmid pHIVRep contains the AAV *rep* gene expressed from the human immunodeficiency virus long terminal repeat (1). HeLa cells grown on glass coverslips were transfected with 0.5 μg of plasmid by using Lipofectamine reagent (Gibco BRL) as described by the manufacturer. Cells were infected with adenovirus at an MOI of 50 PFU per cell at 24 h posttransfection. Those cells expressing Rep protein were detected by immunofluorescence with an anti-Rep rabbit polyclonal antibody.

Immunofluorescence. Cells were grown and infected on glass coverslips in 24-well dishes. The cells were washed three times with phosphate-buffered saline (PBS) and fixed in freshly prepared 4% paraformaldehyde in PBS for 20 min on ice. After fixation, the cells were permeabilized either for 5 min in sodium dodecyl sulfate (SDS) buffer (0.05% SDS, 100 mM Tris-HCl [pH 7.8], 150 mM NaCl, 12.5 mM EDTA) or for 10 min on ice in 0.2% Triton X-100 in PBS. Cells were washed twice more in PBS, incubated for 1 h with primary antibodies, washed in PBS, and incubated for 1 h with secondary antibodies. The DBP of adenovirus was detected with a mouse monoclonal antibody (clone B6-8) at a dilution of 1/50 (33). The AAV Rep protein was detected with an anti-Rep specific polyclonal rabbit serum (44) at a dilution of 1/50. Secondary antibodies conjugated to fluorescein isothiocyanate (FITC) or Texas Red were obtained from Jackson ImmunoResearch and diluted 1:200 in PBS. Cells were counterstained for DNA with 0.5 μg of bis-benzimide (Hoechst 33258; Sigma) and mounted in Fluoromount G (Fisher Scientific). Fluorescent images were analyzed with a Leica confocal scanning microscope.

In situ hybridization. Biotinylated probes were obtained by labeling DNA (2 μg) by nick translation in the presence of biotin 16-dUTP alone or together with biotin 11-dCTP (Sigma). Directly labeled probes were obtained by nick translation in the presence of Fluorogreen or Fluorored (Amersham). Reactions proceeded for 2 to 3 h at 14°C, and the sizes of the resulting fragments were monitored by agarose gel electrophoresis. Fragments with sizes of 200 to 500 bp were selected and purified either by ethanol precipitation or with a Sephadex G-50 column (Boehringer Mannheim Biochemicals). The hybridization mixture was prepared by dissolving 20 to 50 ng of the probe and 10 μg of competitor *E. coli* tRNA in 4 μl of deionized formamide per reaction. Probes were denatured by heating them to 70°C for 10 min and immediately chilling them on ice prior to the addition of dextran sulfate and SSC (1× SSC is 0.15 M NaCl plus 0.015 M sodium citrate). The final concentrations in the hybridization mixture were 2 to 5 ng of probe per μl, 1.25 μg of tRNA per μl, 2× SSC, 10% dextran sulfate, and 50% deionized formamide.

Cells grown and infected on coverslips were washed three times in PBS and fixed in 4% paraformaldehyde in PBS for 20 min on ice. Cells were again washed in PBS and permeabilized by incubation in SDS buffer for 5 min at room temperature. Hybridizations and washings were carried out essentially as described by Pombo et al. (31). Hybridization signals were amplified with a sandwich of avidin-FITC and biotinylated anti-avidin and then with avidin-FITC (Vector Labs).

Histochemical detection of β-galactosidase expression. Infected cells were washed twice in PBS, fixed in 0.5% glutaraldehyde for 10 min at room temperature, and washed twice with 1 mM $MgCl_2$ in PBS. Cells were incubated in 5-bromo-4-chloro-3-indolyl-β-D-galactopyranoside (X-Gal) in 5 mM $K_3Fe(CN)_6$, 5 mM $K_4Fe(CN)_6$, and 1 mM $MgCl_2$ in PBS for 2 to 3 h at 37°C.

RESULTS

AAV nucleic acids and proteins localize to adenovirus replicative domains in coinfected cells. We used in situ DNA hybridization to visualize the nucleic acid of replicating AAV in the nuclei of cells coinfected with adenovirus as a helper. HeLa cells coinfected with AAV and Ad5 at an MOI of 50 were hybridized under nondenaturing and denaturing conditions with a biotinylated AAV genomic DNA probe. A strong nuclear fluorescence hybridization signal was detected in adenovirus-plus-AAV-infected cells at 20 h postinfection (Fig. 1). No labeling signal was detected in uninfected cells or cells infected with adenovirus alone, demonstrating that the labeled probe was specific and did not cross-hybridize with cellular or helper virus nucleic acid (data not shown). Three distinct patterns of in situ hybridization signal were observed for AAV nucleic acid in infected cell nuclei, including small discrete intranuclear foci (Fig. 1a), larger more diffuse foci (Fig. 1b), and an extensive staining spread throughout the nucleus (Fig. 1c). Cytoplasmic staining was also detected, but only in cells with the diffuse nuclear labeling. Time course studies suggested that these patterns represent progressive stages of the AAV lytic life cycle. At 10 to 12 h postinfection, infected cells displayed only the punctate nuclear foci, and by 22 to 24 h postinfection, the diffuse overall nuclear pattern predominated. At intermediate times, all three patterns could be observed in infected monolayers.

Hybridization under nondenaturing conditions will display the localization of both viral RNA and ssDNA. To differentiate between these two signals, nuclease digestions with either RNase A or DNase I were performed prior to hybridization. Without nuclease treatments, the signal under nondenaturing conditions was very similar to that under denaturing conditions, although slightly less intense (Fig. 1d). Following digestion of the cells with RNase A, the hybridization signal ap-

PAGE 17/77 * RCVD AT 8/29/2005 7:17:05 PM [Eastern Daylight Time] * SVR:USPTO-EFXRF-6/26 * DNIS:2738300 * CSID:6504936811 * DURATION (mm-ss):60-28

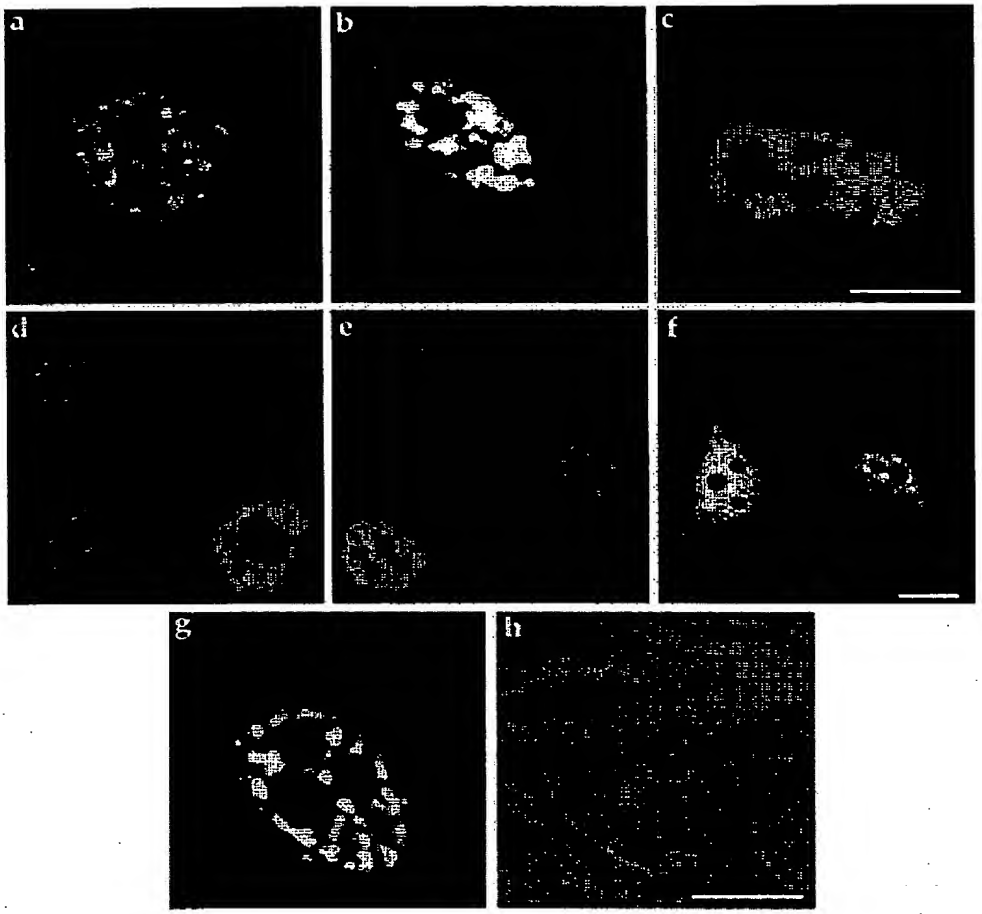

FIG. 1. In situ visualization of total viral nucleic acid for wild-type AAV in the presence of adenovirus. HeLa cells were coinfected with AAV and Ad5 for 20 h and hybridized in situ under denaturing (a, b, and c) and nondenaturing (d to g) conditions with double-biotinylated AAV probes, and nucleic acid was detected with an avidin-FITC complex. Hybridization under denaturing conditions shows total viral nucleic acid, including RNA and both ss- and dsDNA (a, b, and c). The hybridization signal for AAV is variable from cell to cell and ranges from small discrete intranuclear foci early in infection (a) to larger foci (b) and eventually to a diffuse pattern throughout the nucleus, with some staining also in the cytoplasm (c). Hybridization under nondenaturing conditions detects viral RNA and ssDNA (d). In order to visualize specifically viral ssDNA, infected cells were digested with RNase prior to hybridization under nondenaturing conditions (e). To specifically visualize viral RNA alone, infected cells were digested with DNase I prior to nondenaturing in situ hybridization (f). The localization of replication centers for AAV within the nucleus is shown in panels g and h, which show the in situ hybridization pattern under denaturing conditions (g) and the phase contrast image for the same cell (h). Bars, 10 μm.

peared in the same three pattern types as described above under both denaturing and nondenaturing conditions (Fig. 1e). Digestion with DNase I followed by in situ hybridization under nondenaturing conditions showed RNA diffusely distributed in the nucleoplasm and cytoplasm (Fig. 1f). In conclusion, the three patterns of hybridization signal are indicative of both ssDNA and dsDNA and therefore the sites of replication, which proceeds via dsDNA intermediates. Late in infection, the DNA is spread throughout the nucleoplasm, and RNA can be detected in situ under nondenaturing conditions, diffused throughout the nucleus and cytoplasm.

To characterize further the intranuclear location of AAV, we simultaneously localized the AAV Rep protein and the sites of AAV replication in the nuclei of cells coinfected with Ad5 and AAV (Fig. 2a and b). Localization of the AAV Rep proteins was determined by indirect immunofluorescence with a Rep-specific polyclonal rabbit-antiserum and a rhodamine-conjugated secondary antibody. The Rep proteins (Fig. 2b) colocalized with AAV DNA (Fig. 2a) at the replication centers. The pattern of Rep distribution mirrored that seen for DNA (Fig. 1) in that early in infection, fluorescence was detected in numerous distinct foci within the nucleus, and later in infection, it was present as a large diffuse signal (data not shown).

To colocalize the two viruses in cells coinfected with adenovirus and AAV, we carried out in situ hybridization with two different probes, one specific for each viral genome. The Ad5 genomic probe was directly labeled with rhodamine-dUTP, and the AAV probe was biotinylated and detected indirectly with an FITC-avidin complex. Previous studies have described the formation of replication centers following infection with wild-type adenovirus. These centers appear as distinct intranu-

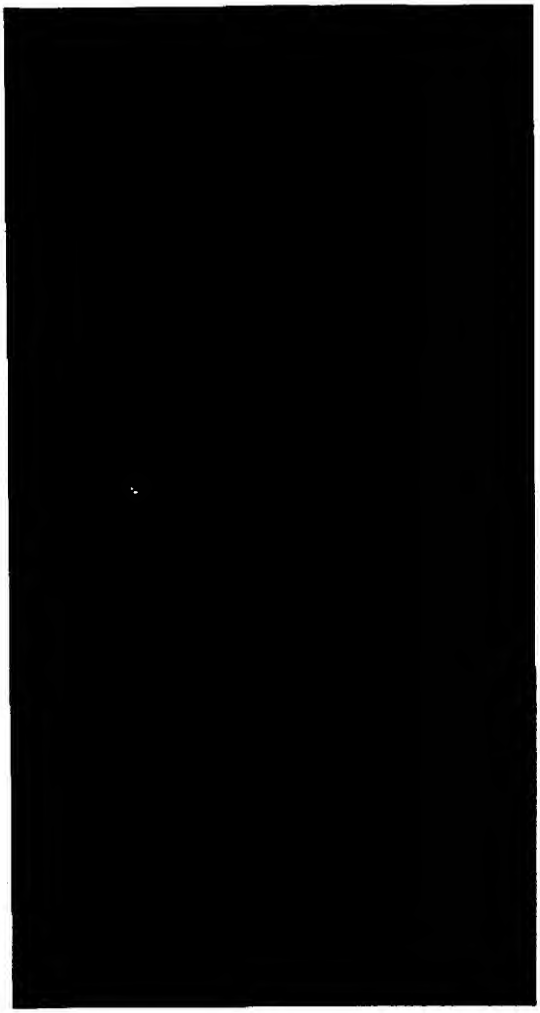

FIG. 2. Colocalization of adenovirus and AAV centers of replication. HeLa cells were coinfected with AAV and Ad5 for 20 to 22 h and hybridized in situ under denaturing conditions with AAV genomic DNA that was biotinylated or adenovirus genomic DNA probe directly labeled with rhodamine-dUTP. DBP and Rep were detected by immunocytochemistry with specific antibodies. The following colocalizations were performed: AAV DNA (a) and Rep protein (b), AAV DNA (c) and Ad DNA (d), AAV DNA (e) and DBP (f), and Rep protein (g) and DBP (h). The left column shows the image with a fluorescein filter, and the right column shows the same cells photographed with a rhodamine filter. Bar, 10 μm.

clear foci at early times in the infection cycle (25, 31, 32) at points where ssDNA and the adenovirus DBP colocalize (45). Both AAV and adenoviral genomes colocalized within the nucleus in common replication centers seen as distinct foci (Fig. 2c [AAV] and d [adenovirus]). We colocalized adenoviral DBP (Fig. 2f) with replicating AAV (Fig. 2e) in the punctate nuclear domains. A combination of double in situ hybridization followed by immunofluorescence with the anti-DBP antibody detected with an AMCA-conjugated second antibody was used to detect all three signals colocalized to replication domains (data not shown). The AAV viral replication protein Rep (Fig. 2g) was also shown to localize with adenovirus DBP (Fig. 2h) at the intranuclear foci.

AAV inhibits adenovirus replication through the Rep protein. During the course of the studies with colocalized adenovirus and AAV nucleic acid in coinfected cells, we noted a dramatic difference in the appearance of adenoviral domains as AAV replication progressed. Infection of cells with Ad5 alone established replication centers that matured through three phases as described previously (25, 31). The patterns observed included fine nuclear dots (Fig. 3a), crescent- and ring-shaped inclusions (Fig. 3b), and an extensive network of large rings and dots (Fig. 3c). Double labeling with anti-DBP antibody showed that the protein colocalized with replication sites (Fig. 2). Cells infected with AAV and adenovirus demonstrated colocalization of the two viral genomes in discrete foci at early time points as described in detail above. As the AAV replication progressed, the foci increased in size and began to spread out into a less discrete pattern. The DBP of adenovirus, initially colocalized at the distinct foci with both viral DNAs, appeared to spread out following the dispersed arrangement of the AAV nucleic acid (Fig. 3d). Concomitant with the spread of DBP was an apparent inhibition of the development of the adenovirus replicating domain. In cells showing an extensive pattern of AAV replication, very little adenovirus replication could be detected (Fig. 3d).

We attempted to quantitate the distribution of replication centers in cells infected with adenovirus in the presence and absence of AAV. A scoring system to quantitate the extent of adenovirus replication in HeLa cells infected with Ad5 at an MOI of 50 PFU per cell for 20 h was devised on the basis of signals for in situ hybridization with adenovirus genomic DNA probe and anti-DBP immunofluorescence. Adenovirus-infected cells in which the hybridization signal was detected as only fine intranuclear dots were scored as "+." Cells with larger foci in crescent-shaped inclusions were scored as "++," and cells with extensive signals in large ring shapes were scored as "+++." In the presence of coinfecting AAV, the additional pattern for decreased adenovirus DNA signal accompanied by dispersed DBP was scored as "SPREAD." This adenovirus pattern was only seen in cells coinfected with AAV. Examples of these patterns are presented in Fig. 3, with a quantitative summary provided in Fig. 4. Infection with adenovirus alone showed the majority of cells were in the later stage, with large inclusions of replicating adenovirus. The frequency of cells in this category was dramatically reduced when AAV was included in infections. An increasing number of cells demonstrated the more spread-out pattern in dually infected cells (Fig. 4).

The Rep protein of AAV has been shown to be responsible for AAV inhibition of replication by other viruses (1, 4, 21, 36, 51). We examined whether Rep was responsible for inhibition of adenovirus replication and if the effect could be observed at the single-cell level. Plasmids expressing Rep78 under the control of the human immunodeficiency virus long terminal repeat were transfected into HeLa cells, and the cells were infected with Ad5 24 h later. The extent of adenovirus replication was determined by in situ hybridization at 20 h postinfection, and cells expressing Rep78 protein were identified by immunofluorescence with the Rep-specific antibody (Fig. 5). The Rep protein was detected in a diffuse pattern throughout the nucleus of transfected cells (Fig. 5b). The degree of adenovirus replication (Fig. 5a) was inhibited in cells that expressed Rep (Fig. 5c). In cells that showed a high level of Rep protein expression, mature adenovirus replication centers could not be detected (Fig. 5c). The adenovirus signal in Rep-containing cells sometimes showed a scattered pattern but did not appear

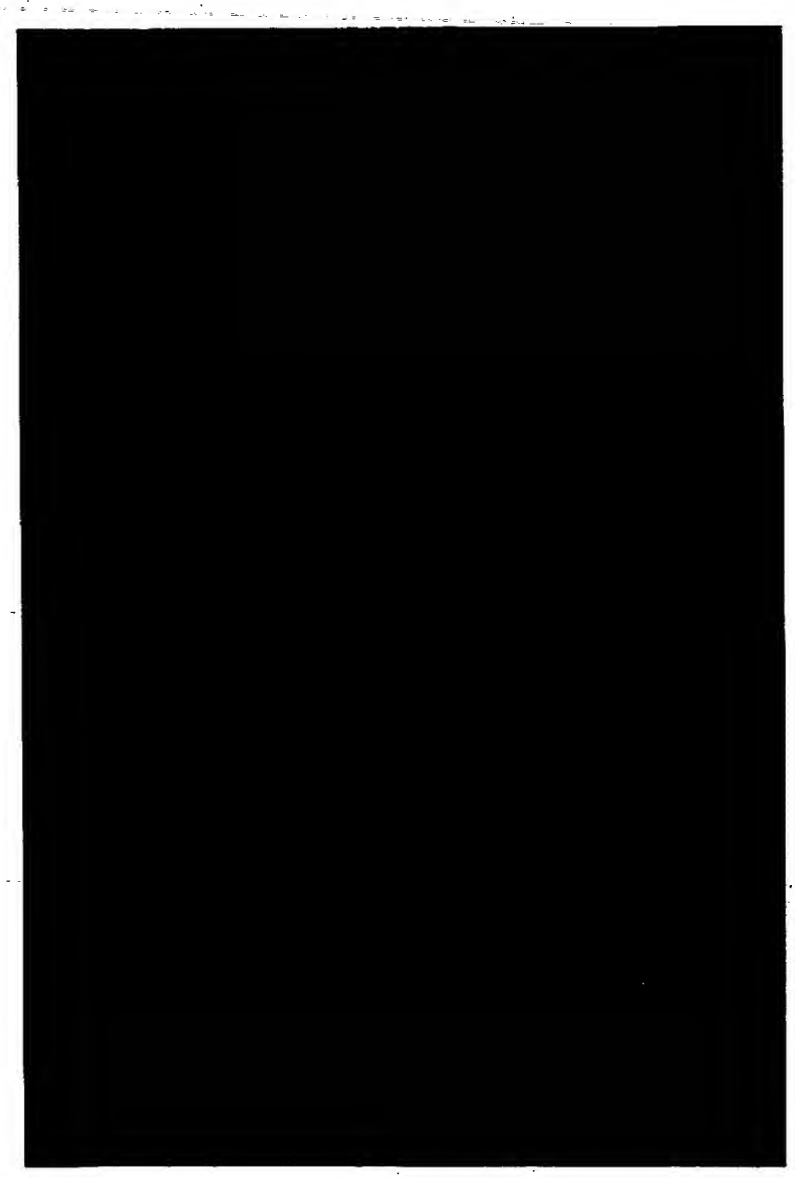

FIG. 3. Examples of the different in situ hybridization patterns for adenovirus infections. HeLa cells were infected with adenovirus in the absence (a, b, and c) and presence of coinfecting AAV (d) for 20 h. The left column shows detection of adenovirus DNA with an avidin-FITC complex formed on hybridized, biotinylated Ad5. The right column shows the same cells double labeled with an anti-DBP antibody and a rhodamine-conjugated secondary antibody. To the right are the scores used for quantitation (see Results and the legend to Fig. 4). Ad, adenovirus.

in the diffuse spread-out pattern observed with AAV replication. In addition, Rep-minus rAAV vectors had no effect on adenovirus replication (see below).

Subcellular localization of mutant adenoviruses. We characterized the intracellular localization of viral nucleic acids in cells infected with a series of adenoviruses from which essential genes had been deleted (Fig. 6). In a wild-type Ad5 infection, most cells displayed an extensive hybridization signal at 20 to 24 h postinfection (see above) (Fig. 6a). For a virus from which E4 had been deleted (*dl*1004), there was a decrease in the number of cells in the late stage of infection (Fig. 6j), with most cells showing only small intranuclear foci. Signals could be detected in crescent and ring shapes, but this pattern was less extensive than that seen with wild-type virus, and there was no detectable cytoplasmic staining. The E1b mutant (H5*dl*110) showed active centers of adenovirus replication, and the frequency of each category appeared to be intermediate between those of the E4 mutant and the wild type (Fig. 6g). Many more smaller foci with very few interconnected rings could be seen. Virus *dl*802 contains a deletion that disrupts the E2a gene,

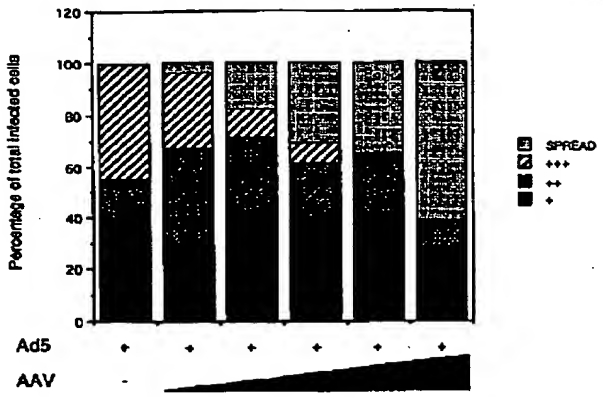

FIG. 4. Quantitation of adenovirus replication and AAV inhibition. The extent of adenovirus replication was determined for HeLa cells infected with Ad5 at an MOI of 50 PFU per cell alone or with increasing amounts of wild-type AAV lysate. Infected cells were fixed and hybridized in situ with Ad5 and AAV genomic probes as described in Materials and Methods. Adenovirus-infected cells in the absence of AAV were scored on a scale described in Results and shown in Fig. 3. In the presence of AAV, cells displaying a diffuse pattern of adenovirus DNA and DBP were scored as "SPREAD" (Fig. 3d). Ten randomly chosen fields were counted, with a total of approximately 100 cells being scored for each infection. Numbers are expressed as percentages of the total number of infected cells counted.

resulting in a truncated DBP and a defect in replication (34). Cells infected with this virus showed signals for both Ad5 DNA and DBP (Fig. 6d) (data not shown). The signal of this viral DNA was significantly different from that in a wild-type infection, with the distribution being in a speckled pattern and no large ring-shaped structures. There was a detectable signal for immunofluorescence with the anti-DBP antibody, but the location appeared to be around the nucleus, possibly in the endoplasmic reticulum (data not shown). Cells infected with a recombinant adenovirus from which E1 had been deleted and which contained the human placental alkaline phosphatase gene in place of the E1 region had a barely detectable hybridization signal, with only a very faint perinuclear pattern at 24 h postinfection (Fig. 6m). At a high MOI and later time points, a hybridization signal could be detected at discrete intranuclear foci, suggesting virus replication (data not shown).

rAAV is recruited to intranuclear domains in cells coinfected with adenovirus. The degree of gene transfer obtained with rAAV vectors is relatively poor but can be enhanced by coinfection with adenovirus (16a). We have demonstrated the importance of adenoviral early genes E1 and E4 in this augmentation of rAAV transduction; however, the underlying mechanisms are unknown. We explored the hypothesis that adenovirus enhancement of AAV transduction is mediated by compartmentalization of viral nucleic acid and protein within the nucleus. To evaluate this hypothesis, we used double in situ hybridization to detect genomic DNA in dually infected cells (Fig. 6). rAAV *lacZ* alone displayed a weak perinuclear hybridization (Fig. 6n). Coinfection of Ad5 with rAAV *lacZ* led to a dramatic augmentation in the expression of β-galactosidase (Fig. 6c) that was accompanied by a striking rearrangement of the rAAV genome (Fig. 6b). Adenovirus centers were established in these cells, and the rAAV *lacZ* genome was recruited to the distinct foci within the nucleus, as was revealed by the in situ hybridization signal (Fig. 7). The discrete dots within the nucleus were detected under nondenaturing conditions and after RNase treatment, indicating that at least part of the signal is due to the direct movement of the ssDNA genome; the signal did appear to be stronger under denaturing conditions, suggesting that some represents dsDNA. This observation conforms with our molecular analysis, which demonstrates that Ad5 coinfection can lead to the conversion of incoming recombinant ssDNA genomes to dsDNA conformations (16a). The possibility of contaminating wild-type AAV was ruled out by the lack of immunofluorescent signals for Rep or Cap proteins (data not shown).

We have previously documented the importance of the E1 and E4 gene products of adenovirus in the augmentation of expression from rAAV vectors. We investigated the intracellular localization of rAAV coinfected with a series of mutant adenoviruses from which different early regions had been deleted. An adenovirus vector from which E1 had been deleted, Ad*CBALP*, failed to redistribute the rAAV genome and did not enhance the degree of expression from the AAV transgene (Fig. 6m, n, and o). The adenovirus from which E4 had been deleted did not significantly increase expression from rAAV *lacZ*, but it did form small distinct foci within the nucleus to which the rAAV genome was targeted (Fig. 6j, k, and l). The E1b mutant showed an intermediate level of augmentation and also produced an intermediate level of replication domains to which rAAV moved (Fig. 6g, h, and i). The virus from which

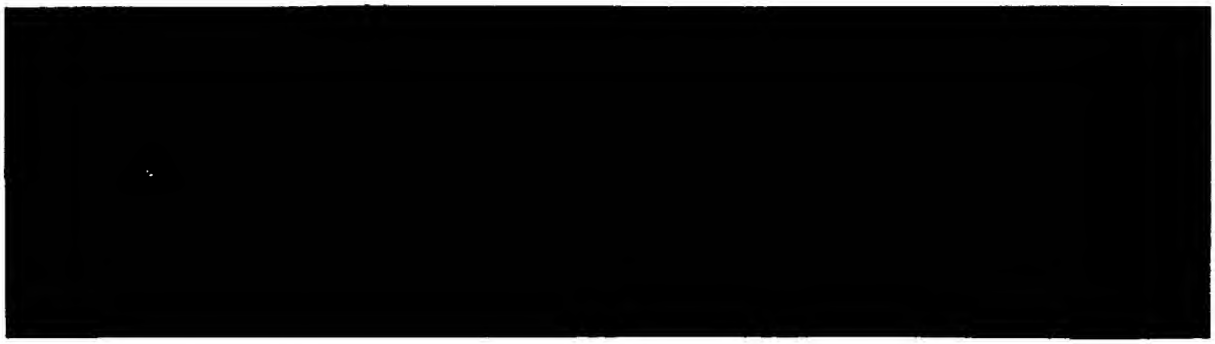

FIG. 5. The Rep protein mediates inhibition of adenovirus replication. HeLa cells were transfected with pIIIVRep (0.5 μg), and 24 h later, the cells were infected with Ad5 (MOI, 50) for a further 20 h. The cells were hybridized under denaturing conditions with biotinylated Ad5 genomic probe, and nucleic acid was detected with an avidin-FITC complex (a). Cells were double labeled with an anti-Rep antibody and a rhodamine-conjugated anti-rabbit secondary antibody (b). The two images have been superimposed in panel c. Bar, 10 μm. Arrow, cell showing a high level of Rep expression and inhibited adenovirus replication.

FIG. 6. Localization of rAAV in HeLa cells coinfected with adenovirus. Left column, adenovirus in situ hybridization with directly labeled Ad5 DNA probe (rhodamine-dUTP); middle column, rAAV *lacZ* in situ hybridization with biotinylated probe (detection with avidin-FITC); right column, X-Gal staining (magnification, ×100). Panels: a, b, and c, rAAV *lacZ* and Ad5; d, e, and f, rAAV *lacZ* and *dl*802; g, h, and i, rAAV *lacZ* and *dl*110; j, k, and l, rAAV *lacZ* and *dl*1004; and m, n, and o, rAAV *lacZ* and AdCBALP.

FIG. 7. Recruitment of rAAV *lacZ* to adenovirus centers of replication. HeLa cells were coinfected with rAAV *lacZ* and Ad5 (MOI, 10) for 22 h and hybridized in situ under denaturing conditions. The probes used were adenovirus genomic DNA probe labeled with rhodamine-dUTP (a) and AAV genomic DNA that was biotinylated and detected with an FITC-avidin complex (b). The two images have been superimposed in panel c. Bar, 10 μm.

E2a had been deleted was associated with a very large increase in expression from the rAAV *lacZ* vector and accompanying intranuclear recruitment of the rAAV genome (Fig. 6e and f).

DISCUSSION

AAV is a human parvovirus that is being evaluated as a vector for human gene therapy (11, 28). rAAV is produced in the context of a lytic infection that is dependent on helper virus, such as human Ad5. Recently, we have shown that transduction with rAAV is greatly enhanced by early gene products of adenovirus. Mechanisms by which these products interact with wild-type AAV to facilitate replication and virus biogenesis have been analyzed with well-characterized adenovirus variants. This previous work has identified adenoviral gene products essential to the AAV life cycle; however, the nature of these interactions remains speculative. The current study has extended our understanding of the interaction of wild-type AAV and adenovirus through its analysis of the compartmentalization of AAV nucleic acids and protein within the nucleus. These data suggest a model for replication of wild-type AAV based on structural reorganization within the cell and illustrate a potential mechanism by which adenovirus enhances transduction of rAAV.

The adenoviral genome contains a complex array of genes whose expression is subject to temporal regulation, with the immediate early genes E1a and E1b initiating a cascade of events leading to the expression of other early genes (E2, E3, and E4) and the transcription of the major late promoter coincident with the onset of viral DNA replication (5). These processes are also subject to remarkable spatial regulation by the formation of structures within the nucleus, called replication centers, where viral transcription and replication occur (31). We show in this report that wild-type AAV is sequestered into the adenovirus replication centers to facilitate AAV replication and transcription. From these data, we suggest a model for the lytic phase of AAV replication in which adenovirus is the driving force for the mobilization of its gene products and cellular factors into highly structured compartments within the nucleus, which are used by AAV for its propagation.

The physical sequestration of adenovirus nucleic acids and proteins with AAV represents a structural confirmation of the relationship between these viruses that was previously suggested in studies that demonstrated functional properties of adenoviral proteins that are common to both adenovirus and AAV replication. The adenovirus genes that supply helper functions for AAV have been defined as E1a, E1b, E2a, E4, and VA RNA. The E1a proteins are required directly for activation of the p5 promoter for expression of the Rep proteins (14) and indirectly through the regulation of other early adenovirus promoters (35). The E1b 55-kDa protein modulates the cytoplasmic accumulation of adenovirus late mRNAs while restricting the accumulation of most cellular mRNA (3, 30). This protein forms a physical complex with the 34-kDa product of the E4 ORF6 (40), and mutants in either protein show similar phenotypes (3, 20, 30, 48). The AAV helper functions for these E1b and E4 proteins appear to parallel their role in the adenovirus life cycle in that they are required for efficient and timely accumulation of AAV mRNA (39). The E1b protein has been detected at five distinct intracellular localizations (29), including within and about the periphery of the nuclear viral inclusion bodies. The ORF6 protein is found at a similar location (reference 16 and data not shown), and in its absence, the E1b protein does not associate efficiently with the replication centers (29). The full AAV growth cycle can be achieved in the absence of E2a (12), although the yield of infectious virus is reduced (it should be noted that the virus used in that report was the same as that with the E2a deletion used in our study, and it may therefore also produce some residual DBP). The VA RNA which is transcribed by the cellular RNA polymerase III is necessary for efficient translation of late adenoviral messages (43), and it has a similar role for AAV (23). The VAI RNA is found diffusely distributed in the cytoplasm and in small very intense bright round bodies in the nucleus (24). Thus, the presence of AAV at the replication centers for adenovirus puts it precisely at the location of the proteins required for helper activity. In addition, there are other cellular proteins that are recruited to these domains and that may be important in the AAV life cycle (6, 50). Although it is not required for AAV, the adenovirus polymerase is located at the viral inclusion foci (41), and thus it is possible that the cellular polymerase protein required by AAV is also recruited. This redistribution of nuclear proteins may be a helper function which is common to both adenovirus and herpesvirus and which makes the host cell competent for AAV replication. Recent observations have suggested that specific subnuclear domains in the host cell may represent preferential targets for DNA tumor viruses (13). The biological consequence of this observation remains unclear, but AAV may also benefit from cellular proteins localized at these specialized sites.

6504936811 8/29/2005 4:17 PM PAGE 24/077 Fax Server

AAV functions as a molecular parasite in that it replicates at the expense of the helper adenovirus. Previous studies have shown that AAV inhibits transcription from numerous heterologous promoters and diminishes replication of a number of viruses, including simian virus 40, bovine papillomavirus type 1, human immunodeficiency virus type 1, and adenovirus, as well as inhibits cellular replication (1, 4, 21, 26, 36, 51). Each effect is believed to be mediated by the AAV-encoded Rep protein. Our studies suggest a mechanism by which this occurs. We show that adenovirus replication centers are established in the presence of wild-type AAV; however, their normal evolution from small dispersed foci into large ring-like structures is aborted in the presence of AAV replication, which eventually dominates, leading to the production of AAV virions. Transfection experiments demonstrated that Rep is sufficient to suppress the maturation of adenovirus replication centers. It is possible that Rep mediates inhibition through a direct interaction with sequences in the adenovirus genome and thus affects gene expression. In addition to the AAV ITR, the Rep protein binds to specific DNA sequences within the AAV genome (27) and human genome (49). The inhibition could also be mediated posttranscriptionally or translationally on viral proteins or cellular proteins essential for the adenovirus growth cycle. Alternatively, the low amount of detectable adenovirus replication accompanied by the spread-out pattern of the DBP may suggest that the Rep proteins mediate their inhibition by usurping viral or cellular factors which support adenoviral or cellular DNA synthesis. Understanding the mechanism of Rep inhibition may prove useful in attempts to harness the site-specific integration of AAV, such as incorporating AAV into a hybrid adenovirus. It may be possible to create a mutant version of Rep that would provide some of the attractive features without inhibition, and the ability to view inhibition within the cell by in situ hybridization may provide a convenient assay to screen mutants. Unfortunately, mutational analysis so far suggests that sequences within the protein responsible for inhibition are also required for replication and, therefore, also possibly rescue and integration (26, 52).

rAAV has been used to transduce recombinant genes in applications of gene therapy, with variable results. In general, transduction of nondividing cells with purified rAAV is relatively poor and can be increased by stimulating the target cells to divide or by treating them with genotoxic agents (37, 38). We have extended this concept by demonstrating that E1 and E4 gene products alone can augment rAAV transduction by 2 to 3 orders of magnitude (16a). The increased transduction can be at least partly accounted for by conversion of incoming ssDNA genomes to a transcriptionally competent dsDNA conformation, although the effects of RNA transport, stability, or transduction could also contribute. One conclusion of these previous studies is that a step subsequent to viral entry limits transduction and that conversion of the incoming AAV genome to a transcriptionally active, double-stranded, nonintegrated form of the viral genome is necessary. Experiments in this paper confirm this hypothesis and suggest potential mechanisms of enhancement. Analysis of cells infected with a high MOI of rAAV in the absence of adenovirus demonstrated the presence of rAAV genomic DNA in virtually all cells, distributed around the perimeter of the nucleus. Infection with adenovirus was associated with an apparent redistribution of the rAAV DNA from around the nucleus to replication centers within the nucleus colocalized with adenoviral nucleic acids and proteins. The autonomous parvoviruses can replicate independently but can still be helped by coinfection with adenovirus (17, 46). The replication of the minute virus of mice is increased markedly by Ad2 coinfection, and the virus is recompartmentalized to the adenovirus replication domains (17) in a manner similar to that seen with rAAV. Mobilization of rAAV DNA into replication centers demonstrated some correlation with the ability of adenovirus mutants to enhance transduction. Viruses from which E1 had been deleted failed to augment transduction and establish replication centers, while fully mature replication centers with sequestered AAV were established with the wild-type virus and virus from which E2a had been partially deleted, both of which provided the greatest enhancement of rAAV transduction. Intermediate results were obtained with the virus from which E1b and E4 had been deleted. The appearance of some rAAV mobilization into replication centers in the presence of virus from which E4 had been deleted was somewhat surprising in that this helper virus was associated with no enhancement of transduction. This may suggest that E4 gene products are required to establish fully functional replication centers or that they contribute to efficient posttranscriptional steps, such as RNA transport, that may be necessary for transduction.

Analysis of the rAAV hybridization signal in infected HeLa cells indicated the effects of adenovirus not only on the distribution but also on the intensity of the signal in that the strength of fluorescence in the replication centers of dual-infected cells exceeded that found in the perinuclear area of rAAV-infected cells. This result may simply be the effect of the concentration at a specific locale. Alternatively, the signal may represent some concatemerization, which would give a larger target for hybridization and therefore a more intense signal. It is unlikely to be due to contaminating wild-type AAV, as none was detected in rAAV stocks. It is possible that some Rep protein is packaged into the AAV virion and allows a limited amount of replication within the cell. In addition to possible DNA synthesis, the signal also reflects an increase in transcription.

In summary, we have studied the relationship between wild-type AAV and adenovirus as it relates to structural reorganization that occurs within the nucleus. AAV takes up residence in adenovirus replication centers, where it replicates and transcribes, possibly by usurping the viral and cellular proteins that have been mobilized to replicate adenovirus. Expression of Rep aborts the normal maturation of the replication complex, giving way to a picture dominated by AAV. Similar principles apply to the use of rAAV for gene therapy in that mobilization of the rAAV genome into active domains within the nucleus greatly enhances its conversion to transcriptionally active genomic forms. A greater understanding of the biology of both wild-type and rAAV should suggest strategies to improve its ability to transduce cells for use as a gene therapy vector.

ACKNOWLEDGMENTS

We are grateful to G. Ketner, D. F. Klessig, A. J. Levine, R. A. Owens, and J. P. Trempe for their generous gifts of reagents. We thank Mitch Goldman, Mark Kelley, and Philippe Moullier for helpful discussions.

This work was supported by grants from the NIDDKD and the NHLBI of the NIH and the Cystic Fibrosis Foundation.

REFERENCES

1. Antoni, B. A., A. B. Rabson, I. L. Miller, J. P. Trempe, N. Chejanovsky, and B. J. Carter. 1991. Adeno-associated virus Rep protein inhibits human immunodeficiency virus type 1 production in human cells. J. Virol. 65:396–404.
2. Babiss, L. E., and H. S. Ginsberg. 1984. Adenovirus type 5 early region 1b gene product is required for efficient shutoff of host protein synthesis. J. Virol. 50:202–212.
3. Babiss, L. E., H. S. Ginsberg, and J. E. Darnell, Jr. 1985. Adenovirus E1b proteins are required for accumulation of late viral mRNA and for effects on cellular mRNA translation and transport. Mol. Cell. Biol. 5:2552–2558.
4. Bantel-Schaal, U., and H. zur Hausen. 1988. Adeno-associated viruses inhibit SV40 DNA amplification and replication of herpes simplex virus in SV40-transformed hamster cells. Virology 164:64–74.

PAGE 24/77 * RCVD AT 8/29/2005 7:17:05 PM [Eastern Daylight Time] * SVR:USPTO-EFXRF-6/26 * DNIS:2738300 * CSID:6504936811 * DURATION (mm-ss):60-28

6504936811 8/29/2005 4:17 PM PAGE 25/077 Fax Server

5. Berk, A. J. 1986. Adenovirus promoters and E1a transactivation. Annu. Rev. Genet. 20:45–79.
6. Bosher, J., A. Dawson, and R. T. Hay. 1992. Nuclear factor I is specifically targeted to discrete subnuclear sites in adenovirus type 2-infected cells. J. Virol. 66:3140–3150.
7. Bridge, E., and G. Ketner. 1989. Redundant control of adenovirus late gene expression by early region 4. J. Virol. 63:631–638.
8. Bridge, E., D.-X. Xia, M. Carmo-Fonseca, B. Cardinali, A. I. Lamond, and U. Pettersson. 1995. Dynamic organization of splicing factors in adenovirus-infected cells. J. Virol. 69:281–290.
9. Brough, D. E., V. Cleghon, and D. F. Klessig. 1992. Construction, characterization and utilization of cell lines which inducibly express the adenovirus DNA-binding protein. Virology 190:624–634.
10. Carter, B. J. 1990. Adeno-associated virus helper functions, p. 255–282. *In* P. Tijssen (ed.), Handbook of parvoviruses, vol. 1. CRC Press, Boca Raton, Fla.
11. Carter, B. J. 1992. Adeno-associated virus vectors. Curr. Opin. Biotechnol. 3: 533–539.
12. Carter, B. J., B. A. Antoni, and D. F. Klessig. 1992. Adenovirus containing a deletion of the early region 2A gene allows growth of adeno-associated virus with decreased efficiency. Virology 191:473–476.
13. Carvalho, T., J.-S. Seeler, K. Ohman, P. Jordan, U. Pettersson, G. Akusjarvi, M. Carmo-Fonseca, and A. Dejean. 1995. Targeting of adenovirus E1A and E4-ORF3 proteins to nuclear matrix-associated PML bodies. J. Cell Biol. 131:45–56.
14. Chang, L.-S., Y. Shi, and T. Shenk. 1989. Adeno-associated virus p5 promoter contains an adenovirus E1A-inducible element and a binding site for the major late transcription factor. J. Virol. 63:3479–3488.
15. Chejanovsky, N., and B. J. Carter. 1989. Replication of a human parvovirus nonsense mutant in mammalian cells containing an inducible amber suppressor. Virology 171:239–247.
16. Cutt, J. R., T. Shenk, and P. Hearing. 1987. Analysis of early region 4-encoded polypeptides synthesized in productively infected cells. J. Virol. 61: 543–552.
16a. Fisher, K. J., G.-P. Gao, M. D. Weitzman, R. DeMatteo, J. F. Burda, and J. M. Wilson. 1996. Transduction with recombinant adeno-associated virus for gene therapy is limited by leading-strand synthesis. J. Virol. 70:520–532.
17. Fox, E., P. T. Moen, and J. W. Bodnar. 1990. Replication of minute virus of mice DNA in adenovirus-infected or adenovirus-transformed cells. Virology 176:403–412.
18. Graham, F. L., J. Smiley, W. C. Russell, and R. Nairn. 1977. Characteristics of a human cell line transformed by DNA from human adenovirus 5. J. Gen. Virol. 36:59–72.
19. Greber, U. F., M. Willetts, P. Webster, and A. Helenius. 1993. Stepwise dismantling of adenovirus 2 during entry into cells. Cell 75:477–486.
20. Halbert, D. N., J. R. Cutt, and T. Shenk. 1985. Adenovirus early region 4 encodes functions required for efficient DNA replication, late gene expression, and host cell shutoff. J. Virol. 56:250–257.
21. Hermonat, P. L. 1992. Inhibition of bovine papillomavirus plasmid DNA replication by adeno-associated virus. Virology 189:329–333.
22. Hunter, L. A., and R. J. Samulski. 1992. Colocalization of adeno-associated virus Rep and capsid proteins in the nuclei of infected cells. J. Virol. 66:317–324.
23. Janik, J. E., M. M. Huston, K. Cho, and J. A. Rose. 1989. Efficient synthesis of adeno-associated virus structural proteins requires both adenovirus DNA binding protein and VA I RNA. Virology 168:320–329.
24. Jimenez-Garcia, L. F., S. R. Green, M. B. Mathews, and D. L. Spector. 1993. Organization of the double-stranded RNA-activated protein kinase DAI and virus-associated VA RNA I in adenovirus-2-infected HeLa cells. J. Cell Sci. 106:11–22.
25. Jimenez-Garcia, L. F., and D. L. Spector. 1993. In vivo evidence that transcription and splicing are coordinated by a recruiting mechanism. Cell 73:47–59.
26. Kleinschmidt, J. A., M. Mohler, F. W. Weindler, and R. Heilbronn. 1995. Sequence elements of the adeno-associated virus *rep* gene required for suppression of herpes-simplex-virus-induced DNA amplification. Virology 206:254–262.
27. McCarty, D. M., D. J. Pereira, I. Zolotukhin, X. Zhou, J. H. Ryan, and N. Muzyczka. 1994. Identification of linear DNA sequences that specifically bind the adeno-associated virus Rep protein. J. Virol. 68:4988–4997.
28. Muzyczka, N. 1992. Use of adeno-associated virus as a general transduction vector in mammalian cells. Curr. Top. Microbiol. Immunol. 158:97–129.
29. Oroelles, D. A., and T. Shenk. 1991. Localization of the adenovirus early region 1B 55-kilodalton protein during lytic infection: association with nuclear viral inclusions requires the early region 4 34-kilodalton protein. J. Virol. 65:424–439.
30. Pilder, S., M. Moore, J. Logan, and T. Shenk. 1986. The adenovirus E1B-55K transforming polypeptide modulates transport or cytoplasmic stabilization of viral and host cell mRNAs. Mol. Cell. Biol. 6:470–476.
31. Pombo, A., J. Ferreira, E. Bridge, and M. Carmo-Fonseca. 1994. Adenovirus replication and transcription sites are spatially separated in the nucleus of infected cells. EMBO J. 13:5075–5085.
32. Puvion-Dutilleul, F., J. Pedron, and C. Cajean-Feroldi. 1984. Identification of intranuclear structures containing the 72K DNA binding protein of human adenovirus type 5. Eur. J. Cell Biol. 34:313–322.
33. Reich, N. C., P. Sarnow, E. Duprey, and A. J. Levine. 1983. Monoclonal antibodies which can recognize native and denatured forms of the adenovirus DNA-binding protein. Virology 128:480–484.
34. Rice, S. A., and D. F. Klessig. 1985. Isolation and analysis of adenovirus type 5 mutants containing deletions in the gene encoding the DNA-binding protein. J. Virol. 56:767–778.
35. Richardson, W. D., and H. Westphal. 1981. A cascade of adenovirus early functions is required for expression of adeno-associated virus. Cell 27:133–141.
36. Rittner, K., R. Heilbronn, J. A. Kleinschmidt, and G. Sczakiel. 1992. Adeno-associated virus type 2-mediated inhibition of human immunodeficiency virus type 1 (HIV-1) replication: involvement of p78rep/p68rep and the HIV-1 long-terminal repeat. J. Gen. Virol. 73:2977–2981.
37. Russell, D., A. Miller, and I. Alexander. 1994. Adeno-associated virus vectors preferentially transduce cells in S phase. Proc. Natl. Acad. Sci. USA 91: 8915–8919.
38. Russell, D. W., I. E. Alexander, and A. D. Miller. 1995. DNA synthesis and topoisomerase inhibitors increase transduction by adeno-associated virus vectors. Proc. Natl. Acad. Sci. USA 92:5719–5723.
39. Samulski, R. J., and T. Shenk. 1988. Adenovirus E1B 55-*M*, polypeptide facilitates timely cytoplasmic accumulation of adeno-associated virus mRNAs. J. Virol. 62:206–210.
40. Sarnow, P., P. Hearing, C. W. Anderson, D. N. Halbert, T. Shenk, and A. J. Levine. 1984. Adenovirus early region 1B 58,000-dalton tumor antigen is physically associated with an early region 4 25,000-dalton protein in productively infected cells. J. Virol. 49:692–700.
41. Sasagari, Y., T. Sanford, P. Aguire, and R. Padmanbahn. 1987. Immunological analysis of 140-kDa adenovirus-encoded DNA polymerase in adenovirus type 2-infected HeLa cells using antibodies raised against the protein expressed in *Escherichia coli*. Virology 160:389–399.
42. Schaak, J., W. Y.-W. Ho, P. Freimuth, and T. Shenk. 1990. Adenovirus terminal protein mediates both nuclear matrix association and efficient transcription of adenovirus DNA. Genes Dev. 4:1197–1208.
43. Thimmappaya, B., C. Weinberger, R. J. Schneider, and T. Shenk. 1982. Adenovirus VA I RNA is required for efficient translation of viral mRNAs at late times after infection. Cell 31:543–551.
44. Trempe, J. P., E. Mendelson, and B. J. Carter. 1987. Characterization of adeno-associated virus Rep proteins in human cells by antibodies raised against Rep expressed in *Escherichia coli*. Virology 161:18–28.
45. Voelkerding, K., and D. F. Klessig. 1986. Identification of two nuclear subclasses of the adenovirus type 5-encoded DNA-binding protein. J. Virol. 60: 353–362.
46. Walton, T. H., P. T. Moen, Jr., E. Fox, and J. W. Bodnar. 1989. Interactions of minute virus of mice and adenovirus with host nucleoli. J. Virol. 63: 3651–3660.
47. Weinberg, D. H., and G. Ketner. 1983. A cell line that supports growth of a defective early region 4 deletion mutant of human adenovirus type 2. Proc. Natl. Acad. Sci. USA 80:5383–5386.
48. Weinberg, D. H., and G. Ketner. 1986. Adenoviral early region 4 is required for efficient viral DNA replication and for late gene expression. J. Virol. 57: 833–838.
49. Weitzman, M. D., S. R. M. Kyostio, R. M. Kotin, and R. A. Owens. 1994. Adeno-associated virus (AAV) Rep proteins mediate complex formation between AAV DNA and its integration site in human DNA. Proc. Natl. Acad. Sci. USA 91:5808–5812.
50. Wilcock, D., and D. P. Lane. 1991. Localization of p53, retinoblastoma and host replication proteins at sites of viral replication in herpes-infected cells. Nature (London) 349:429–431.
51. Yang, Q., F. Chen, J. Ross, and J. P. Trempe. 1995. Inhibition of cellular and SV40 DNA replication by the adeno-associated virus Rep proteins. Virology 207:246–250.
52. Yang, Q., A. Kadam, and J. P. Trempe. 1992. Mutational analysis of the adeno-associated virus *rep* gene. J. Virol. 66:6058–6069.

PAGE 25/77 * RCVD AT 8/29/2005 7:17:05 PM [Eastern Daylight Time] * SVR:USPTO-EFXRF-6/26 * DNIS:2738300 * CSID:6504936811 * DURATION (mm-ss):60-28

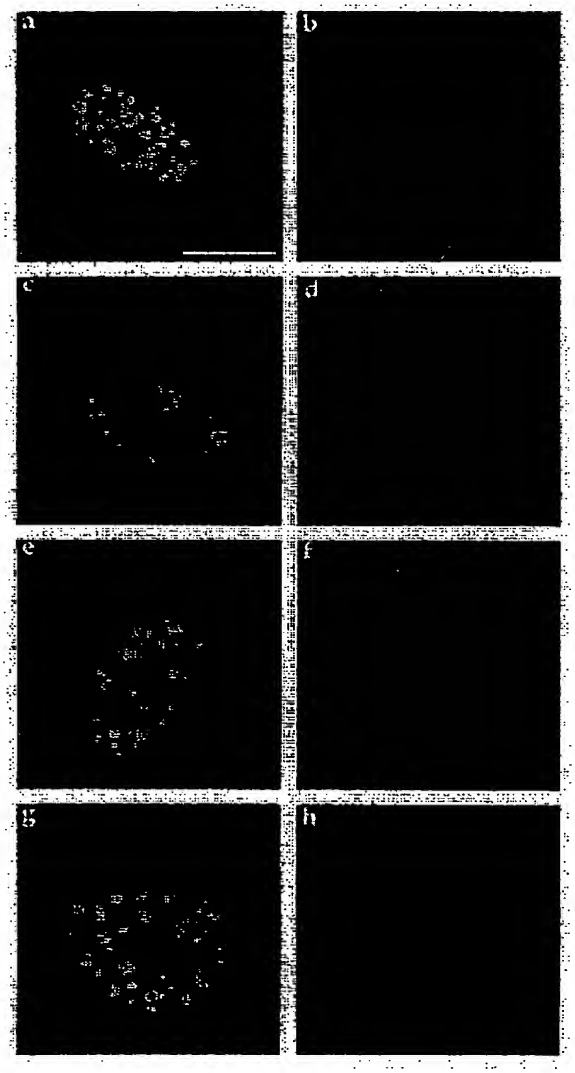
a
b
c
d
e
f
g
h

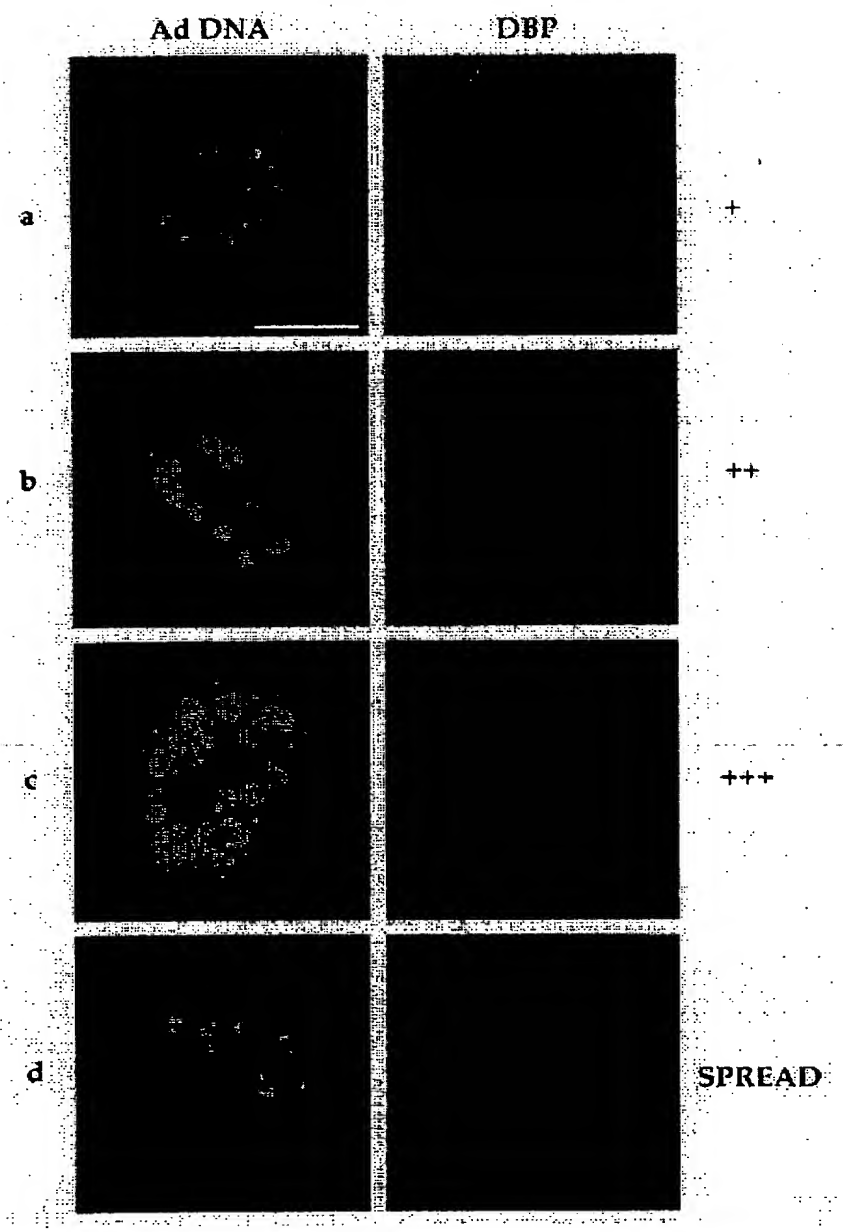
Ad DNA
DBP
a
+
b
++
c
+++
d
SPREAD


c
b
a

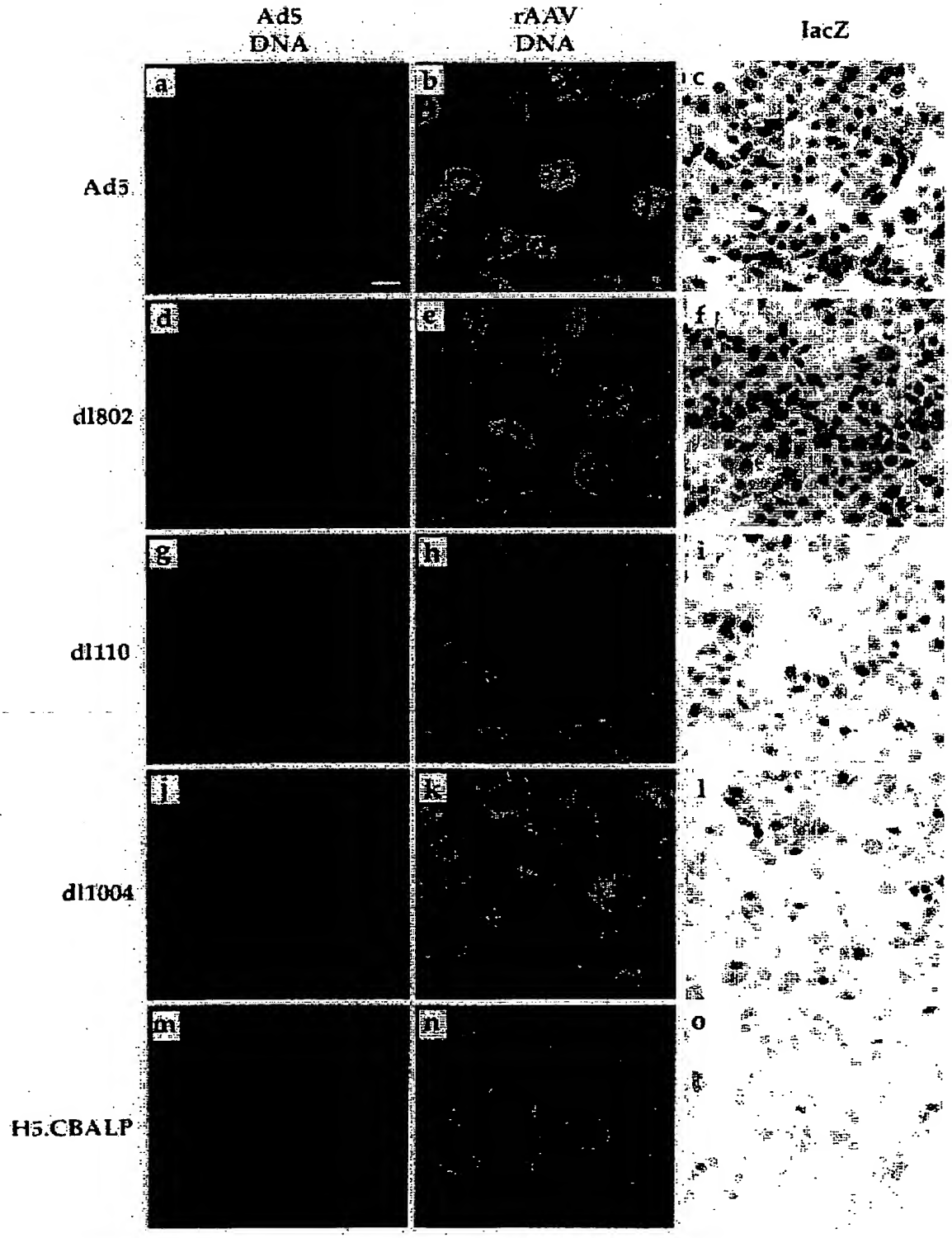
Ad5 DNA
rAAV DNA
lacZ
Ad5
dl802
dl110
dl1004
H5.CBALP
a
b
c
d
e
f
g
h
i
j
k
l
m
n
o

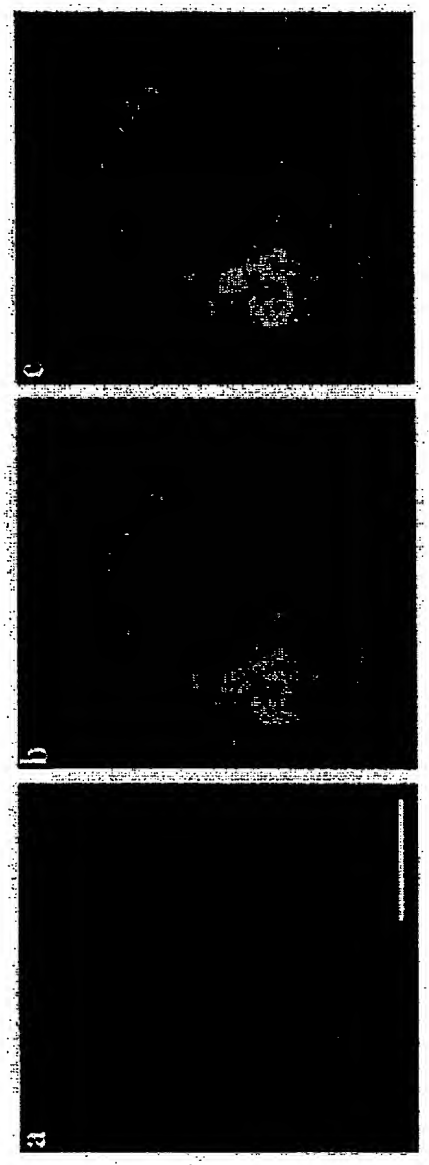
c
b
a

JOURNAL OF VIROLOGY, Jan. 1996, p. 520–532 Vol. 70, No. 1
0022-538X/96/$04.00+0
Copyright © 1996, American Society for Microbiology

Transduction with Recombinant Adeno-Associated Virus for Gene Therapy Is Limited by Leading-Strand Synthesis

KRISHNA J. FISHER, GUANG-PING GAO, MATTHEW D. WEITZMAN, RONALD DEMATTEO, JOHN F. BURDA, AND JAMES M. WILSON*

Institute for Human Gene Therapy and Department of Molecular and Cellular Engineering, University of Pennsylvania Health System, and The Wistar Institute, Philadelphia, Pennsylvania 19104

Received 13 July 1995/Accepted 2 October 1995

Adeno-associated virus is an integrating DNA parvovirus with the potential to be an important vehicle for somatic gene therapy. A potential barrier, however, is the low transduction efficiencies of recombinant adeno-associated virus (rAAV) vectors. We show in this report that adenovirus dramatically enhances rAAV transduction in vitro in a way that is dependent on expression of early region 1 and 4 (E1 and E4, respectively) genes and directly proportional to the appearance of double-stranded replicative forms of the rAAV genome. Expression of the open reading frame 6 protein from E4 in the absence of E1 accomplished a similar but attenuated effect. The helper activity of adenovirus E1 and E4 for rAAV gene transfer was similarly demonstrated in vivo by using murine models of liver- and lung-directed gene therapy. Our data indicate that conversion of a single-stranded rAAV genome to a duplex intermediate limits transduction and usefulness for gene therapy.

Adeno-associated virus (AAV) is a human parvovirus being considered as a gene delivery vehicle for human gene therapy. This small, nonenveloped virus contains a 4.7-kb single-stranded DNA genome that encodes regulatory and structural genes called *rep* and *cap*, respectively (13). Recombinant forms of AAV (rAAV) have been developed as vectors by substituting all viral open reading frames (ORFs) with a therapeutic minigene while retaining necessary *cis* elements contained in the 146-bp inverted terminal repeats (ITRs) (14, 30, 41). The AAV life cycle is biphasic, composed of both latent and lytic phases. rAAV is produced from a plasmid-based vector by stimulating a lytic infection with helper adenovirus or herpesvirus while supplying AAV *rep* and *cap* functions in *trans* (31). Although the mechanism of AAV-mediated transduction with a recombinant virus is poorly understood, it is most often equated with the latent phase of the wild-type AAV life cycle (18). Transduction with rAAV has been demonstrated in a wide variety of cell types, including differentiated, nondividing cells, suggesting the potential of this vector system for in vivo gene delivery to organs such as muscle, the liver, the central nervous system, and the lungs (10, 17, 22).

A greater understanding of the biology of the rAAV vector system would greatly accelerate its development for human gene therapy. Features of the lytic phase of the wild-type virus are of potential importance to both the production of the recombinant and its interaction with the target cell during transduction. When a cell harboring an integrated AAV provirus is challenged with a secondary infection by adenovirus or herpesvirus, a series of events unfold that result in cell lysis and propagation of AAV (6). Helper viruses encode functions that, along with products from cellular genes, are recruited by AAV to aid in rescue of the viral genome from the chromosome. Interactions between AAV and helper virus have been most thoroughly studied in the setting of an adenovirus infection in which it has been suggested that the genes in early regions E1A, E1B, E4, and E2A and VA RNA have pivotal roles (7, 16, 29, 44). Interestingly, the adenovirus gene products directly involved in adenovirus DNA replication (i.e., E2A, E2B, and terminal protein) do not contribute similar activities during replication of the AAV genome (24, 25, 39). In fact, host cellular functions can replace helper functions under conditions that activate endogenous pathways such as DNA repair (37, 46, 47). In a general sense, virus helper activities act to enhance or regulate AAV and cellular gene expression, while cellular proteins or factors direct replication of the rescued AAV genome.

Critical to the success of rAAV in gene therapy of chronic diseases such as cystic fibrosis are efficient transduction and prolonged expression of the therapeutic transgene. In its most stable form, wild-type AAV exists as a latent provirus preferentially targeting sites to human chromosome 19 (19, 33). Although the site-specific nature of AAV integration has been proposed for rAAV vectors, this behavior has only been fully characterized in terms of the wild-type virus. AAV relies heavily on the host cell machinery for establishing a latent infection; however, the mechanism of integration remains unknown. Important for the development of rAAV vectors is the observation that the viral ITRs represent the minimal elements necessary for integration (23, 31). It is unclear which features of wild-type AAV latency are relevant to transduction with rAAV.

In this study, we evaluated the potential of rAAV for gene therapy. Our findings indicate that transduction with purified rAAV is limited not by transfer of the single-stranded (SS) viral genome but rather by subsequent conversion of the viral genome to a transcriptionally active double-stranded template. This rate-limiting step is substantially enhanced by expression of adenovirus genes E1 and E4. Experiments with cell lines indicate that ORF6 of the adenovirus E4 gene locus is sufficient to enhance rAAV transduction significantly. Principles of rAAV transduction learned in vitro were confirmed with murine models of rAAV-mediated gene transfer to both lung and liver tissues. These studies illustrate important limitations of

* Corresponding author. Mailing address: The Wistar Institute, Room 204, 3601 Spruce St., Philadelphia, PA 19104-4268. Phone: (215) 898-3000. Fax: (215) 898-6588.

PAGE 31/77 * RCVD AT 8/29/2005 7:17:05 PM [Eastern Daylight Time] * SVR:USPTO-EFXRF-6/26 * DNIS:2738300 * CSID:6504936811 * DURATION (mm-ss):60-28

rAAV vectors as they currently exist and suggest strategies for improving their potential.

MATERIALS AND METHODS

Viruses. Wild-type adenovirus type 5 (Ad5) and mutant strains *dl*110 (2), H5.CBALP, and *ts*125 (8) were propagated in 293 cells. H5.CBALP (H5.010CBALP) is a recombinant adenovirus that contains an alkaline phosphatase minigene in place of adenovirus E1A and E1B gene sequences (map units 1 to 9.2). The alkaline phosphatase (ALP) cDNA is under the transcriptional control of a cytomegalovirus (CMV)-enhanced β-actin promoter. The titer of this virus was assessed in limiting-dilution infections on 293 cells, which measured PFU, and on HeLa cells, which measured ALP-expressing cells. The titer based on ALP expression was generally 10-fold higher than that based on PFU measurements. Virus *dl*802 was grown in E2A-complementing gmDBP cells as previously described (27). Viruses *dl*1004 and *dl*1010 were grown in E4-complementing Vero W162 cells (42). All viruses were purified by two sequential rounds of buoyant density ultracentrifugation in CsCl.

E1-E4 cell lines. The entire E4 region from Ad5 or an ORF6 minigene was subcloned into a shuttle plasmid that contained a neomycin resistance gene. Two versions of the ORF6 minigene that differ in the promoter element were developed. The first used a Zinc-inducible sheep metallothionein (MT) promoter to drive ORF6 expression. The second used a dexamethasone-inducible mouse mammary tumor virus promoter. Plasmids were transfected by calcium phosphate precipitation into 293 or HeLa cells seeded on 100-mm-diameter plates (10 μg of plasmid per plate). At 24 h posttransfection, cells were harvested and seeded at various dilutions (1:10 to 1:100) in 100-mm-diameter plates. Seeding medium contained G-418 (Geneticin; Bethesda Research Laboratories) at 1 mg/ml. Resistant colonies that developed were selected and expanded. Selected clones were analyzed for expression of ORF6 by several criteria, including (i) relative plaquing efficiency of *dl*1004, (ii) complementation of *dl*1004 based on late-gene expression, (iii) enhancement of rAAV transduction, and (iv) expression of ORF6 protein as measured by immunocytochemistry and Western blot (immunoblot) analyses. A detailed characterization of these cell lines will be presented elsewhere (11).

rAAV production and purification. rAAV was generated by plasmid transfections in the presence of helper adenovirus (31). The *cis*-acting plasmid pAV.CMV.LacZ was derived from psub201 (30) and contains a *lacZ* minigene in place of the AAV *rep* and *cap* genes. Expression of the *lacZ* reporter was driven by the immediate-early CMV enhancer-promoter. Therefore, the 5′-to-3′ organization of the recombinant AV.CMV.LacZ genome (4.9 kb) includes an AAV ITR, a CMV enhancer-promoter element, a simian virus 40 (SV40) splice site donor-acceptor, *lacZ* cDNA, an SV40 polyadenylation signal, and an AAV ITR. *rep* and *cap* functions were provided by *trans*-acting plasmid pAAV/Ad (31).

Production of lots of the AV.CMV.LacZ vector involved the following steps. Monolayers of 293 cells (certified AAV free; Human Applications Laboratory, University of Pennsylvania, Philadelphia) grown to 90% confluency in 150-mm-diameter culture dishes (5×10^7 cells per plate; 90 plates total) were infected with H5.CBALP at a multiplicity of infection (MOI) of 10. Infections were done in Dulbecco's modified Eagle medium (DMEM) supplemented with 2% fetal bovine serum (FBS) at 20 ml of medium per 150-mm-diameter plate. At 2 h postinfection, 50 μg of plasmid DNA (37.5 μg of *trans*-acting DNA and 12.5 μg of *cis*-acting DNA) was added to each plate as a calcium phosphate precipitate and evenly distributed. Cells were left in this condition for 10 to 14 h, after which the infection-transfection medium was replaced with 20 ml of fresh DMEM-2% FBS. Following transfection (~50 h), cells were harvested and suspended in 10 mM Tris-Cl (pH 8.0) buffer (45-ml final volume) and a lysate was prepared by sonication. The lysate was brought to 10 mM manganese chloride, after which bovine pancreatic DNase I (20,000 U) and RNase (0.2-mg/ml final concentration) were added and the reaction mixture was incubated at 37°C for 30 min. Sodium deoxycholate was added to a final concentration of 1%, and the mixture was incubated at 37°C for an additional 10 min. The treated lysate was chilled on ice for 10 min, and solid CsCl was added to a final density of 1.3 g/ml. The lysate was brought to a final volume of 60 ml with a 1.3-g/ml CsCl solution in 10 mM Tris-Cl (pH 8.0) and divided into three equal aliquots. Each 20-ml sample was layered onto a CsCl step gradient composed of two 9.0-ml tiers with densities of 1.45 and 1.60 g/ml. Centrifugation was performed at 25,000 rpm in a Beckman SW-28 rotor for 24 h at 4°C. One-milliliter fractions were collected from the bottom of the tube and analyzed on 293 or 293(E4) cells for *lacZ* transduction. Fractions containing peak titers of the functional AV.CMV.LacZ vector were combined and subjected to three sequential rounds of equilibrium sedimentation in CsCl. The rotors used included Beckman NVT-90 (80,000 rpm for 4 h) and SW-41 (35,000 rpm 20 h) rotors. At equilibrium, AV.CMV.LacZ appeared as an opalescent band at 1.40 to 1.41 g/ml of CsCl. Densities were calculated from refractive index measurements. The purified vector was transferred to 20 mM *N*-2-hydroxyethylpiperazine-*N*′-2-ethanesulfonic acid (HEPES) buffer (pH 7.8) containing 150 mM NaCl by dialysis and stored frozen at −80°C in the presence of 10% glycerol or as a liquid stock at −20°C in 20 mM HEPES buffer (pH 7.8)–150 mM NaCl–40% glycerol.

Characterization of purified AV.CMV.LacZ vector. The purified vector was tested for AV.CMV.LacZ peptides and transducing virions, as well as contaminating H5.CBALP helper virus. Helper virus was monitored by histochemical staining for reporter ALP activity. A sample of purified vector representing 1.0% of the final product was added to a growing monolayer of 293 cells seeded in a 60-mm-diameter plate. Forty-eight hours later, cells were fixed in 0.5% glutaraldehyde–phosphate-buffered saline (PBS) for 10 min at room temperature, washed in PBS (3 × 10 min), and incubated at 65°C for 40 min to inactivate endogenous ALP activity. The monolayer was allowed to cool to room temperature, rinsed once briefly in 100 mM Tris-Cl (pH 9.5)–100 mM NaCl–5 mM MgCl, and incubated at 37°C for 30 min in the same buffer containing 0.33 mg of nitroblue tetrazolium chloride per ml and 0.165 mg of 5-bromo-4-chloro-3-indolylphosphate *p*-toluidinium salt per ml. Color development was stopped by washing the monolayer in 10 mM Tris-Cl (pH 8.0)–5 mM EDTA. Routinely, the purification scheme described above removed all detectable H5.CBALP helper virus by the third round of buoyant density ultracentrifugation.

AV.CMV.LacZ titers were measured according to genome copy number (vector particles per milliliter), A_{260}, and *lacZ*-forming units (LFU) per milliliter. Vector particle concentrations were based on Southern blotting. Briefly, a sample of purified AV.CMV.LacZ was treated with capsid digestion buffer (50 mM Tris-Cl [pH 8.0], 1.0 mM EDTA [pH 8.0], 0.5% sodium dodecyl sulfate, 1.0 mg of proteinase per ml) at 50°C for 1 h to release vector DNA. The reactions were allowed to cool to room temperature, loading dye was added, and the mixtures were electrophoresed through a 1.2% agarose gel. Standard quantities of the double-stranded AV.CMV.LacZ genome were also resolved on the gel. DNAs were electroblotted onto a nylon membrane, hybridized with a ^{32}P-random-primer-labeled restriction fragment, and the resulting blot was scanned on a PhosphorImager 445 SI (Molecular Dynamics). A standard curve was generated from the duplex forms and used to extrapolate the number of vector genomes in the sample. LFU titers were generated by infecting indicator cells with limiting dilutions of the vector sample. Indicator cells included the HeLa, 293, and 293(E4) lines. Twenty-four hours later, cells were fixed in glutaraldehyde as described above and histochemically stained for β-galactosidase activity (45). One LFU is the quantity of the vector sufficient to cause visually detectable *lacZ* expression in one cell at 24 h postinfection.

Transduction of cells in culture. (i) HeLa cells infected with adenovirus. HeLa cells seeded in six-well 36-mm-diameter culture plates (2×10^6 cells per well) were infected with wild-type Ad5 or an early region mutant (see Table 1) at an MOI of 10 PFU per cell. Infections were done in 1.0 ml of DMEM–2% FBS. Six hours postinfection, monolayers were washed and 1.0 ml of fresh DMEM–2% FBS containing AV.CMV.LacZ at 4×10^9 vector particles per ml was added. Although the AV.CMV.LacZ vector lot used in these experiments was shown to be free of H5.CBALP helper virus by histochemical staining, the vector sample was subjected to heat treatment (60°C for 20 min) prior to use to ensure the absence of contaminating adenovirus. Two hours later, 1.0 ml of DMEM–15% FBS was added to each well. Twenty-four hours after the addition of AV.CMV.LacZ, cells were harvested. Each test condition was done in triplicate to enable vector transduction to be evaluated in terms of three outputs: histochemical staining for *lacZ* activity (45), intracellular β-galactosidase specific activity, and the molecular form of the vector DNA. For β-galactosidase assays, cell pellets were suspended in 0.5 ml of PBS and sonicated. Cell debris was removed by centrifugation (15,000 × *g* for 10 min), and the clarified extract was assayed for total protein and β-galactosidase activity with *o*-nitrophenyl-β-D-galactopyranoside as the substrate. Episomal DNA was extracted from cell pellets by a modification of the procedure originally described by Hirt (15). Briefly, cells were suspended in 320 ml of Tris-Cl (pH 8.0)–10 mM EDTA–1% (final concentration) sodium dodecyl sulfate. The mixture was incubated at 37°C for 30 min. Pronase and proteinase K were added to final concentrations of 500 and 20 mg/ml, respectively, and the reaction mixture was incubated at 37°C for 2 h. Sodium chloride was added to a final concentration of 1.1 M, and the mixture was incubated at 4°C overnight. The precipitate that developed during the 4°C incubation was pelleted at 20,000 × *g* (30 min), and the clear supernatant was carefully removed. The supernatant was extracted once with phenol-chloroform-isoamyl alcohol (25:24:1) and then chloroform-isoamyl alcohol (24:1). Nucleic acids were precipitated with ethanol. The final pellet was suspended in 50 ml of Tris-Cl (pH 8.0)–1.0 mM EDTA. Samples (5 ml) of each Hirt extract were resolved through a 1.2% agarose gel, electroblotted onto a nylon membrane, and hybridized with a ^{32}P-random-primer-labeled cDNA of the SV40 polyadenylation signal used in AV.CMV.LacZ.

(ii) Inducible ORF6 cell lines. 293(MT-ORF6) and HeLa(MT-ORF6) cells seeded in six-well 35-mm-diameter culture plates (2×10^6 cells per well) were infected with purified, heat-treated AV.CMV.LacZ at an MOI of 1,000 vector particles per cell. Induction of ORF6 expression with zinc sulfate was initiated 2 h before addition of the vector and continued through the duration of the experiment. Twenty-four hours postinfection, cells were harvested and analyzed for *lacZ* expression and vector DNA as described above.

Animals and histology. BALB/c mice 4 to 6 weeks old were purchased from Jackson Laboratory (Bar Harbor, Maine). All animal procedures were approved by the Institutional Animal Care and Use Committee of the University of Pennsylvania and The Wistar Institute. Animals were anesthetized by an intraperitoneal injection of ketamine (70 mg/kg) and xylazine (10 mg/kg). For liver studies, a 1-cm left-flank incision was made and the spleen was exposed. The purified, heat-treated AV.CMV.LacZ vector in 50 μl of 20 mM HEPES buffer (pH 7.8)–150 mM NaCl (10^{11} vector particles) was injected just beneath the

TABLE 1. Early region mutants used to demonstrate adenovirus-mediated enhancement of AV.CMV.LacZ vector transduction

Helper	Mutant locus	Reference
Ad5	Wild-type Ad5	26
*dl*110	E1B-55kDa	2
H5.CBALP	E1A/E1B	20
*ts*125	E2A	8
*dl*802	E2A	27
*dl*1004	E4 (+ORF1)[a]	4
*dl*1010	E4 (−ORF6)[b]	4

[a] The deletion encoded by *dl*1004 ablates expression of all E4 ORFs except ORF1.
[b] The deletion encoded by *dl*1010 selectively disrupts E4 ORF6 expression.

splenic capsule, and the abdomen was closed with 3-0 vicryl. Vector samples spiked with helper adenovirus contained 2×10^{10} A_{260} particles of purified *dl*1004, *ts*125, or H5.CBALP in a final volume of 50 μl. For lung studies, vector samples (30 μl) were slowly infused into a mainstem bronchus through polyethylene tubing inserted into the trachea through a midline incision. Samples contained the same formulation of purified, heat-treated AV.CMV.LacZ with or without helper adenovirus as described for liver injections. Necropsies were performed 3 days postinfusion, and tissue was frozen in optimum cutting temperature cryoembedding compound. Frozen sections (6 μm) were prepared and histochemically stained for reporter enzyme activity as described earlier. Sections were counterstained with neutral red and mounted.

RESULTS

Adenovirus enhances rAAV transduction in cultured cells. The present study evolved from observations made during the production and characterization of a *lacZ* rAAV vector (AV.CMV.LacZ) that was generated in 293 cells with an E1-deleted adenovirus as a helper. Heat inactivation of contaminating adenovirus from purified rAAV stocks resulted in a 100-fold drop in the AV.CMV.LacZ functional titer assayed on 293 cells. Interestingly, *lacZ* transducing activity could be recovered by adding adenovirus back to the heat-treated vector. This provided the first indication that adenovirus significantly enhances the transduction efficiency of rAAV.

To better define the role of adenovirus in rAAV transduction, a series of complementation groups were generated by mixing different adenovirus early gene mutants with purified *lacZ* rAAV (Table 1). HeLa cells were infected with mixtures of adenovirus and rAAV and analyzed for *lacZ* transduction by histochemical staining of cell monolayers (Fig. 1) and intracellular enzyme activity (Fig. 2). Reporter β-galactosidase levels were substantially increased in cells infected with wild-type Ad5 (107-fold) and E2a-defective viruses *ts*125 (134-fold) and *dl*802 (225-fold) compared with β-galactosidase activity in cells infected with rAAV alone (Fig. 2A); histochemical analysis demonstrated a corresponding increase in *lacZ*-expressing cells (Fig. 1). The increase in β-galactosidase activity in lysates was greater than the apparent increase in *lacZ*-expressing cells detected by 5-bromo-4-chloro-3-indolyl-β-D-galactopyranoside (X-Gal) histochemistry. This was due, in part, to the high MOIs used for rAAV infection. A better correlation was demonstrated in coinfections with limiting dilutions of rAAV (data not shown). Enhancement of rAAV transduction was proportional to input helper adenovirus from MOIs of 1 to 50 for both wild-type Ad5 and *dl*802 (Fig. 2B); higher virus doses led to a fall in β-galactosidase expression, presumably because of adenovirus toxicity. In contrast to results obtained with the wild-type virus and the E2A mutants, an adenovirus with an E1 (H5.CBALP) or E4 (*dl*1004) deletion provided no significant increase in rAAV transduction (Fig. 1 and 2A). An intermediate level of enhancement (Fig. 1 and 2A) was achieved with an adenovirus with a partial E1 (*dl*110, ΔE1B) or E4 (*dl*1010, ΔORF6) deletion. These results implicated early regions E1 and E4 in the augmentation of rAAV.

Conversion of SS to double-stranded genome limits rAAV transduction efficiency. Studies with adenovirus early gene mutants suggested that expression of adenovirus genes, rather than the virion itself, is responsible for enhancement of rAAV transduction. To investigate these mechanisms further, we characterized the molecular state of the rAAV genome in infected cells. Hirt extracts were prepared from HeLa cultures transduced with *lacZ* rAAV with or without helper adenovirus and analyzed by Southern blot hybridization (Fig. 3). The full spectrum of molecular species present during a lytic AAV infection was demonstrated in cells infected with *lacZ* rAAV and wild-type adenovirus (Fig. 3A, lane +Ad5) or *ts*125 (Fig. 3A, lane +*ts*125); the input SS genome and monomeric and dimeric double-stranded replicative-form intermediates (RFm and RFd, respectively) were present. This result is in contrast to that obtained with cells infected with purified rAAV alone, in which the SS genome was the sole molecular form detected (Fig. 3A, lane AV.CMV.LacZ).

Analysis of cells coinfected with adenoviruses with early gene deletions revealed a direct correlation between formation of double-stranded forms of the rAAV genome and enhancement of *lacZ* transduction. Mutant adenoviruses that were ineffective in enhancing rAAV transduction (H5.CBALP and *dl*1004) failed to promote the formation of double-stranded forms of rAAV (Fig. 3A). Cells infected with adenovirus with E2A deleted (*dl*802) or E1 (*dl*110) or E4 (*dl*1010) partially deleted additionally demonstrated a band whose size was identical to RFm of the *lacZ* rAAV genome and whose abundance correlated directly with the expression of β-galactosidase activity (compare Fig. 2A and 3A). More slowly migrating concatemers of duplex rAAV were also detected (Fig. 3A). The relationship between RFm formation and *lacZ* rAAV transduction was further explored in experiments in which the dose of coinfecting wild-type Ad5 or *dl*802 varied between MOIs of 1 and 10 (Fig. 2B). The level of β-galactosidase and the abundance of RFm increased in proportion to the amount of infecting wild-type Ad5 (Fig. 3B) and *dl*802 (Fig. 3C). The correlation between rAAV transduction and RF synthesis appeared to be influenced by the permissiveness of the adenovirus infection. Cells infected with wild-type Ad5 or *ts*125 revealed proliferative AV.CMV.LacZ duplex synthesis (Fig. 3A); however, the levels of reporter expression generated with these two helper viruses were slightly lower than those achieved with *dl*802 (Fig. 1 and 2A). Unlike the deletion mutants described above, both wild-type Ad5 and *ts*125 are capable of mounting a productive infection in HeLa cells at low MOIs. This is significant because it introduces a multitude of factors that might impact the efficiency of gene expression from a newly synthesized duplex AV.CMV.LacZ sequence. For instance, reorganization of the nucleus in response to an adenovirus infection could lead to entrapment of RF molecules in DNA replication centers and/or their exclusion from active transcription domains (43a). The difference between *dl*802 and wild-type Ad5 could be seen in a direct comparison of *lacZ* transduction and RFm synthesis at low MOIs (≤ 10). Although both viruses maintained a tight linear relationship between the two measured outputs, more copies of the AV.CMV.LacZ duplex were needed to yield a unit of β-galactosidase activity in cells infected with wild-type Ad5 than in cells infected with *dl*802 (Fig. 2A and 3A).

The simplest explanation for the formation of double-stranded *lacZ* rAAV intermediates is extension of the leading DNA strand by DNA polymerase from the free 3′ OH of the duplex region of the vector ITR. In the absence of *rep*, this

6504936811 8/29/2005 4:17 PM PAGE 34/077 Fax Server

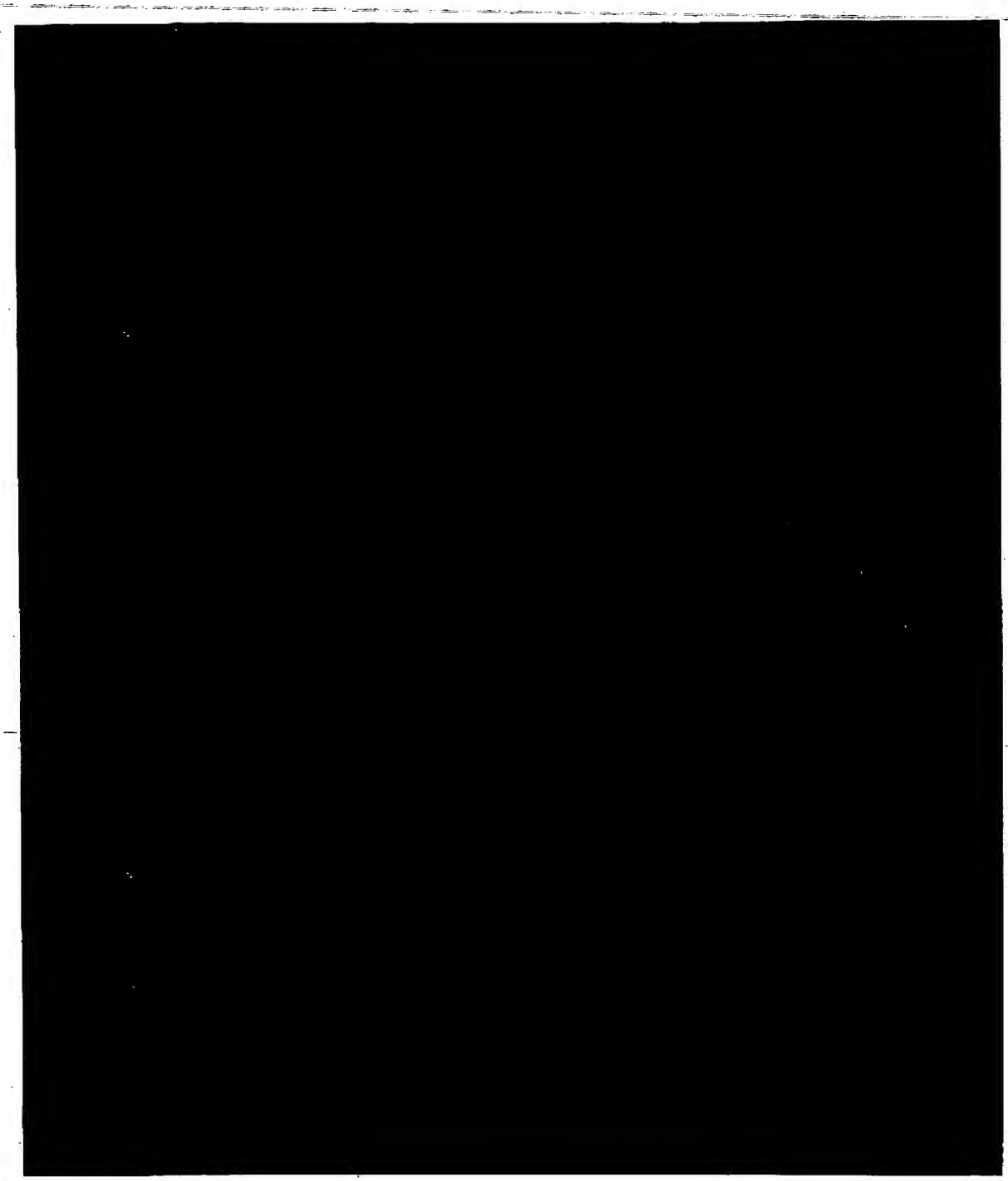

FIG. 1. Transduction efficiency of a recombinant AAV *lacZ* vector (AV.CMV.LacZ) in HeLa cells infected with different adenovirus mutants. HeLa cells infected with wild-type Ad5 or early gene mutants (10 PFU per cell) and AV.CMV.LacZ (2,000 vector particles per cell) were histochemically stained for β-galactosidase expression. Tested were the AAV vector alone (AV.CMV.LacZ), the vector plus wild-type Ad5 (+Ad5), the vector plus *dl*110 (+*dl*110), the vector plus H5.CBALP (+H5.CBALP), the vector plus *ts*125 (+*ts*125), the vector plus *dl*802 (+*dl*802), the vector plus *dl*1004 (+*dl*1004), and the vector plus *dl*1010 (+*dl*1010). Magnification, ×10.

PAGE 34/77 * RCVD AT 8/29/2005 7:17:05 PM [Eastern Daylight Time] * SVR:USPTO-EFXRF-6/26 * DNIS:2738300 * CSID:6504936811 * DURATION (mm-ss):60-28

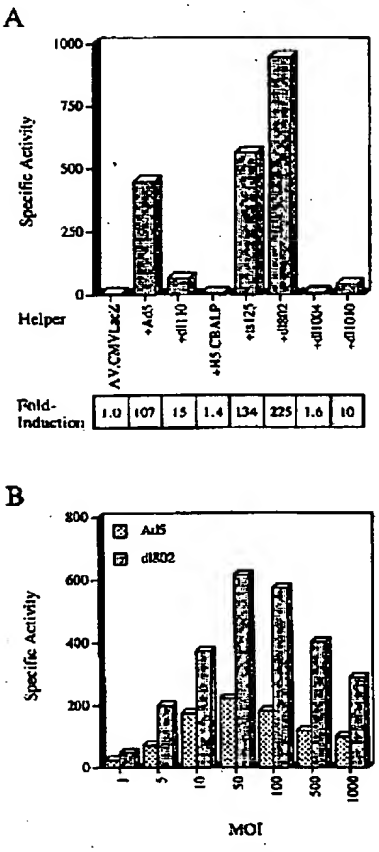

FIG. 2. Quantitation of enhanced vector transduction. (A) A duplicate set of the HeLa cells shown in Fig. 1 were lysed and assayed for total protein and intracellular β-galactosidase activity. The test condition is shown along the horizontal axis, and intracellular β-galactosidase specific activity (in milliunits per milligram of protein) is plotted on the vertical axis. Below each bar, the fold induction in specific activity relative to cells that received the AV.CMV.LacZ vector alone is given. (B) HeLa cells were infected with increasing MOIs of wild-type Ad5 or *dl*802. Six hours postinfection, monolayers were washed and the cells were infected with AV.CMV.LacZ at 1,000 vector particles per cell. Twenty-four hours after the addition of AV.CMV.LacZ, cells were harvested and assayed for total protein and β-galactosidase activity. Adenovirus MOIs are given along the horizontal axis, and intracellular β-galactosidase specific activity is given along the vertical axis.

conversion event would generate molecules in which one end is open and the other is covalently closed (Fig. 4). DNA blot hybridization studies were used to analyze the structure of the ends of RFm. Hirt extracts from cells coinfected with *lacZ* rAAV and wild-type Ad5 were digested with *Not*I to release the termini of the double-stranded intermediate; conformational differences between fragments with a closed or open end would allow separation through a nondenaturing agarose gel. Membranes were hybridized with a probe specific for the SV40 polyadenylation signal positioned immediately upstream of the rightward ITR. At least two forms were released from the right end of duplex genomes, one that migrated to a position in the gel that predicted an open-ended conformation (form II) and a second, more slowly migrating species (form I) (Fig. 4B, lanes 1 and 2). Although this result was consistent with our model (Fig. 4A), it was difficult to predict with certainty the structure of form I. Its retarded mobility did, however, suggest a conformation that differs from that of open-ended form II.

Adenovirus proteins encoded by E1 and E4 enhance rAAV transduction in the absence of adenovirus infection. The experiments described above implicated adenoviral gene expression in rAAV transduction. These data, however, did not directly uncouple the effect of adenovirus infection from adenovirus gene expression, nor did they specifically define the adenovirus gene products involved. Cell lines that stably express adenovirus gene products from constitutive or regulated promoters were established to help elucidate these mechanisms. Experiments with adenoviruses defective in early genes suggested that E1 and E4 gene products contribute to enhancement of rAAV transduction (Fig. 1 and 2). To confirm this observation, we stably transfected 293 cells with a genomic fragment of Ad5 spanning E4 that encodes seven ORFs. This E1-E4-expressing cell line and the parent E1-expressing cell line, 293, were infected with *lacZ* rAAV and analyzed for transduction; the specific activity of β-galactosidase was 196.2 mU/mg in E1-E4-expressing 293 cells, compared with 1.0 mU/mg in 293 cells that express only E1 genes. These experiments support a mechanism for enhancing rAAV transduction that is effected by expression of both E1 and E4 adenoviral genes.

We next considered whether the same effect could be achieved in 293 cells that express one specific ORF from the E4 region, ORF6. Our interest in this protein came from earlier experiments in which we used as a helper the ORF6 deletion mutant *dl*1010, which was much less effective than wild-type Ad5 at enhancing *lacZ* rAAV transduction (Fig. 1 and 2A). The cell line that was developed, 293(MT-ORF6), expresses ORF6 of the E4 gene of Ad5 from the MT promoter, which is relatively inactive at baseline but can be induced with divalent cations. In the absence of zinc, the 293(MT-ORF6) line generated 39-fold higher levels of β-galactosidase when infected with *lacZ* rAAV than did similarly infected control 293 cells (Fig. 5A). Induction of ORF6 expression with increasing amounts of zinc resulted in a concomitant rise in *lacZ* rAAV-mediated transduction to a peak level that was 445-fold greater than that of the parent 293 line (Fig. 5A). Analysis of Hirt extracts revealed the presence of RFm in rAAV-infected 293(MT-ORF6) cells but not in rAAV-infected 293 cells (Fig. 5B and 6). Importantly, the RFm level increased in proportion to the increment in *lacZ* transducing activity that occurred as ORF6 expression was induced with zinc (Fig. 5C) while the level of the SS rAAV genome remained constant. Similar results were obtained with a 293-derived cell line that expresses ORF6 from the glucocorticoid-responsive mouse mammary tumor virus promoter (data not shown).

The experiments described above implicated the combined expression of E1 and E4(ORF6) in the adenovirus-mediated augmentation of rAAV transduction. Expression of E1 alone was insufficient to have an effect, as evidenced by the results obtained when *lacZ* rAAV was used to infect 293 cells (Fig. 5A) or HeLa cells were coinfected with *dl*1004 (Fig. 1). To determine whether ORF6 expression is sufficient to enhance rAAV transduction, we developed a HeLa cell line that stably expresses the inducible MT-ORF6 minigene. This new cell line, HeLa(MT-ORF6), was evaluated for *lacZ* rAAV transduction in response to ORF6 induction. The number of cells that scored *lacZ* positive (Fig. 7A), and the amount of β-galactosidase in lysates (Fig. 7B), increased as the concentration of zinc in the medium was raised from 0 to 200 mM. A concentration of 250 mM zinc was found to be toxic to the cells. Hirt extracts were prepared from HeLa(MT-ORF6) cells to determine whether synthesis of duplex intermediates contrib-

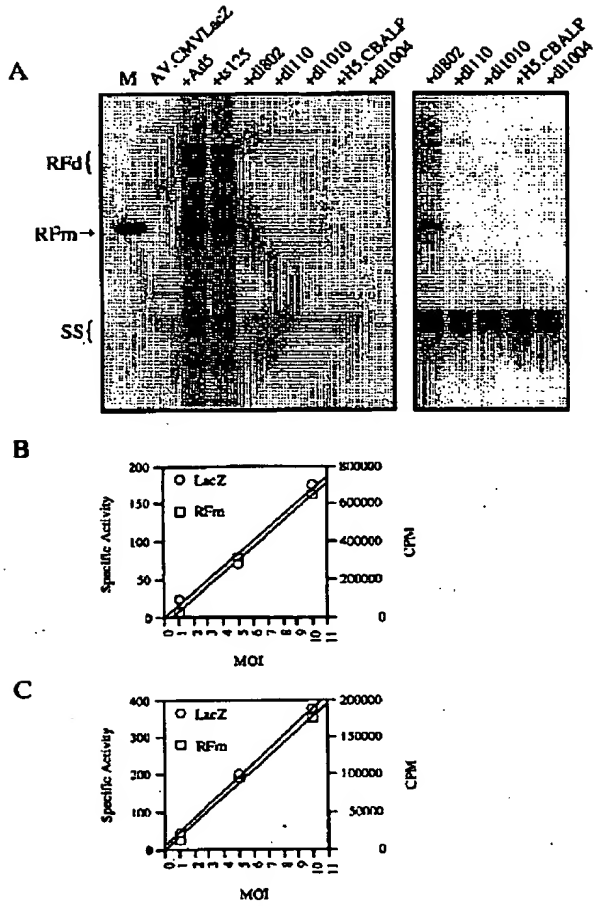

FIG. 3. Analysis of low-molecular-weight DNAs in AV.CMV.LacZ transduced cells. (A) Hirt extracts were prepared from a duplicate set of the HeLa cells shown in Fig. 1. Samples were analyzed by Southern hybridization with a probe specific for the SV40 polyadenylation signal of AV.CMV.LacZ. Bands corresponding to the SS AV.CMV.LacZ genome, RFm, and RFd were identified and labeled. To make the RFm band a reference, a plasmid carrying AV.CMV.LacZ was digested to release the entire genome (lane M). Autoradiogram exposure times were 14 h (left) and 69 h (right). The high-molecular-weight band in sample lane +H5.CBALP is helper virus DNA. Helper virus DNA is recognized by the SV40 probe because the CBALP minigene also utilizes the SV40 polyadenylation signal. (B and C) HeLa cells were infected with Ad5 (B) or *dl*802 (C) as described in the legend to Fig. 2B. Monolayers were harvested 24 h later and analyzed for β-galactosidase activity and RFm synthesis. Monomer bands similar to those shown in panel A were quantitated on a PhosphorImager 445 SI. β-Galactosidase specific activity and monomer counts per minute are plotted along the vertical axis. Adenovirus MOIs are given on the horizontal axis. Data obtained by infections with MOIs of 1, 5, and 10 are shown.

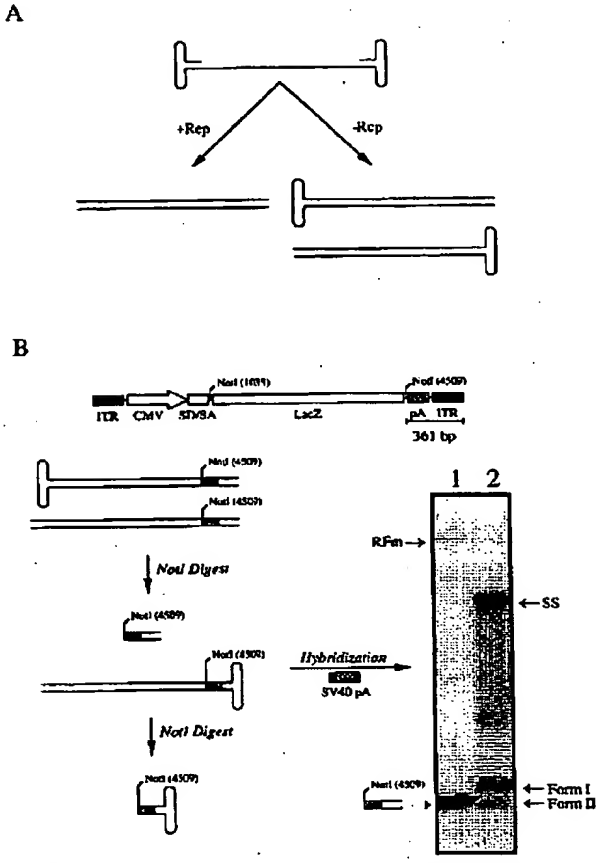

FIG. 4. Duplex end analysis. (A) Model for leading-strand synthesis of a complementary AAV strand in the presence of *rep* (+*rep*) or in the absence of *rep* (−*rep*). *rep* expresses a terminal resolution activity that can convert a duplex structure with closed ends to an open-ended duplex. In the absence of *rep*, terminal resolution is impaired, leaving the covalently closed hairpin structures intact. Under these conditions, hairpins would be expected to be found leftward and rightward since both strands of a rescued double-stranded AAV genome are packaged into virions. (B) Strategy for identifying the terminal structure of duplex RFm that is synthesized from SS AV.CMV.LacZ in response to adenovirus gene expression. At the top is a schematic of AV.CMV.LacZ with special attention to the right end. The domains that are labeled include the AAV ITRs, the CMV immediate-early enhancer-promoter, the SV40 splice donor-splice acceptor (SD/SA), the *Escherichia coli* β-galactosidase gene (*lacZ*), and the SV40 polyadenylation signal (pA). On the right end, a *Not*I site located at bp 4509 provided a convenient means of releasing a 361-bp fragment that contained the right ITR in the context of a hybridization target (i.e., the SV40 polyadenylation signal). In the presence of terminal resolution, only the open-ended 361-bp fragment would be expected to be generated. However, in the absence of such activity, digestion with *Not*I would generate a mixture of open-ended and covalently closed duplex fragments. In lane 1, a plasmid carrying AV.CMV.LacZ was digested to release the vector and then with *Not*I to release the right-terminal 361-bp fragment. In lane 2 is a sample of *Not*I-digested, Hirt-extracted DNA from HeLa cells infected with wild-type Ad5 and transduced with AV.CMV.LacZ (Fig. 3). The *Not*I digestion resulted in the release of two fragments, forms I and II. The migration positions of SS AV.CMV.LacZ and RFm are also shown.

utes to the augmentation in *lacZ* rAAV transduction. HeLa and uninduced HeLa(MT-ORF6) cells demonstrated a single band on Southern blots that comigrated with the SS genome (Fig. 8). Induction of ORF6 resulted in the appearance of detectable levels of a double-stranded monomer, but only at higher concentrations of zinc. A band corresponding to RFd was clearly evident in all cell preparations, and its relevance is unclear since the monomer form is a likely precursor of the dimer. The linear relationship between enhanced transduction and formation of RFm observed in cells expressing E1 and E4 was less obvious than in cells expressing just E4. One model to explain these findings is that formation of double-stranded genomes necessary for transcription is rate limiting for transduction in the presence of both E1 and E4; other steps may become limiting in the presence of only E4.

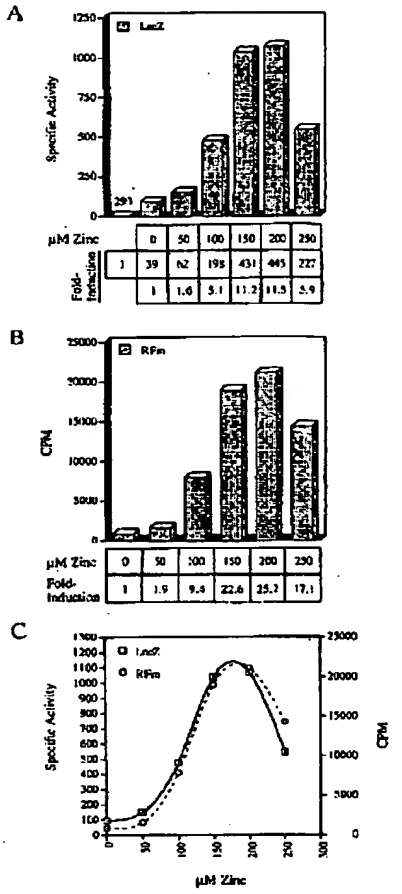

FIG. 5. Analysis of AV.CMV.LacZ transduction efficiency in 293 cells stably transfected with an inducible E4 ORF6 cDNA. 293(MT-ORF6) cells were transduced with an AV.CMV.LacZ vector at an MOI of 1,000 vector particles per cell in the presence or absence of a zinc inducer. Twenty-four hours after addition of the vector, cells were harvested and analyzed for transgene expression. (A) Lysates were assayed for recombinant β-galactosidase activity. 293 cells were included to establish the baseline transduction efficiency. Specific activity (in milliunits of β-galactosidase per milligram of protein) is plotted along the vertical axis. Below each bar is the concentration of zinc used for induction, the fold induction relative to 293 cells, and the fold induction relative to 293(ORF6) cells maintained in the absence of zinc. (B) Low-molecular-weight DNA was prepared from cell extracts and analyzed by Southern hybridization. RFm values (in counts per minute) are plotted along the vertical axis. The concentration of zinc used for induction and the fold induction relative to 293(ORF6) cells maintained in 0 mM zinc are given below each bar. (C) Comparison of the induction profiles that describe AV.CMV.LacZ transduction efficiency. Specific activity (in milliunits of β-galactosidase per milligram of protein) data from panel A and counts-per-minute data for AV.CMV.LacZ RFm from panel B are plotted along the vertical axis, and concentrations of zinc sulfate used during the experiment are shown along the horizontal axis. The two profiles are nearly mirror images.

The influence of factors, such as adenovirus gene expression on the efficiency of rAAV transduction has practical implications for the characterization of purified rAAV stock titers. Figure 9 summarizes various approaches to the assessment of the rAAV titer in a purified stock of AV.CMV.LacZ. Quantitation of viral particles based on A_{260} was consistently twofold higher than the measurement of viral genomes based on DNA hybridization. Direct measurement of viral genomes by hybridization is our standard approach for estimating particle concentration. Characterization of a purified lot of rAAV for function is more difficult because of the influence of the target cell and contaminating adenovirus. Analysis of an AV.CMV.LacZ preparation for *lacZ* transduction in a limiting-dilution assay on growing HeLa cells revealed an LFU titer that was approximately 4 orders of magnitude lower than the genome titer. The proliferative rate of the HeLa cultures at the time of the limiting-dilution assay has a minor (two- to threefold) influence on LFU measurements. The functional transduction titer on confluent cultures was increased 100-fold when adenovirus proteins E1 and E4 were expressed in the target cells by either coinfecting HeLa cells with wild-type adenovirus or infecting a 293-derived cell line that constitutively expresses E4.

Coinfection with adenovirus improves the efficiency of *lacZ* rAAV transduction in mouse liver and lung. In vitro experiments suggest that the efficiency of rAAV transduction is low because of limited conversion of the input SS genome to a transcriptionally active double-stranded intermediate. This conversion is facilitated by expression of adenovirus E1 and E4 gene products. We attempted to validate these principles in murine models of gene therapy directed to liver and lung tissues.

The impact of adenovirus gene expression on rAAV transduction in the murine liver was studied by infusing mixtures of *lacZ* rAAV and adenovirus early gene mutants into the portal circulation via the spleen. Unless otherwise stated, the dose of adenovirus was sufficient to transduce >25% of hepatocytes (i.e., 2×10^{10} particles). Figure 10A shows representative histochemical analyses of liver tissue harvested 3 days after gene transfer. Infusion of 10^{11} vector particles of purified *lacZ* rAAV alone into the portal vein was not associated with appreciable gene transfer (<0.01% of cells), confirming the inherent inefficiency of the rAAV system. Samples containing rAAV and E4-deleted adenovirus had no impact on *lacZ* transduction (Fig. 10A, +*dl*1004), whereas E1-deleted virus demonstrated a modest increment in *lacZ*-positive hepatocytes to ~0.1% (Fig. 10A, +H5.CBALP). The most significant increase in rAAV transduction occurred in the presence of the E2a adenovirus mutant *ts*125, with *lacZ* expression detected in 10 to 25% of hepatocytes (Fig. 10A, +*ts*125). A direct relationship between adenovirus and rAAV transduction was demonstrated in animals infused with a saturating dose of *lacZ* rAAV (10^{11} vector particles) and a limiting dose of the ALP-expressing, E1-deleted adenovirus (i.e., 2×10^9 particles that transduce ~1 to 2% of the liver). Histochemical studies demonstrated colocalization of ALP and *lacZ* in the majority of *lacZ*-expressing hepatocytes (Fig. 10A, +H5.CBALP).

Similar studies were performed with our murine model of lung-directed gene transfer (Fig. 10B). Doses of adenoviruses sufficient to transduce >25% conducing airway epithelial cells were instilled into the trachea with 10^{11} vector particles of rAAV. Analysis of lung tissue 3 days later revealed only a rare *lacZ*-positive cell in animals instilled with rAAV alone (Fig. 10B, AV.CMV.LacZ). No detectable enhancement of rAAV transduction was noted in animals when the vector was supplemented with adenovirus (2×10^{10} particles) with either E1 (Fig. 10B, +H5.CBALP) or E4 (Fig. 10B, +*dl*1004) deleted. However, substantial enhancement of transduction was achieved in cells of the conducting airways and alveoli of animals administered similar quantities of the E2a mutant adenovirus (Fig. 10B, +*ts*125).

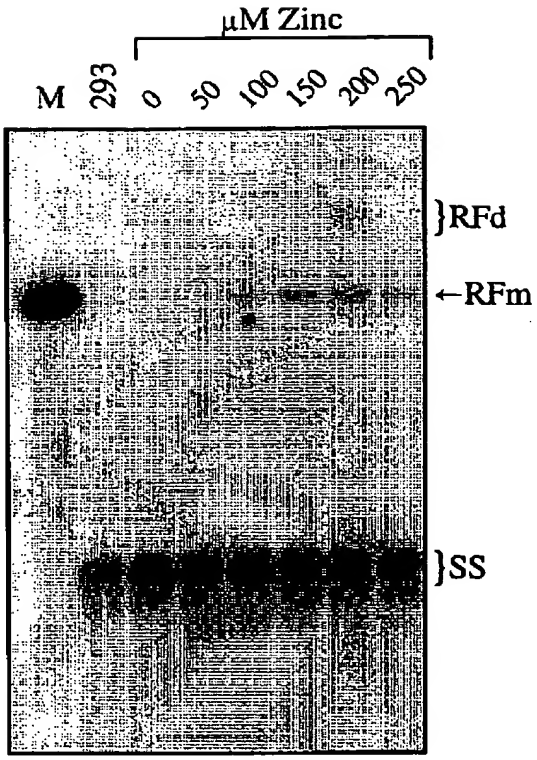

FIG. 6. Molecular analysis of the AV.CMV.LacZ genome in 293(MT-ORF6) cells following induction of E4 ORF6. The autoradiogram shows agarose gel-resolved Hirt extracts from the AV.CMV.LacZ-transduced cells described in Fig. 5. A plasmid carrying AV.CMV.LacZ was digested to release the entire sequence and loaded in lane M. The band that appears in this lane therefore reflects the migration of RFm. The migration positions of the SS AV.CMV.LacZ genome, RFm, and duplex RFd are shown. Lanes 0, 50, 100, 150, 200, and 250 contained samples from 293(MT-ORF6) cells that were induced with the indicated concentration of zinc. A Hirt extract from 293 cells (lane 293) transduced with AV.CMV.LacZ is also shown.

DISCUSSION

AAV is being developed for a wide range of applications in gene therapy both ex vivo and in vivo. The potential of AAV to integrate its genome efficiently into nondividing cells is being exploited in gene therapies based on ex vivo transduction of hematopoietic stem cells (21). In vivo application of rAAV is being developed for the treatment of cystic fibrosis by instillation of purified virus stocks into the airway to transduce the terminally differentiated epithelial cells of the conducting airway (10) and treatment of disorders of the central nervous system, such as Parkinson's disease (17). Efforts in our laboratory to develop rAAV for gene therapy have been hampered by the poor recovery of functional rAAV following purification. We discovered, however, that full rAAV transducing activity could be reconstituted when adenovirus was added back to the purified stocks. Characterization of the molecular basis of this phenomenon revealed issues of AAV and adenovirus biology relevant to the use of rAAV vectors for gene therapy.

The present studies indicated that the limiting step in rAAV-mediated transduction is not internalization of the virus, but rather the synthesis of transcriptionally active double-stranded intermediates from SS genomes. This genomic conversion and subsequent expression of the recombinant reporter gene were greatly facilitated by expression of a subset of adenovirus genes including E1 and E4. Experiments in complementing cell lines were critical for showing the relative contribution of these regions of the adenovirus genome to enhanced rAAV transduction. The data indicated that expression of the ORF6 protein from E4 was sufficient and necessary to increase the efficiency of *lacZ* transduction by an rAAV vector in a way that is dependent on synthesis of double-stranded viral DNAs. Although a similar response was not evident in cells that express E1 proteins alone, when combined with ORF6 expression, maximal transduction and duplex synthesis were achieved. Therefore, the role of E1 in enhanced rAAV transduction is best characterized as cooperative and dependent on the expression of the ORF6 protein.

These findings should be viewed in the context of the classic latency model of AAV transduction in which the SS viral genome is recognized by cellular factors and integrated into host chromosomal DNA. While there is evidence that this process can occur in certain in vitro settings (23, 31), our data strongly suggest that episomal double-stranded intermediates of the rAAV genome can be synthesized and are transcriptionally active. The latter mechanism of AAV transduction more closely resembles the basic mechanism of adenovirus-mediated gene transfer in which the double-stranded viral genome resides as a transcriptionally active episome (20). An important difference, however, is that the input rAAV genome must be converted from SS to double-stranded DNA for it to be functional.

The simplest model that emerged from the data is that adenovirus gene products promote the formation of double-stranded rAAV DNA intermediates which are transcriptionally active, a process that requires, at minimum, a cellular DNA polymerase. Parallels can be drawn to the initial steps in a lytic wild-type AAV infection in which helper gene products recruit cellular factors to facilitate the conversion of SS genomes to form RFm and RFd. The most compelling evidence for the contribution of cellular factors is the observation that radiation or genotoxic chemicals can stimulate replication of wild-type AAV in a helper-independent manner (37, 46, 47). Although the responses to these DNA-damaging agents are wide ranging and not fully understood in mammalian cells, the presumed outcome is an intracellular milieu that permits optimal repair of lesions before the cell reinitiates replicative DNA synthesis (34). It is reasonable to suggest that adenovirus helper activities which enhance rAAV transduction invoke similar responses. This might involve transient alterations in the expression or availability of cellular proteins, including polymerases, that are needed to initiate leading-strand synthesis from the 3'-end palindrome of an SS rAAV genome. Indeed, structural analysis of RFm formed during rAAV transduction suggested a model for DNA replication that mirrors repair-like synthesis.

The precise mechanism(s) by which adenovirus proteins encoded by E1 and E4 interact with rAAV to enhance transduction has not been defined; however, two general categories should be considered. The E1 region of adenovirus exerts pleiotropic effects on cellular gene expression and host cell growth (3). While the proteins from the E1A segment are most often associated with *trans* activation of genes (viral and cellular) and related events that lead to transformation, these proteins can also stimulate DNA synthesis through regulation of the cell cycle (36, 38). In the present report, we show that E1 gene products are not sufficient to enhance leading-strand synthesis or rAAV transduction; however, they may remove important barriers that enable other, related processes to pro-

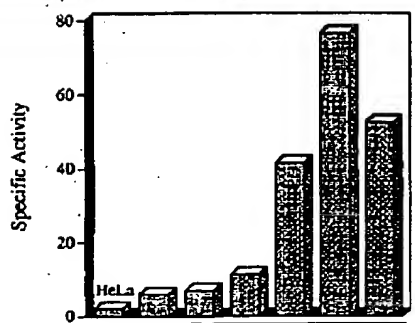

µM Zinc		0	50	100	150	200	250
Fold Induction	1	3	3.5	5.7	20.7	38.3	26.2
		1	1.2	1.9	6.9	12.8	8.7

FIG. 7. Enhanced AV.CMV.LacZ transduction in HeLa cells carrying an inducible ORF6 minigene. HeLa(MT-ORF6) cells were transduced at an MOI of 1,000 AV.CMV.LacZ vector particles per cell in the presence or absence of a zinc inducer. (A) Cell monolayers were histochemically stained for *lacZ* activity. The concentrations of zinc sulfate present in the media during transduction are shown. (B) Cell extracts were prepared and assayed for β-galactosidase activity. Specific activity (in milliunits of β-galactosidase per milligram of protein) is plotted along the vertical axis. Below each bar are the concentration of zinc used for induction, the fold induction relative to HeLa cells, and the fold induction relative to HeLa(MT-ORF6) cells maintained in the absence of zinc.

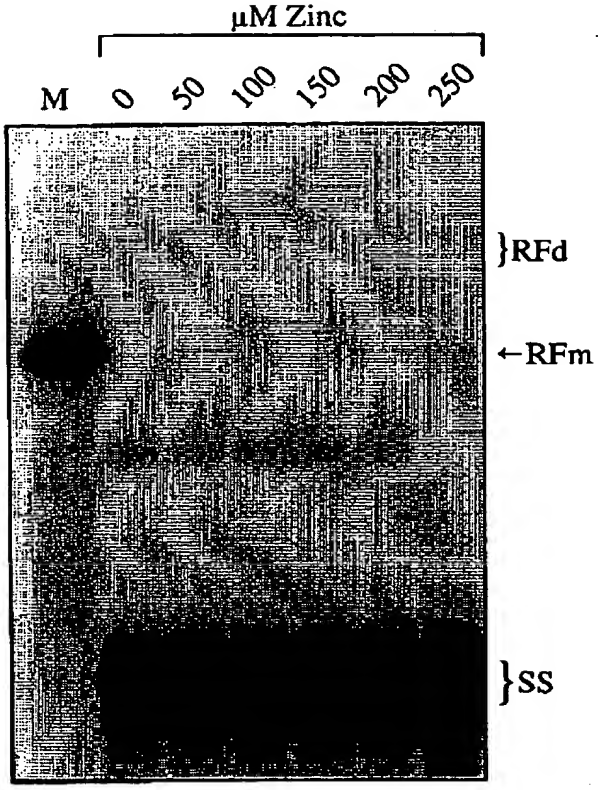

FIG. 8. Southern blot analysis of low-molecular-weight DNA from AV.CMV.LacZ-transduced HeLa(MT-ORF6) cells following induction of E4 ORF6. Hirt extracts were prepared from HeLa(MT-ORF6) cells transduced with AV.CMV.LacZ as described in the legend to Fig. 7. The blot was hybridized with a *lacZ*-specific probe. Lanes 0, 50, 100, 150, 200, and 250 contained samples from HeLa(MT-ORF6) cells that were induced with the indicated concentrations of zinc. Lane M contained a plasmid encoding AV.CMV.LacZ that was digested to release the entire genome. Bands corresponding to the SS AV.CMV.LacZ genome, duplex RFm, and duplex RFd are indicated.

ceed with greater efficiency. This contrasts with the observation that the ORF6 protein of E4 could alone induce the synthesis of duplex rAAV DNAs from SS genomes. This finding is consistent with an earlier proposal that the E4 region of adenovirus functions to promote second-strand synthesis of wild-type AAV (7, 28, 29). These early studies were confounded, however, by the fact that the wild-type AAV genome had not been fully characterized, leaving open the possibility that the effect was due to AAV proteins. With the discovery of the *rep* gene and its functions (13, 40), opinion shifted towards a role of E4 proteins in the modulation of posttranscriptional events (32). This possibility was further supported by the observation that the ORF6 protein of E4 forms a physical association with the E1B 55-kDa protein (35), a complex involved in cytoplasmic transport of mRNAs (12). The E4 region has also been implicated in the control of adenovirus DNA replication by regulation of the expression of the E2 region (5, 12).

Several findings suggested that total reporter transgene expression during rAAV transduction was influenced by factors other than the quantity of episomal double-stranded DNA molecules. This was most evident from experiments with HeLa cells that express the ORF6 protein of E4 from a regulated promoter. Although *lacZ* transduction increased in response to ORF6 expression, the induction profile did not precisely correlate with the accumulation of RFm. This is in contrast to the tight correlation between transduction and RFm synthesis that was shown in cells that express both the ORF6 and E1 proteins. ORF6 of E4 is known to have a pivotal role in the regulation of posttranscriptional events such as RNA transport and processing (12, 43). Furthermore, this activity is dependent on the formation of a complex with the adenovirus E1B 55-kDa protein (35). Our finding that both of these proteins are needed for optimal rAAV transduction suggests a similar role. In the absence of the E1B 55-kDa protein, efficient cytoplasmic transport and accumulation of RNA transcripts could be diminished. Therefore, while the formation of double-stranded DNA intermediates is an obligatory first step for rAAV transduction, transgene expression is likely further modulated through posttranscriptional mechanisms.

These studies are of potential importance to the development of rAAV for gene therapy. The encouraging conclusion is that rAAV can efficiently transfer its SS genome to a variety of cell types both in vitro and in vivo. The utility of rAAV is

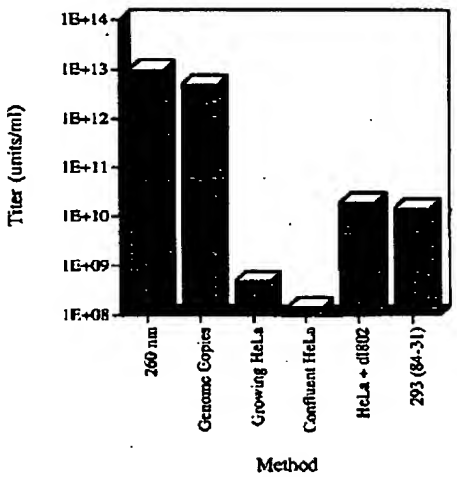

FIG. 9. Determination of *lacZ* rAAV titer. The titer of the purified recombinant AV.CMV.LacZ used in this study was measured in accordance with six different criteria. Titers in units per milliliter are on the vertical axis. The titer determination methods used are on the horizontal axis. Vector particle titers were initially determined by measuring A_{260} (bar labeled 260 nm) by using the formula $A_{260} \times$ dilution factor $\times 1.3 \times 10^{13}$. The constant was derived from the predicted absorbance of an SS DNA 4.7 kb long. The A_{260}/A_{250} ratio of the purified preparation was 0.71, in agreement with previous reports. Vector particle concentrations were also determined by using a Southern blot procedure (bar labeled Genome Copies) as described in Materials and Methods. This method more accurately measures the number of particles containing a genome copy of AV.CMV.LacZ. The titers reported in this study were determined by using vector particles per milliliter based on the Southern blot procedure. Titers based on functional *lacZ*-transducing virions (in LFU) were also determined as described in Materials and Methods. This method of titer determination is largely dependent on the condition of the indicator cell line, as shown here. The different conditions that were tested included HeLa cells that were confluent at the time of infection with AV.CMV.LacZ (bar labeled Confluent HeLa), HeLa cells that were confluent at the time of infection with AV.CMV.LacZ and infected with *dl*802 virus at an MOI of 25 (bar labeled HeLa + *dl*802), HeLa cells that were newly seeded at a low density (bar labeled Growing HeLa), and 293 cells that contained a stable copy of E4 [bar labeled 293 (84-31)]. The cell line 293 (84-31) contains all of E4, including the E4 promoter. This cell line is preferred over the 293 (MT-ORF6) cell line for titer determination because it does not require induction for expression of E4 proteins.

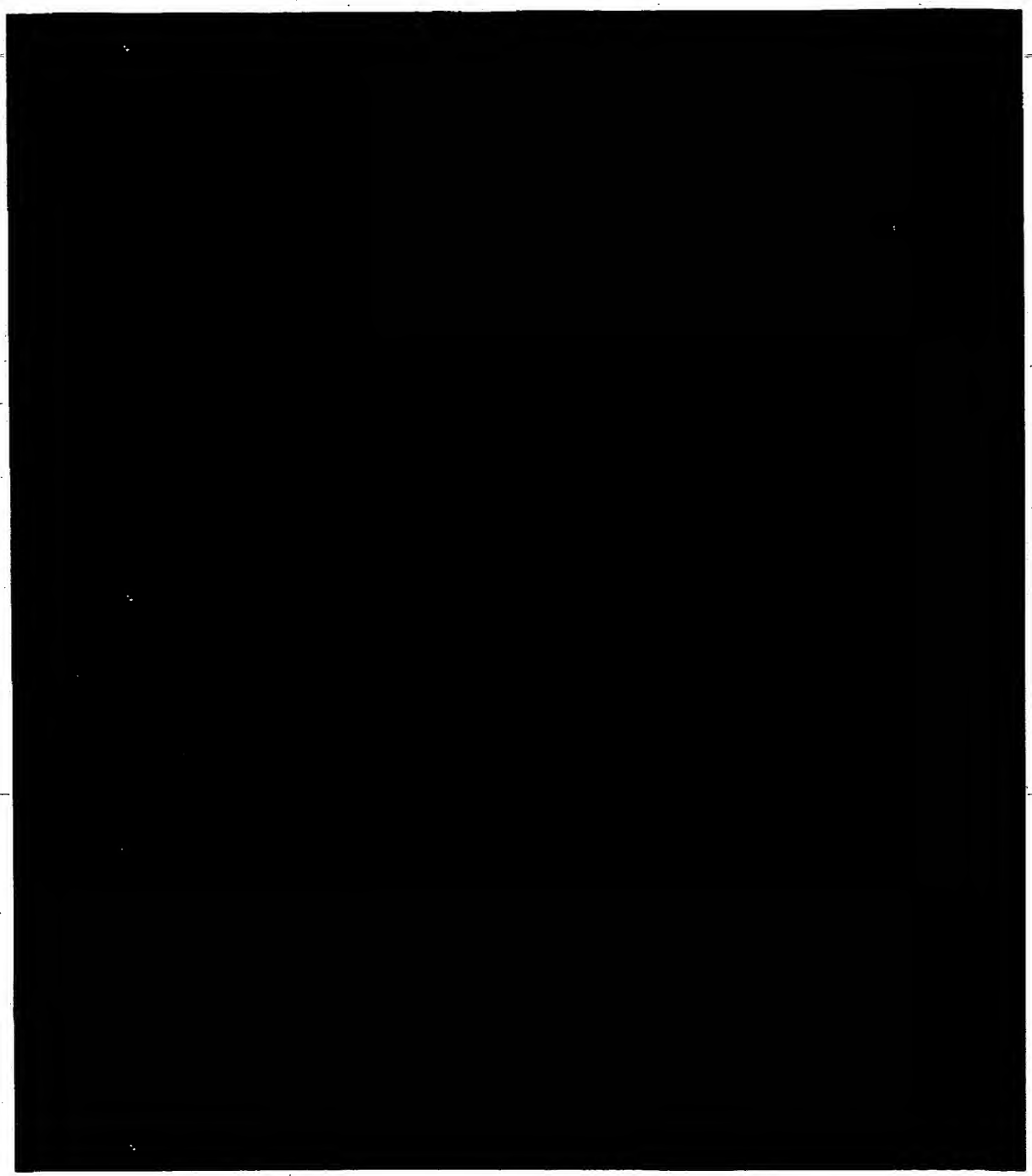

FIG. 10. Effect of adenovirus infection on in vivo AV.CMV.LacZ targeting efficiency. Mixtures of rAAV and helper adenovirus were delivered to the livers and lungs of adult BALB/c mice. Injection samples included 10^{11} vector particles of purified AV.CMV.LacZ or the same vector sample spiked with 2×10^{10} A_{260} particles of *dl*1004, H5.CBALP, or *tr*125. Tissue was harvested 72 h postinfusion. Frozen sections were histochemically stained for *lacZ* expression and counterstained with neutral red. This experiment utilized a total of six animals (three animal lungs and three animal livers), and sections spanning >50% of the cross section of each organ were analyzed. The experiment was repeated in part on two occasions. The data presented represent the predominant findings in these experiments. (A) Frozen liver sections. The inset in panel AV.CMV.LacZ shows a *lacZ*-positive hepatocyte targeted with AV.CMV.LacZ (arrow). The material labeled both +H5.CBALP and *lacZ*+ALP was from an animal infused with a mixture of AV.CMV.LacZ (10^{11} vector particles) and 2×10^{9} A_{260} particles of H5.CBALP. The section was histochemically stained for both β-galactosidase and ALP. The thin arrow identifies a cell targeted with AV.CMV.LacZ and H5.CBALP, while the thick arrow shows a cell positive for H5.CBALP alone. ALP gave a characteristic peripheral staining pattern (9). (B) Frozen lung sections. Airways are labeled with the letter A. The inset in panel AV.CMV.LacZ shows a *lacZ*-positive airway epithelial cell targeted with AV.CMV.LacZ. The upper panel labeled +*tr*125 emphasizes staining of airway epithelial cells (arrow), while the lower panel shows *lacZ*-positive cells in the airway and airspace (arrow). Magnification, ×20.

PAGE 41/77 * RCVD AT 8/29/2005 7:17:05 PM [Eastern Daylight Time] * SVR:USPTO-EFXRF-6/26 * DNIS:2738300 * CSID:6504936811 * DURATION (mm-ss):60-28

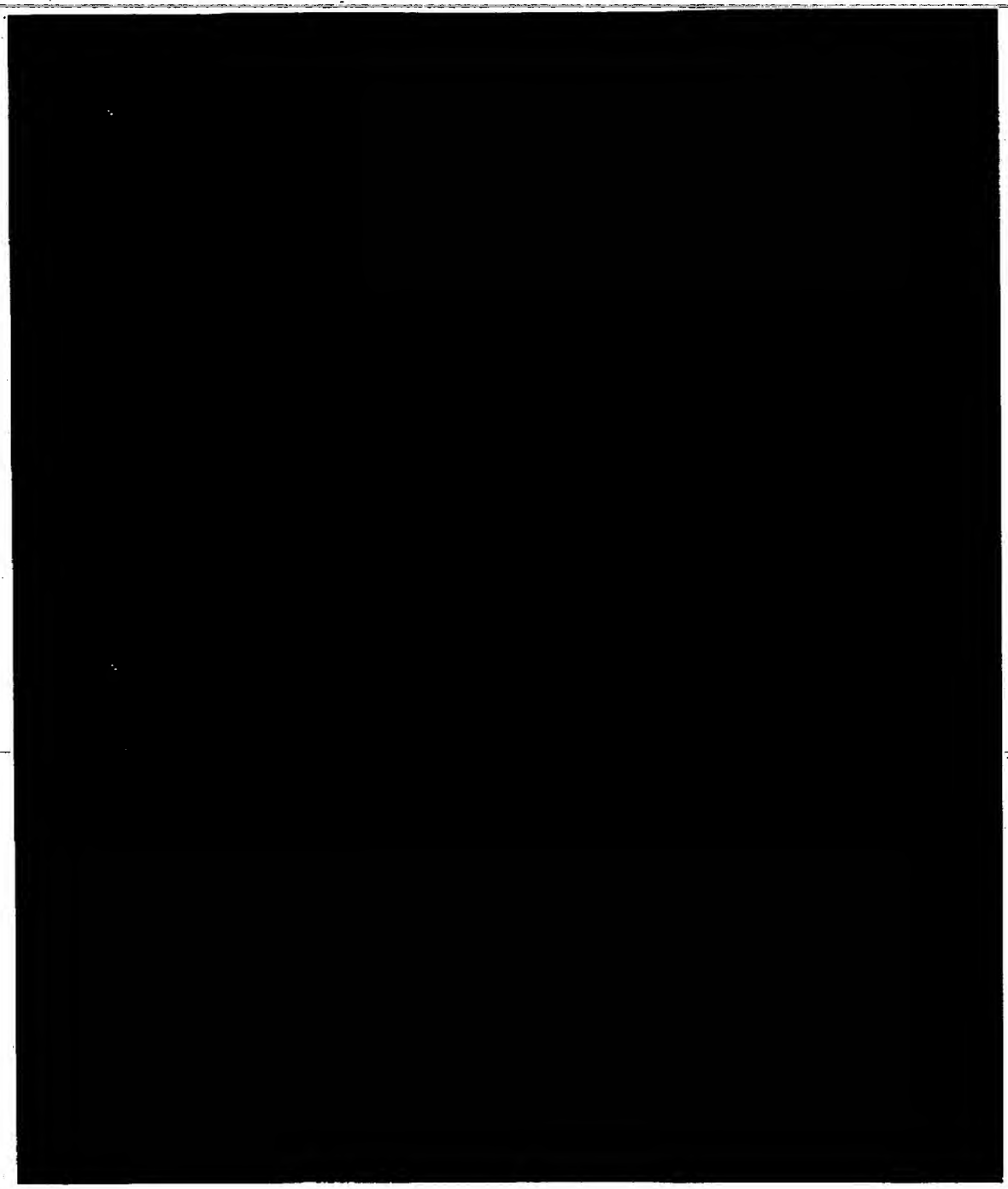

FIG. 10—*Continued.*

limited, however, by the relative inefficiency with which the cell converts the SS genome to a transcriptionally active duplex form. The simplest of models suggests that this conversion requires a cellular DNA polymerase to extend the leading strand from a duplex ITR. Our data suggest that expression of one adenovirus gene, ORF6 of E4, can facilitate this process. The effect of ORF6, whose product is not a DNA polymerase, is likely secondary to another cellular function. Miller and

coworkers have described a variety of agents that enhance rAAV transduction in cultured cells (1). The relevance of this work to our studies is unclear because they did not correlate enhanced transduction with the molecular state of the rAAV genome. However, most of the exogenous agents they found to be effective in enhancement of rAAV transduction were suggested to impact host cell DNA synthesis or repair pathways. This is consistent with a model of enhanced rAAV transduction in which the final common pathway is activation of cellular factors that assemble to convert the rAAV genome to a transcriptionally active duplex form.

ACKNOWLEDGMENTS

We gratefully thank Lorita Dudus and the Cell Morphology and Vector Cores for excellent support.

This work was supported by grants from the NIDDK and the NHLBI of the NIH and the Cystic Fibrosis Foundation.

REFERENCES

1. **Alexander, I. E., D. W. Russell, and A. D. Miller.** 1994. DNA-damaging agents greatly increase the transduction of nondividing cells by adeno-associated virus vectors. J. Virol. 68:8282–8287.
2. **Babiss, L. E., and H. S. Ginsberg.** 1984. Adenovirus type 5 early region 1b gene product is required for efficient shutoff of host protein synthesis. J. Virol. 50:202–212.
3. **Berk, A. J.** 1986. Functions of adenovirus E1A. Cancer Surv. 5:367–387.
4. **Bridge, E., and G. Ketner.** 1989. Redundant control of adenovirus late gene expression by early region 4. J. Virol. 63:631–638.
5. **Bridge, E., S. Medghalchi, S. Ubol, M. Leesong, and G. Ketner.** 1993. Adenovirus early region 4 and viral DNA synthesis. Virology 193:794–801.
6. **Carter, B. J.** 1990. The growth cycle of adeno-associated virus, p. 155–168. *In* P. Tijsser (ed.), Handbook of parvoviruses. CRC Press, Inc., Boca Raton, Fla.
7. **Carter, B. J., C. J. Marcus-Sekura, C. A. Laughlin, and G. Ketner.** 1983. Properties of an adenovirus type 2 mutant, Ad2dl807, having a deletion near the right-hand genome terminus: failure to help AAV replication. Virology 126:505–516.
8. **Ensinger, M. J., and H. S. Ginsberg.** 1972. Selection and preliminary characterization of temperature-sensitive mutants of type 5 adenovirus. J. Virol. 10:328–339.
9. **Fields-Berry, S. C., A. L. Halliday, and C. L. Cepko.** 1992. A recombinant retrovirus encoding alkaline phosphatase confirms clonal boundary assignment in lineage analysis of murine retina. Proc. Natl. Acad. Sci. USA 89: 693–697.
10. **Flotte, T. R., S. A. Afione, R. Solow, M. L. Drumm, D. Markakis, W. B. Guggino, P. L. Zeitlin, and B. J. Carter.** 1993. Expression of the cystic fibrosis transmembrane conductance regulator from a novel adeno-associated virus promoter. J. Biol. Chem. 268:3781–3790.
11. **Gao, G.** Unpublished data.
12. **Halbert, D. N., J. R. Cutt, and T. Shenk.** 1985. Adenovirus early region 4 encodes functions required for efficient DNA replication, late gene expression, and host cell shutoff. J. Virol. 56:250–257.
13. **Hermonat, P. L., M. A. Labow, R. Wright, K. I. Berns, and N. Muzyczka.** 1984. Genetics of adeno-associated virus: isolation and preliminary characterization of adeno-associated virus type 2 mutants. J. Virol. 51:329–339.
14. **Hermonat, P. L., and N. Muzyczka.** 1984. Use of adeno-associated virus as a mammalian DNA cloning vector: transduction of neomycin resistance into mammalian tissue culture cells. Proc. Natl. Acad. Sci. USA 81:6466–6470.
15. **Hirt, B.** 1967. Selective extraction of polyoma DNA from infected mouse cell cultures. J. Mol. Biol. 26:365–369.
16. **Janik, J. E., M. M. Huston, K. Cho, and J. A. Rose.** 1989. Efficient synthesis of adeno-associated virus structural proteins requires both adenovirus DNA binding protein and VA1 RNA. Virology 168:320–329.
17. **Kaplitt, M. G., R. Leone, R. J. Samulski, X. Xiao, D. W. Pfaff, K. L. O'Malley, and M. J. During.** 1994. Long-term gene expression and phenotypic correction using adeno-associated virus vectors in the mammalian brain. Nature Genet. 8:148–154.
18. **Kotin, R. M.** 1994. Prospects for the use of adeno-associated virus as a vector for human gene therapy. Hum. Gene Ther. 5:793–801.
19. **Kotin, R. M., M. Siniscalco, R. J. Samulski, X. Zhu, L. Hunter, C. A. Laughlin, S. McLaughlin, N. Muzyczka, M. Rocchi, and K. I. Berns.** 1990. Site-specific integration by adeno-associated virus. Proc. Natl. Acad. Sci. USA 87:2211–2215.
20. **Kozarsky, K. F., and J. M. Wilson.** 1993. Gene therapy: adenovirus vectors. Curr. Opin. Genet. Dev. 3:499–503.
21. **LaFace, D., P. Hermonat, E. Wakeland, and A. Peck.** 1988. Gene transfer into hematopoietic progenitor cells mediated by an adeno-associated virus vector. Virology 162:483–490.
22. **Lehkowski, J. S., M. M. McNally, T. B. Okarma, and L. B. Lerch.** 1988. Adeno-associated virus: a vector system for efficient introduction and integration of DNA into a variety of mammalian cell types. Mol. Cell. Biol. 8:3988–3996.
23. **McLaughlin, S. K., P. Collis, P. L. Hermonat, and N. Muzyczka.** 1988. Adeno-associated virus general transduction vectors: analysis of proviral structures. J. Virol. 62:1963–1973.
24. **McPherson, R. A., H. S. Ginsberg, and J. A. Rose.** 1982. Adeno-associated virus helper activity of adenovirus DNA binding protein. J. Virol. 44:666–673.
25. **Myers, M. W., C. A. Laughlin, F. T. Jay, and B. J. Carter.** 1980. Adenovirus helper function for growth of adeno-associated virus: effect of temperature-sensitive mutants in adenovirus early region 2. J. Virol. 35:65–75.
26. **Pina, M., and M. Green.** 1965. Biochemical studies on adenovirus multiplication. IX. Chemical and base composition of 28 human adenoviruses. Proc. Natl. Acad. Sci. USA 54:547–551.
27. **Rice, S. A., and D. F. Klessig.** 1985. Isolation and analysis of adenovirus type 5 mutants containing deletions in the gene encoding the DNA-binding protein. J. Virol. 56:767–778.
28. **Richardson, W. D., and H. Westphal.** 1983. Adenovirus early gene regulation and the adeno-associated virus helper effect. Curr. Top. Microbiol. Immunol. 109:147–165.
29. **Richardson, W. D., and H. Westphal.** 1984. Requirement for either early region 1a or early region 1b adenovirus gene products in the helper effect for adeno-associated virus. J. Virol. 51:404–410.
30. **Samulski, R. J., L.-S. Chang, and T. Shenk.** 1987. A recombinant plasmid from which an infectious adeno-associated virus genome can be excised in vitro and its use to study viral replication. J. Virol. 61:3096–3101.
31. **Samulski, R. J., L.-S. Chang, and T. Shenk.** 1989. Helper-free stocks of recombinant adeno-associated viruses: normal integration does not require viral gene expression. J. Virol. 63:3822–3828.
32. **Samulski, R. J., and T. Shenk.** 1988. Adenovirus E1B 55-*M*, polypeptide facilitates timely cytoplasmic accumulation of adeno-associated virus mRNAs. J. Virol. 62:206–210.
33. **Samulski, R. J., X. Zhu, X. Xiao, J. D. Brook, D. E. Housman, N. Epstein, and L. A. Hunter.** 1991. Targeted integration of adeno-associated virus (AAV) into human chromosome 19. EMBO J. 10:3941–3950. (Erratum, 11:1228, 1992.)
34. **Sarasin, A.** 1985. SOS response in mammalian cells. Cancer Invest. 3:163–174.
35. **Sarnow, P., P. Hearing, C. W. Anderson, D. N. Halbert, T. Shenk, and A. J. Levine.** 1984. Adenovirus early region 1B 58,000-dalton tumor antigen is physically associated with an early region 4 25,000-dalton protein in productively infected cells. J. Virol. 49:692–700.
36. **Sarnow, P., Y. Ho, J. Williams, and A. J. Levine.** 1982. Adenovirus E1B-55 kD tumor antigen and SV40 large tumor antigen are physically associated with the same 54 kD cellular protein in transformed cells. Cell 28:387–394.
37. **Schlehofer, J. R., M. Ehrbar, and H. zur Hausen.** 1986. Vaccinia virus, herpes simplex virus, and carcinogens induce DNA amplification in a human cell line and support replication of a helper virus dependent parvovirus. Virology 152:110–121.
38. **Shepherd, S. E., J. A. Howe, J. S. Mymryk, and S. T. Bayley.** 1993. Induction of the cell cycle in baby rat kidney cells by adenovirus type 5 E1A in the absence of E1B and a possible influence of p53. J. Virol. 67:2944–2949.
39. **Straus, S. E., H. S. Ginsberg, and J. A. Rose.** 1976. DNA-minus temperature-sensitive mutants of adenovirus type 5 help adenovirus-associated virus replication. J. Virol. 17:140–148.
40. **Tratschin, J.-D., I. L. Miller, and B. J. Carter.** 1984. Genetic analysis of adeno-associated virus: properties of deletion mutants constructed in vitro and evidence for an adeno-associated virus replication function. J. Virol. 51:611–619.
41. **Tratschin, J.-D., I. L. Miller, M. G. Smith, and B. J. Carter.** 1985. Adeno-associated virus vector for high-frequency integration, expression, and rescue of genes in mammalian cells. Mol. Cell. Biol. 5:3251–3260.
42. **Weinberg, D. H., and G. Ketner.** 1983. A cell line that supports the growth of a defective early region 4 deletion mutant of human adenovirus type 2. Proc. Natl. Acad. Sci. USA 80:5383–5386.
43. **Weinberg, D. H., and G. Ketner.** 1986. Adenoviral early region 4 is required for efficient viral DNA replication and for late gene expression. J. Virol. 57:833–838.

43a. **Weitzman, M. D., et al.** Unpublished data.

44. **West, M. H., J. P. Trempe, J. D. Tratschin, and B. J. Carter.** 1987. Gene expression in adeno-associated virus vectors: the effects of chimeric mRNA structure, helper virus, and adenovirus VA1 RNA. Virology 160:38–47.
45. **Wilson, J. M., D. M. Jefferson, J. R. Chowdhury, P. M. Novikoff, D. E. Johnston, and R. C. Mulligan.** 1988. Retrovirus-mediated transduction of adult hepatocytes. Proc. Natl. Acad. Sci. USA 85:3014–3018.
46. **Yakobson, B., T. Koch, and E. Winocour.** 1987. Replication of adeno-associated virus in synchronized cells without the addition of a helper virus. J. Virol. 61:972–981.
47. **Yankinoglu, A. O., R. Heilbronn, A. Burkle, J. R. Schlehofer, and H. zur Hausen.** 1988. DNA amplification of adeno-associated virus as a response to cellular genotoxic stress. Cancer Res. 48:3123–3130.

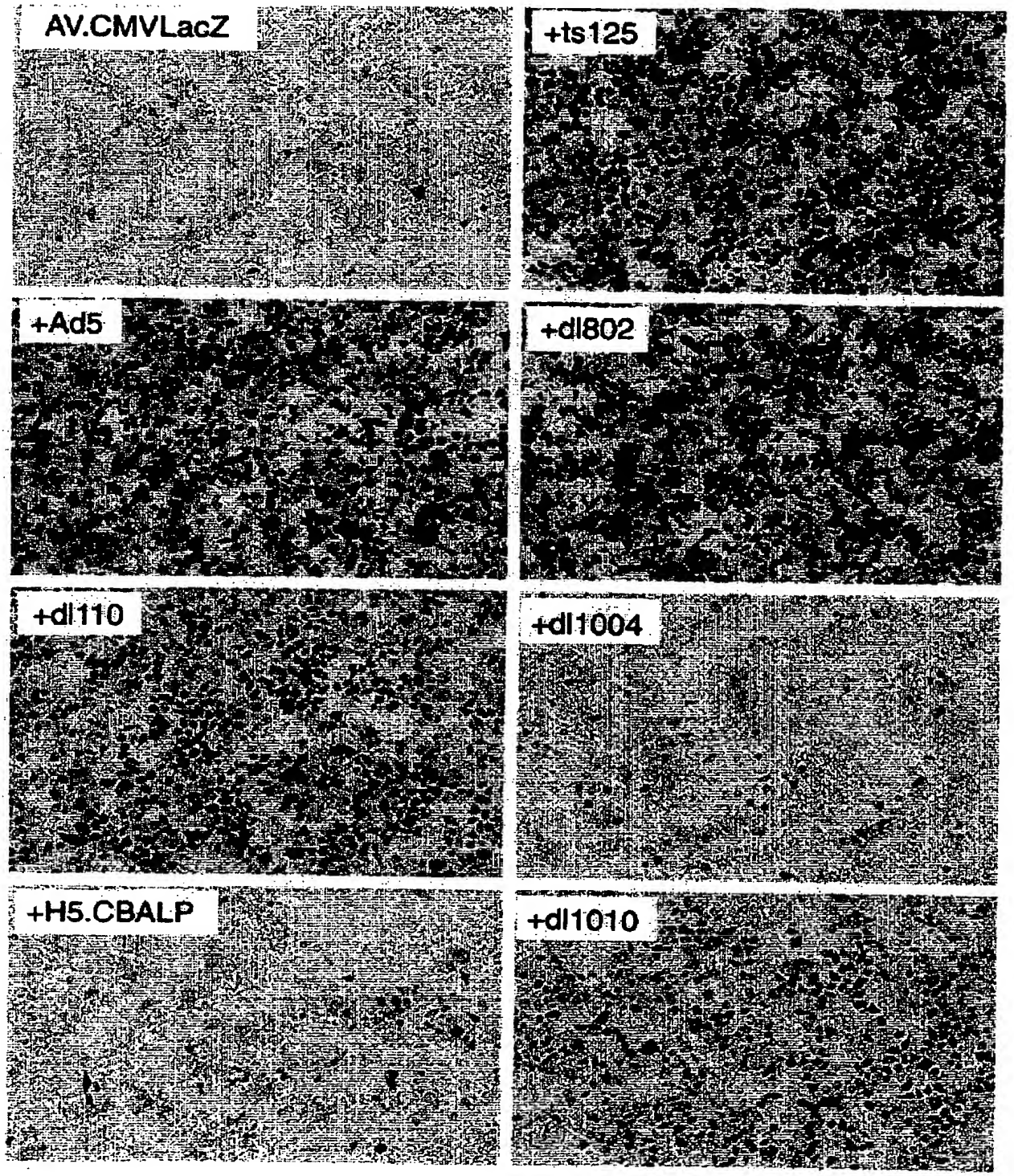
AV.CMVLacZ
+ts125
+Ad5
+dl802
+dl110
+dl1004
+H5.CBALP
+dl1010

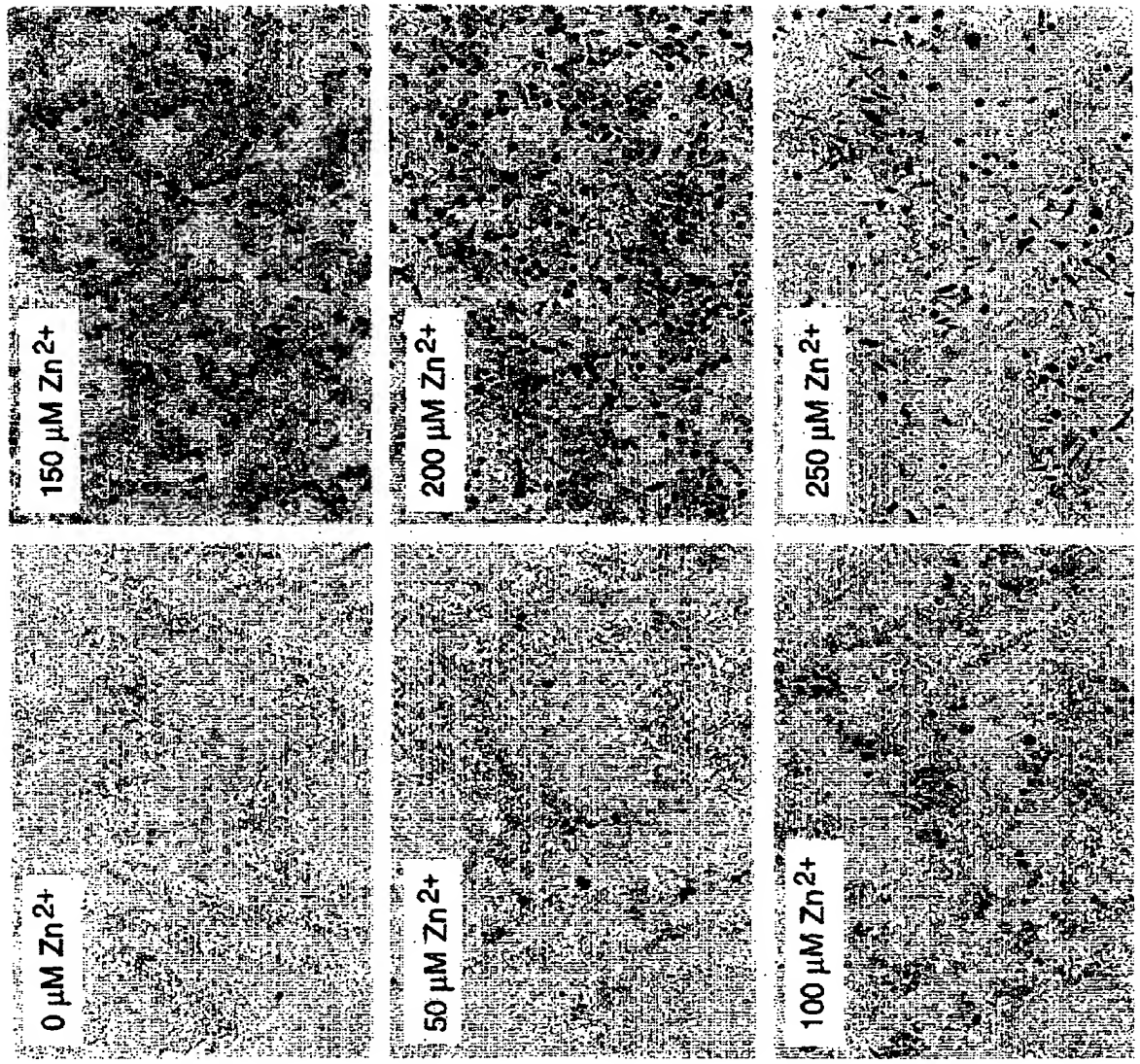
150 µM Zn^{2+}
200 µM Zn^{2+}
250 µM Zn^{2+}
0 µM Zn^{2+}
50 µM Zn^{2+}
100 µM Zn^{2+}

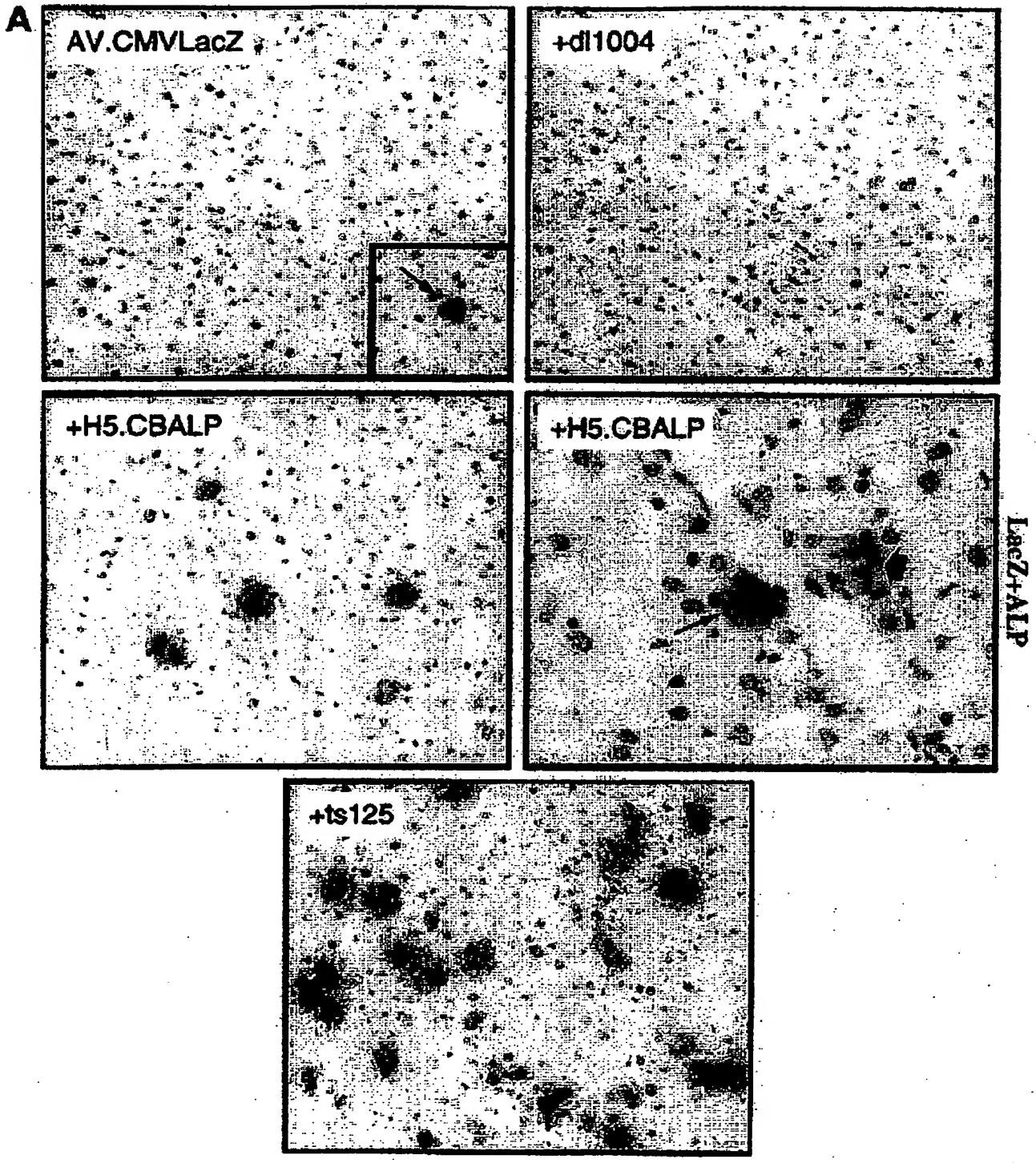
A
AV.CMVLacZ
+dl1004
+H5.CBALP
+H5.CBALP
+ts125
LacZ+ALP

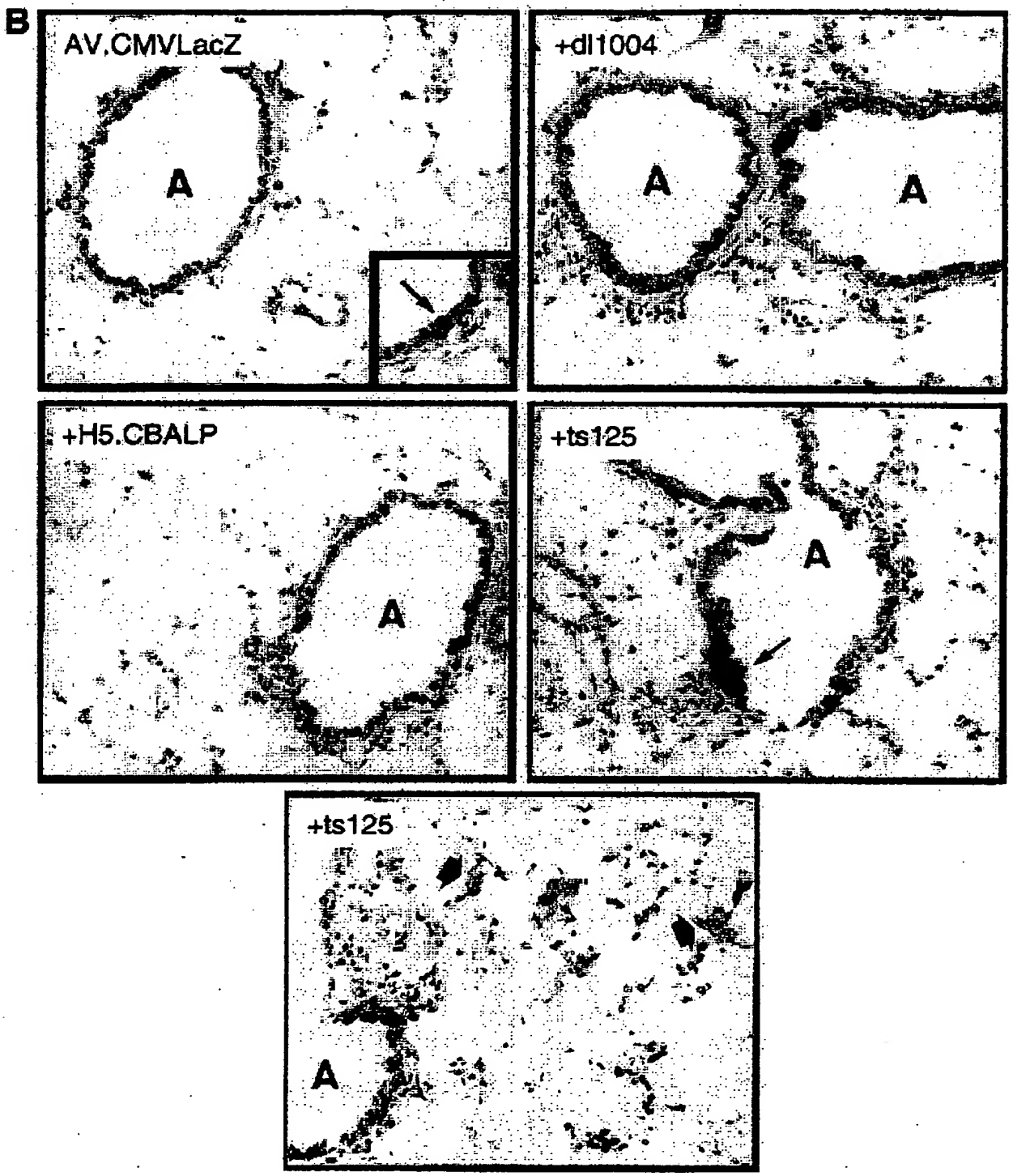
B
AV.CMVLacZ
A
+dl1004
A
A
+H5.CBALP
A
+ts125
A
+ts125
A

Proc. Natl. Acad. Sci. USA
Vol. 91, pp. 10183–10187, October 1994
Genetics

Recombinant adeno-associated virus (rAAV)-mediated expression of a human γ-globin gene in human progenitor-derived erythroid cells

JEFFERY L. MILLER†, ROBERT E. DONAHUE†, STEPHANIE E. SELLERS†, RICHARD JUDE SAMULSKI‡, NEAL S. YOUNG†, AND ARTHUR W. NIENHUIS§¶

†National Heart, Lung and Blood Institute, Bethesda, MD 20892; ‡University of North Carolina, Chapel Hill, NC 27599; and §St. Jude Children's Research Hospital, Memphis, TN 38101

Communicated by Helen M. Ranney, June 28, 1994 (received for review April 1, 1994)

ABSTRACT Effective gene therapy for the severe hemoglobin (Hb) disorders, sickle-cell anemia and thalassemia, will require an efficient method to transfer, integrate, and express a globin gene in primary erythroid cells. To evaluate recombinant adeno-associated virus (rAAV) for this purpose, we constructed a rAAV vector encoding a human γ-globin gene (pJM24/vHS432$^{A}\gamma^{s}$). Its 4725-nucleotide genome consists of two 150-bp AAV inverted terminal repeats flanking the core elements of hypersensitive sites 2, 3, and 4 from the locus control region of the β-globin gene cluster, linked to a mutationally marked $^{A}\gamma$-globin gene ($^{A}\gamma^{s}$) containing native promoter and RNA processing signals. CD34^{+} human hematopoietic cells were exposed to rAAV particles at a multiplicity of infection of 500–1000 and cultured in semisolid medium containing several cytokines. A reverse transcriptase polymerase chain reaction assay distinguished mRNA signals derived from transduced and endogenous human γ-globin genes. Twenty to 40% of human erythroid burst-forming unit-derived colonies expressed the rAAV-transduced $^{A}\gamma^{s}$-globin gene at levels 4–71% that of the endogenous γ-globin genes. The HbF content of pooled control colonies was 26%, whereas HbF was 40% of the total in pooled colonies derived from rAAV transduced progenitors. These data establish that rAAV containing elements from the locus control region linked to a γ-globin gene are capable of transferring and expressing that gene in primary human hematopoietic cells resulting in a substantial increase in HbF content.

Human hemoglobin (Hb) disorders such as thalassemia and sickle-cell disease are a prevalent cause of significant morbidity and mortality worldwide. Therapeutic strategies directed toward genetic modification involve replacement of the defective gene via allogeneic bone marrow transplantation or the addition of a functional gene to the defective bone marrow cells. Characterization of the gene defects in patients with these hemoglobinopathies, as well as extensive characterization of the human β-globin locus in cultured cells and transgenic mice, have made gene transfer potentially feasible (1, 2).

Retroviral vectors have been studied extensively as vehicles for the delivery of globin genes. Successful transduction of cell lines (3–5), hematopoietic progenitor cells (6, 7), and pluripotent hematopoietic stem cells (PHSCs) (8–10) has been achieved using these vectors. Studies in cell lines and transgenic mice have demonstrated that the locus control region (LCR), specific sequences distributed over 20 kb upstream from the β-globin gene cluster, is required for high-level, integration position-independent expression of transferred genes (1, 11, 12). The core elements located within the hypersensitivity sites (HSs) of the LCR have been incorporated into retroviral vectors linked to a globin gene, but such vectors have been genetically unstable. Only recently has limited success been reported in achieving significant globin gene expression using a retroviral vector (13, 14). Low transduction efficiencies of primate PHSCs (15, 16), despite up to nearly 100% efficiency of gene transfer into progenitors (17, 18), remain a persistent problem.

Recently, recombinant adeno-associated virus (rAAV) vectors have emerged as an alternative to retroviral vectors for the delivery and expression of globin genes (19). High-level, cell type expression of rAAV transduced globin genes was shown in hemin-induced K562 cells containing a single copy of the rAAV genome. Precise LCR regulation of the rAAV globin gene transcription in these cells was demonstrated through mutational analysis (20). Using wild-type AAV and rAAV containing the β-galactosidase gene, conclusive evidence for transduction, integration, and expression of a proviral AAV genome in primary hematopoietic cells has been obtained (21). High efficiency transduction of mouse progenitor cells has been suggested with vectors containing a gene that confers resistance to neomycin (22).

In the present study, we report transduction of human hematopoietic progenitor cells with a rAAV vector containing LCR elements linked to a human $^{A}\gamma^{s}$ globin gene with its native promoter, introns, and poly(A) signal. Analysis of erythroid burst-forming unit (BFU-E)-derived colonies provided evidence for rAAV-directed γ-globin gene transcription and HbF production in primary erythroid cells.

MATERIALS AND METHODS

Construction of Plasmid JM24/vHS432$^{A}\gamma^{s}$ and Preparation of rAAV. The human β-globin LCR fragments HS4, HS3, HS2, and the $^{A}\gamma^{s}$ globin gene (23) were subcloned into pUC007 (24). A *Bgl* II/*Sal* I fragment of this construct was subcloned into pUC008 (19), which was then digested with *Nhe* I and ligated to the *Xba* I fragment of pSUB201. Fig. 1*A* depicts the structure of the HS432$^{A}\gamma^{s}$ genome and the legend provides the details of fragments used in its construction. This plasmid construct, pJM24/vHS432$^{A}\gamma^{s}$, was cotransfected with the complementing plasmid, pAAV/ad (25), into 293 cells previously infected with adenovirus type 5 to make the rAAV, vHS432$^{A}\gamma^{s}$. Preparation of cell lysates containing rAAV, Hirt extracts, and Southern blot analyses are described elsewhere (19, 25, 26). All rAAV cell lysates were concentrated by ultrafiltration using a model 8400 stir cell apparatus and XM300 membrane (Amicon) prior to heat inactivation of adenovirus (56°C, 30 min). The final volume of concentrated cell lysate was ≈1 ml per 10-cm^{2} dish of 293 cells used for cotransinfection.

The publication costs of this article were defrayed in part by page charge payment. This article must therefore be hereby marked "*advertisement*" in accordance with 18 U.S.C. §1734 solely to indicate this fact.

Abbreviations: rAAV, recombinant adeno-associated virus; LCR, locus control region; RT-PCR, reverse transcriptase polymerase reaction; BFU-E, erythroid burst-forming unit; HS, hypersensitivity site; DPP, DNase-protected particle.

¶To whom reprint requests should be addressed at: St. Jude Children's Research Hospital, 332 N. Lauderdale, Memphis, TN 38101.

PAGE 48/77 * RCVD AT 8/29/2005 7:17:05 PM [Eastern Daylight Time] * SVR:USPTO-EFXRF-6/26 * DNIS:2738300 * CSID:6504936811 * DURATION (mm-ss):60-28

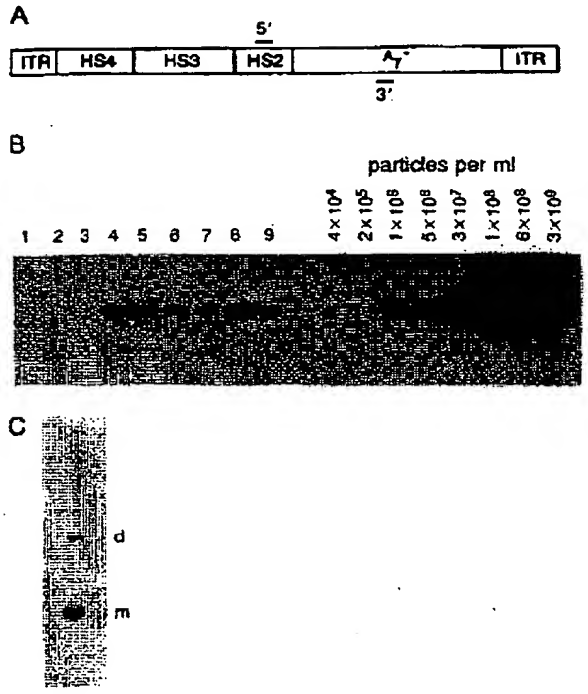

FIG. 1. Characterization of vHS432$^{A}\gamma^{*}$. (*A*) Schematic of the rAAV genome and relative position of the primers used to estimate the particle titer of the cell lysate preparations. The pSUB201-derived AAV inverted terminal repeats (ITR) flank core regions of the human β-globin LCR: HS4 (GenBank, 958–1714 bp), HS3 (GenBank, 4281–5179 bp), HS2 (GenBank, 8486–8860 bp), and the mutationally marked human $^{A}\gamma^{*}$ gene (23). (*B*) DPP titer of vHS432$^{A}\gamma^{*}$. Bands represent the 665-bp PCR product spanning the region defined by the 5' and 3' primers shown above. The PCR templates were as follows: lane 1, H_2O blank; lane 2, mock adenovirus-infected cell lysate from cells cotransfected with pAAV/ad and pJM24/HS432$^{A}\gamma^{*}$; lane 3, vHS432$^{A}\gamma^{*}$ cell lysate extracted with Stat-60 prior to DNase treatment; lanes 4–6, vHS432$^{A}\gamma^{*}$ in triplicate; lanes 7–9, vHS2/$^{A}\gamma^{*}$/neo (19) cell lysate stock (10^4 neo^R per ml) in triplicate. A standard curve generated from pJM24/HS432$^{A}\gamma^{*}$ DNA of known concentration is shown on the right. (*C*) Southern blot analysis of Hirt extracted DNA from cells producing vHS432$^{A}\gamma^{*}$ showing dimer (d) and monomer (m) bands. A 1975-bp fragment (*Apa* I restriction enzyme fragment of the parent plasmid) containing the $^{A}\gamma^{*}$ globin gene was used as a probe.

Assay for Estimation of rAAV Particle Titer. A variation of previous assays (25) was used to estimate particle number. Twenty microliters of rAAV cell lysate was incubated (37°C, 1 hr) with 200 units of DNase (Boehringer Mannheim) in a final volume of 200 μl (20 mM Tris·HCl, pH 8.0/10 mM $MgCl_2$ buffer). DNase-protected particle (DPP) viral DNA was extracted with RNA STAT-60 (Tel-Test, Friendswood, TX) using the manufacturer's protocol with a final volume of 20 μl. This technique favors recovery of the low molecular weight single-stranded DNA genome of the rAAV vector particles. The polymerase chain reaction (PCR) generated a 665-bp fragment spanning the junction between HS2 and the $^{A}\gamma^{*}$ globin gene in HS432$^{A}\gamma^{*}$ (Fig. 1*A*). PCR conditions were as follows: 23 cycles; 95°C/1 min, 58°C/1 min, 72°C/1.5 min; 5' primer, 5'-TCTCAGCCTAGAGTGATGAC; 3' primer, 5'-ATAGTAGCCTTGTCCTCCTC.

Preparation and Transduction of CD34^{+} Selected Progenitor Cells. Human peripheral blood mononuclear cells were obtained by hemapheresis of a patient with Hb SS disease after informed consent under a protocol approved by Institute Review Board of the National Heart, Lung and Blood Institute. A Ceprate kit (CellPro, Bethell, WA) was used for CD34^{+} cell enrichment according to the manufacturer's protocol. One thousand CD34^{+} selected cells were exposed to 500 μl of rAAV-containing cell lysate (10^6 particles) in a total volume of 1000 μl of tissue culture medium (Dulbecco's modified Eagle medium, 15% fetal calf serum, 50 ng of interleukin 6 per ml, and 100 ng of stem cell factor per ml). One transduction (see Fig. 3) was done in tissue culture medium without growth factors. After an overnight exposure with gentle rocking at 37°C in 5% CO_2, the cells were resuspended to 10^3 cells per ml and plated at 1000 cells per plate in methylcellulose containing growth factors (10 ng of granulocyte/macrophage colony-stimulating factor per ml, 10 ng of interleukin 3 per ml, 100 ng of stem cell factor per ml, and 5 units of erythropoietin per ml). Cells were incubated at 37°C in 5% CO_2 for 13–19 days prior to analysis of progenitor-derived colonies.

Gene Transfer and Expression. RNA extraction from individual colonies was performed by placing each colony (<10 μl of methylcellulose) in 250 μl of Stat-60 (Tel-Test) according to the manufacturer's protocol and maintained at −70°C until reverse transcriptase PCR (RT-PCR) analysis. RT-PCR reagents and the thermal-cycler were obtained from Perkin–Elmer. The reverse transcriptase reactions (42°C/30 min,

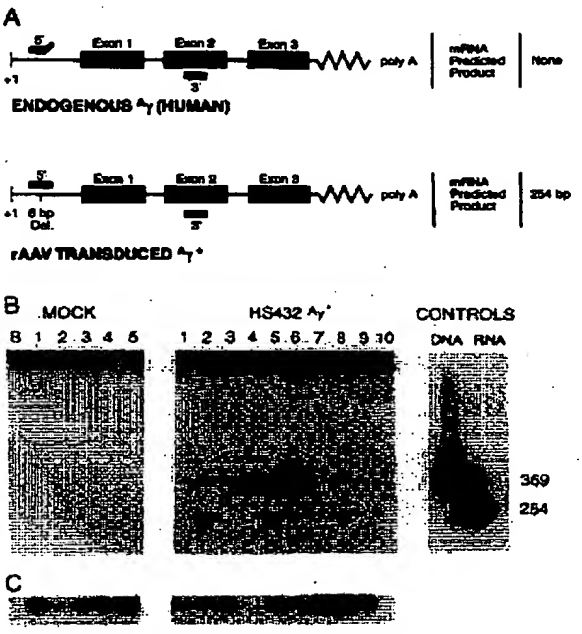

FIG. 2. Analysis of RNA from colonies derived from human BFU-E transduced with rAAV, vHS432$^{A}\gamma^{*}$. (*A*) Schematic of RT-PCR assay showing position of the PCR primers. Primer–template mismatches with the 5' primer that spanned the 6-bp deletion in the $^{A}\gamma^{*}$ genes prevented efficient amplification of the endogenous gene or mRNA sequences; intron-spanning primers (5', 5'-TCGCTTC-TGGAACGTCTATC; 3', 5'-CACCTTCTTGCCATGTGCCT) differentiate $^{A}\gamma^{*}$ DNA and RNA. Conversely, the 5' primer specific for the endogenous gene included nucleotides at its 3' end that are part of the 6-bp deletion in the $^{A}\gamma^{*}$-globin gene. (*B*) Analysis of 5 mock and 10 vHS432$^{A}\gamma^{*}$ transduced sickle-cell BFU-E-derived colonies harvested after 14 days in methylcellulose. Lane B is the minus template control. Other controls on far right show predicted DNA (369 bp) and RNA (254 bp) signals. (*C*) PCR product derived from 10% of the cDNA template using primers specific for the endogenous γ-globin genes. RT-PCR conditions are given in the text.

6504936811 8/29/2005 4:17 PM PAGE 50/077 Fax Server

95°C/5 min) were performed as single or double volume mixtures, followed by single or matched PCRs (35 cycles; 95°C/1 min, 60°C/1 min) using the appropriate primers. RNA-derived PCR mixtures, which included [^{32}P]CTP, were electrophoresed on 10% denaturing polyacrylamide gels and dried prior to autoradiogram or PhosphorImager analysis. Comparison of the polyacrylamide gel band intensities was made using the densitometry function of a PhosphorImager (Molecular Dynamics). High-performance liquid chromatography HPLC was used for Hb analysis as described (27).

RESULTS

Virus Production. Using the DPP titering assay, the concentration of rAAV genome in the cell lysate preparations was reproducibly estimated (Fig. 1*B*). DNase treatment was effective in eliminating amplification of plasmid and genomic DNA in the cell lysates. Control lysate samples were prepared from 293 cells cotransfected with the pJM24/vHS432$^{A}\gamma^{s}$ and pAAV/AD plasmids but not infected with adenovirus. The PCR amplified signals from these mock cell lysates were reduced to <1% of untreated samples by DNase treatment (Fig. 1*B*, lane 2). When the rAAV-containing lysates were extracted with Stat-60 (the commercial product contains phenol) prior to DNase treatment, the rAAV particle genomes were not protected by their capsids from DNase and therefore the signal was eliminated (Fig. 1*B*, lane 3). A standard curve was generated from the band intensities of PCR products amplified from serial dilutions of plasmid DNA, and the DPP titer of vHS432$^{A}\gamma^{s}$ lysates was estimated at 1–5 × 10^{6} particles per ml. Stocks of vHS2/$^{A}\gamma^{s}$/neo^{R} (Fig. 1*B*, lanes 7–9) were estimated to have a titer of 10^{6} physical particles per ml by the DPP assay; these stocks had an infectious unit titer of ≈10^{4} neo^{R} colonies on Detroit 6 cells in a standard biological titering assay (19). Thus, the DPP titering assay is consistent with previous data that predict a particle-to-infectious unit ratio of ≥100 (25, 28, 29). Southern blot analysis of Hirt extracted DNA demonstrated the replicated forms of the vHS432$^{A}\gamma^{s}$ genome in 293 cells 24 hr after transduction (Fig. 1*C*).

rAAV Transduction of Human BFU-E and $^{A}\gamma^{s}$ Gene Expression in Progenitor-Derived Colonies. The results of the DPP assay and knowledge that the ratio of physical-to-infectious titers of the vector preparations was ≥100 allowed us to establish transduction conditions in which the estimated ratio of infectious particles to target cells was ≈5–10. Preliminary experiments indicated that vector DNA in medium or associated with colonies compromised attempts to estimate transduction frequency of clonogenic progenitors by DNA-based PCR methodologies (data not shown; Fig. 2*B*). $^{A}\gamma^{s}$ DNA signals of variable intensity were present in 80% of the transduced BFU-E-derived colonies. Because of these fluctuations, we relied on RT-PCR to evaluate gene transfer and expression. Using intron-spanning primers, the RT-PCR assay was designed to distinguish rAAV-derived $^{A}\gamma^{s}$ RNA and DNA. The nucleic acids derived from the endogenous globin genes were not amplified above background levels with the primers specific for the transduced $^{A}\gamma^{s}$ globin gene (Fig. 2*B*). Distinct $^{A}\gamma^{s}$ RNA-derived signals were found in 20–30% of the colonies derived from erythroid progenitors exposed to HS432$^{A}\gamma^{s}$ rAAV (Figs. 2 and 3), while no $^{A}\gamma^{s}$ RNA-derived signal was present in a similar number of nonerythroid colonies (data not shown). In the mRNA positive BFU-E-derived colonies, comparison of RT-PCR signals from the rAAV $^{A}\gamma^{s}$ and endogenous genes (Fig. 2*B*) suggested that $^{A}\gamma^{s}$ globin gene expression was around 10% that of the total γ-globin expression. Hence, our initial data provided strong evidence for rAAV transduced $^{A}\gamma^{s}$ gene transcription in BFU-E exposed to the HS432$^{A}\gamma^{s}$ vector. A DNA-derived signal of variable intensity was observed on analysis in a larger proportion of colonies; in some or all cases, this signal may represent contamination by viral DNA, as the physical multiplicity of infection was ≈1000.

These results have been reproduced in several separate analyses of vHS432$^{A}\gamma^{s}$ transduced peripheral CD34^{+} progenitor cells; a second experiment is shown in Fig. 3. In the 19 erythroid colonies analyzed, equal amounts of cDNA were taken from a common RT reaction mixture and used as template for the PCR amplification of endogenous and $^{A}\gamma^{s}$ signals. As shown, evidence of transcription from the transduced rAAV genome was present in 7 of 19 colonies analyzed, and the $^{A}\gamma^{s}$ RNA-derived signals had intensities from 4% to 71% of those amplified using the same RT reaction mixture with primers specific for cDNA from the four endogenous γ-globin genes. The range of rAAV-derived and endogenous signal intensities in Figs. 2 and 3 supports their use in providing a semiquan-

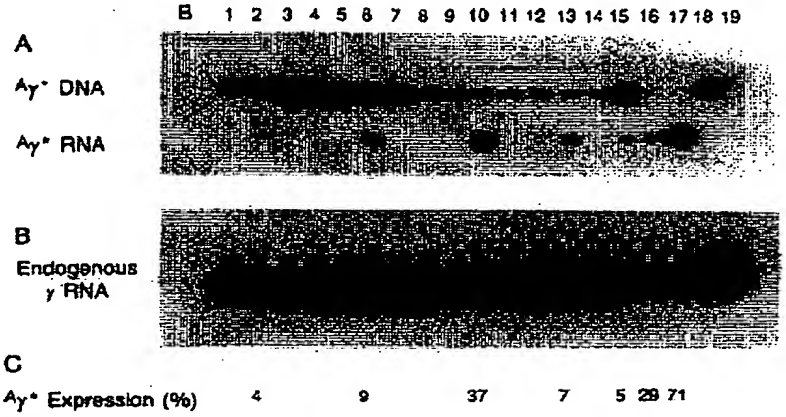

FIG. 3. Comparison of RT-PCR signals for the transduced and endogenous γ-globin genes. After completion of the RT reaction, the reaction mixture for each individual colony was split into equal volumes and used as matched templates for the primer-specific PCRs. (*A*) Analysis of 19 sickle-cell BFU-E-derived colonies using the assay and $^{A}\gamma^{s}$-specific primers shown in Fig. 2. Identification of each signal appears on the far left. (*B*) PCR products using the endogenous γ-globin specific primers. (*C*) Percent expression from the rAAV transduced $^{A}\gamma^{s}$ gene compared to the γ-globin genes in that colony. Each lane contained an equal volume of the PCR mixture. The gels containing endogenous and $^{A}\gamma^{s}$ generated signals were then exposed for identical times using a single PhosphorImager screen. Polyacrylamide gel electrophoresis on each sample was performed twice and signals were averaged. The percentages were calculated by multiplying the ratio of the $^{A}\gamma^{s}$ RNA-derived signal intensity and the endogenous γ-globin RNA signal intensity by 100.

PAGE 50/77 * RCVD AT 8/29/2005 7:17:05 PM [Eastern Daylight Time] * SVR:USPTO-EFXRF-6/26 * DNIS:2738300 * CSID:6504936811 * DURATION (mm-ss):60-28

titative estimate of the level of rAAV transduced gene expression. The small amount of RNA available from each colony precluded other quantitative assays of transcriptional activity.

Quantitation of Hb Expression in BFU-E-Derived Colonies. The results of HPLC analysis of the Hbs in colony erythroblasts are shown in Fig. 4. The Hb composition of pooled colonies (>50 erythroid) derived from 1000 mock transduced progenitors was 26% HbF and 70% HbS, consistent with the high level of HbF production in erythroblasts derived from adult BFU-E when cultured in fetal serum containing medium (30). The HbF concentration in pooled colonies derived from an equal number of BFU-E transduced with vHS432$^{A}\gamma^{s}$ was 40% of the total. Since less than one-half of the colonies were expressing the vHS432$^{A}\gamma^{s}$ transferred gene, these data suggested a substantial increase in fetal Hb content in erythroblasts derived from transduced progenitors.

DISCUSSION

These experiments were undertaken to evaluate the ability of rAAV to introduce a globin gene into primitive human hematopoietic cells and to express the gene in maturing erythroblasts without selection for cells in which the vector genome had been successfully introduced. The $^{A}\gamma^{s}$-globin gene linked to the core elements of three of the HSs from the β-globin gene cluster LCR was expressed at a level that approximated that of an endogenous globin gene. The conditions established for successful transduction of erythroid progenitors are potentially applicable to the *ex vivo* transduction of repopulating hematopoietic stem cells. Our results suggest that rAAV vectors may be useful for gene therapy of human Hb disorders.

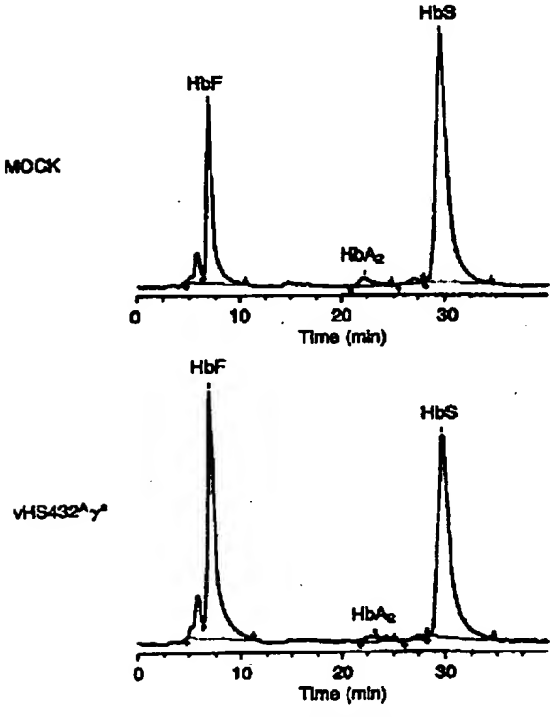

FIG. 4. Hb composition of colonies derived from peripheral blood BFU-E of a patient with sickle-cell anemia. One thousand control (MOCK) or vHS432$^{A}\gamma^{s}$-transduced cells were plated in methylcellulose. After 19 days, the colonies (>50 erythroid) from the control or experimental plates were pooled, washed, and analyzed on cation-exchange HPLC. Major Hb species are identified by their time of elution. The integrated area under each peak provided an estimate of the Hb composition of each pool of colonies. The HbF content was 26% in the control (MOCK) and 40% in the colonies derived from progenitors transduced with vHS432$^{A}\gamma^{s}$.

Our prior work had established that a rAAV vector (vHS2/$^{A}\gamma^{s}$/neo^{R}) containing the $^{A}\gamma^{s}$-globin gene linked to the core region of HS2 and the neo^{R} gene was able to transfer and express the globin gene in clones of human erythroleukemia cells selected in G418 (19, 20). The transferred globin gene was expressed at levels equivalent to that of an endogenous globin gene. One unrearranged, integrated proviral genome was present in most drug-selected human erythroleukemia cell clones, but rearrangement of the integrated vector genome occurred in a minority of such clones (20). This vector, however, worked poorly in primary hematopoietic cells, rearranging if selection was imposed or expressing the transferred globin gene at low levels in those colonies derived without drug selection (J.L.M., A. Moulten, and A.W.N., unpublished observations). By eliminating the drug-resistance gene and adding the core elements of HS3 and HS4, we have now derived a vector that appears to be more stable and to express the transferred globin gene at high levels in primary erythroid cells. The ability to introduce the vector genome without selection is a particularly attractive feature for gene therapy targeted to stem cells.

A larger proportion of colonies was positive for the vector genome than exhibited expression of the transferred globin gene when assayed by PCR analysis (Figs. 2 and 3). It is possible that some progenitors incorporated the vector genome without expressing it. However, results obtained in transgenic mice suggest that the combination of HS2, HS3, and HS4 should be sufficient to ensure high-level expression of a linked globin gene even in single-copy integrants (11, 12). Rearrangement of the vector genome with loss of regulatory sequences may have occurred in a proportion of clones (20). An alternative explanation is that residual vector DNA gave an artificially high or false signal in DNA from some colonies. Without appropriate controls and careful quantitative comparison of the PCR amplified signals from a transferred and endogenous gene (21), DNA-based PCR may be unreliable in estimating rAAV-directed gene transfer efficiencies. The rAAV viral genome consists of complementing single-stranded DNAs that are very efficiently amplified by PCR so that even a low level of contamination may give a false-positive signal. For this reason, we have relied on the RT-PCR as a more accurate method of estimating rAAV transduction efficiency.

rAAV vectors have been shown to transfer and express exogenous genes in several cell types (31, 32), including respiratory epithelium (29, 33, 34) and brain cells *in vivo* (R.J.S., unpublished observations). As we have shown for primary hematopoietic cells, efficient transduction requires a high multiplicity of infection to ensure an excess of biologically active vector particles over the target cell population. Stable expression of the gene for the cystic fibrosis transmembrane conductance regulator (CFTR) in rabbit respiratory epithelium *in vivo* for >6 months is most consistent with integration of the rAAV proviral genome (34), and, indeed, rAAV vector-mediated integration of the CFTR gene in nonselected cell lines *in vitro* has been documented by Southern blot analysis (33). Although we have not formally demonstrated integration of the vHS432$^{A}\gamma^{s}$ proviral genome in erythroid colonies, the high level of transferred globin gene expression over 13–19 days in maturing colonies composed of >1000 cells derived from a single transduced progenitor is most consistent with proviral integration at an early stage in colony development. Successful transduction of hematopoietic long-term culture initiating cells by other investigators using a rAAV vector containing the neo^{R} gene with derivation

6504936811 8/29/2005 4:17 PM PAGE 52/077 Fax Server

of G418-resistant progenitors over 5 weeks in culture also supports the ability of rAAV to integrate the proviral genome in primitive hematopoietic cells (35). Transduction and integration of a rAAV into murine repopulating cells were suggested by detection of the proviral sequences in hematopoietic tissues by PCR analysis 12 weeks posttransplantation (36). These data all support the potential of rAAV for stem cell-targeted gene therapy. However, a formal evaluation of integration efficiency in cultured cells and demonstration and expression of the rAAV genome in hematopoietic cells from long-term transplant recipients will be necessary.

Of interest in our experiments is the increased HbF content in progenitor-derived erythroid colonies following rAAV-mediated transfer of the $^A\gamma^s$-globin gene. Many factors, including the source of progenitor cells, the culture medium and conditions in which they are allowed to differentiate, and the concerted expression of endogenous and transduced globin genes, may contribute to the total HbF content in these cells. Introduction and high-level expression of an exogenous γ-globin gene into erythroblasts of patients with sickle-cell anemia are likely to cause unbalanced globin chain synthesis and a relative excess of non-α chains. Under these conditions, the Hb composition of erythrocytes should reflect the relative affinity of the β^S and γ chains for the limiting number of α chains. The γ-globin chain preferentially associates with α-globin when in competition with the β^S subunit (37). As predicted from these observations, rAAV-mediated expression of the γ-globin gene in colony erythroblasts increased HbF content at the apparent expense of HbS.

The utility of rAAV vectors for gene therapy of Hb disorders can only be established by testing their ability to transfer a globin gene linked to LCR elements into repopulating stem cells with subsequent expression in erythroblasts *in vivo*. The rhesus autologous bone marrow transplantation model (16, 38) will be useful for this experiment, as rhesus hematopoietic progenitors appear to be as efficiently transduced with rAAV as are human cells (21). Although current methods of vector production yield crude preparation with relatively low titer, the experiments reported here have established conditions in which early primate hematopoietic cells can be efficiently transduced. In the future, improved packaging systems and methods of vector purification must be developed if rAAV are to reach clinical application.

We thank Dr. Eitan Fibach and Dr. Griffin Rodgers for performing the HPLC analysis. We credit Dr. Susan Leitman for furnishing the hemapheresed cells and Amgen Biologicals for supplying the growth factors used to culture those cells. We also thank Drs. Christopher Walsh, Paul Ney, David Bodine, and Steven Farina for helpful discussions throughout the course of this work.

1. Stamatoyannopoulos, G. & Nienhuis, A. W. (1994) in *The Molecular Basis of Blood Diseases*, eds. Stamatoyannopoulos, G., Nienhuis, A. W., Majerus, P. & Varmus, H. E. (Saunders, Philadelphia), 2nd Ed., pp. 107–156.
2. McDonagh, K. & Nienhuis, A. W. (1993) in *Hematology of Infancy and Childhood*, eds. Nathan, D. G. & Oski, F. A. (Saunders, Philadelphia), pp. 783–846.
3. Karlsson, S., Papayannopoulou, T., Schweiger, S. G., Stamatoyannopoulos, G. & Nienhuis, A. W. (1987) *Proc. Natl. Acad. Sci. USA* **84**, 2411–2415.
4. Cone, R. D., Weber-Bernarous, A., Baurte, D. & Mulligan, R. C. (1987) *Mol. Cell. Biol.* **7**, 887–897.
5. Lerner, N., Brigham, S., Goff, S. & Bank, A. (1987) *DNA* **6**, 573–582.
6. Bender, M. A., Miller, A. D. & Gelinas, R. E. (1988) *Mol. Cell. Biol.* **8**, 1725–1735.
7. Karlsson, S., Bodine, D. M., Perry, L., Papayannopoulou, T. & Nienhuis, A. W. (1988) *Proc. Natl. Acad. Sci. USA* **85**, 6062–6066.
8. Dzierzak, E. A., Papayannopoulou, T. & Mulligan, R. C. (1988) *Nature (London)* **331**, 35–41.
9. Bender, M. A., Gelinas, R. E. & Miller, A. D. (1989) *Mol. Cell. Biol.* **9**, 1426–1434.
10. Bodine, D. M., Karlsson, S. & Nienhuis, A. W. (1989) *Proc. Natl. Acad. Sci. USA* **86**, 8897–8901.
11. Crossley, M. & Orkin, S. H. (1993) *Curr. Opin. Genet. Dev.* **3**, 232–237.
12. Dillon, N. & Grosveld, F. (1993) *Trends Genet.* **9**, 134–137.
13. Novak, U., Harris, E. A. S., Forrester, W., Groudine, M. & Gelinas, R. (1990) *Proc. Natl. Acad. Sci. USA* **87**, 3386–3390.
14. Plavec, I., Papayannopoulou, T., Maury, C. & Meyer, F. (1993) *Blood* **81**, 1384–1392.
15. Brenner, M. K., Rill, D. R., Holladay, M. S., Heslop, H. E., Moen, R. C., Buschle, M., Krance, R. A., Anderson, W. F. & Ihle, J. N. (1993) *Lancet* **342**, 1134–1137.
16. Bodine, D. M., Moritz, T., Donahue, R. E., Luskey, B. D., Kessler, S. W., Martin, D. I. K., Orkin, S. H., Nienhuis, A. W. & Williams, D. A. (1993) *Blood* **82**, 1975–1980.
17. Bregni, M., Magni, M., Siena, S., Di Nicola, M., Bonadonna, G. & Gianni, A. M. (1992) *Blood* **80**, 1418–1422.
18. Cassel, A., Cottler-Fox, M., Doren, S. & Dunbar, C. E. (1993) *Exp. Hematol.* **21**, 585–591.
19. Walsh, C. E., Liu, J. M., Xiao, X., Young, N. S., Nienhuis, A. W. & Samulski, R. J. (1992) *Proc. Natl. Acad. Sci. USA* **89**, 7257–7261.
20. Miller, J. L., Walsh, C. W., Ney, P. A., Samulski, R. J. & Nienhuis, A. W. (1993) *Blood* **82**, 1900–1906.
21. Goodman, S., Xiao, X., Donahue, R. E., Moulton, A., Miller, J., Walsh, C., Young, N. S., Samulski, R. J. & Nienhuis, A. W. (1994) *Blood*, in press.
22. Zhou, S. Z., Broxmeyer, H. E., Cooper, S., Harrington, M. A. & Srivastava, A. (1993) *Exp. Hematol.* **21**, 928–933.
23. Sorrentino, B. P., Ney, P. A. & Nienhuis, A. W. (1990) *Ann. N.Y. Acad. Sci.* **612**, 141–151.
24. Ney, P. A., Sorrentino, B. P., McDonough, K. T. & Nienhuis, A. W. (1990) *Genes Dev.* **4**, 993–1006.
25. Samulski, R. J., Chang, L. S. & Shenk, T. (1989) *J. Virol.* **63**, 3822–3828.
26. Hirt, B. (1967) *J. Mol. Biol.* **26**, 365–369.
27. Fibach, E., Burke, K. P., Schechter, A. N., Noguchi, C. T. & Rodgers, G. P. (1993) *Blood* **82**, 162–165.
28. Tratschin, J., Miller, I. L., Smith, M. G. & Carter, B. J. (1985) *Mol. Cell. Biol.* **5**, 3251–3260.
29. Flotte, T. R., Solow, R., Owens, R. A., Afione, S., Zeitlin, P. L. & Carter, B. J. (1992) *Am. J. Respir. Cell Mol. Biol.* **7**, 349–356.
30. Constantoulakis, P., Nakamoto, B., Papayannopoulou, T. & Stamatoyannopoulos, G. (1990) *Blood* **75**, 1862–1869.
31. Samulski, R. J., Berns, K. I., Tan, M. & Muzyczka, N. (1982) *Proc. Natl. Acad. Sci. USA* **79**, 2077–2081.
32. Muzyczka, N. (1992) *Curr. Top. Microbiol. Immunol.* **158**, 97–129.
33. Flotte, T. R., Afione, S. A., Solow, R., Drumm, M. L., Markakis, D., Guggino, W. B., Zeitlin, P. L. & Carter, B. J. (1993) *J. Biol. Chem.* **268**, 3781–3790.
34. Flotte, T. R., Afione, S. A., Conrad, C., McGrath, S. A., Solow, R., Oka, H., Zeitlin, P. L., Guggino, W. B. & Carter, B. J. (1993) *Proc. Natl. Acad. Sci. USA* **90**, 10613–10617.
35. Srivastava, A., Zhou, S. Z., Brandt, J. E., Munshi, N. C., Nahreini, P. & Hoffman, R. (1992) *Blood* **80**, Suppl. 1, 178 (abstr.).
36. Yoder, M. C., Kang, L. Y., Zhou, S. Z., Luo, F. & Srivastava, A. (1993) *Blood* **82**, Suppl. 1, 347 (abstr.).
37. Bunn, H. F. (1987) *Blood* **69**, 1–6.
38. Donahue, R. E., Kessler, S. W., Bodine, D., McDonough, K., Dunbar, C., Goodman, S., Agricola, B., Byrne, E., Raffeld, M., Moen, R., Bacher, J., Zsebo, K. M. & Nienhuis, A. W. (1992) *J. Exp. Med.* **176**, 1125–1135.

PAGE 52/77 * RCVD AT 8/29/2005 7:17:05 PM [Eastern Daylight Time] * SVR:USPTO-EFXRF-6/26 * DNIS:2738300 * CSID:6504936811 * DURATION (mm-ss):60-28

Phenotypic Correction of Fanconi Anemia in Human Hematopoietic Cells with a Recombinant Adeno-associated Virus Vector

Christopher E. Walsh,* Arthur W. Nienhuis,‡ Richard Jude Samulski,§ Michael G. Brown,‖ Jeffery L. Miller,* Neal S. Young,* and Johnson M. Liu*

*Hematology Branch, National Heart, Lung, and Blood Institute, National Institutes of Health, Bethesda, Maryland 20892; ‡St. Jude Children's Research Hospital, Memphis, Tennessee 38112; §Department of Pharmacology, University of North Carolina, Chapel Hill, North Carolina 27599; and ‖Oregon Health Sciences University, Portland, Oregon 97201

Abstract

Fanconi anemia (FA) is a recessive inherited disease characterized by defective DNA repair. FA cells are hypersensitive to DNA cross-linking agents that cause chromosomal instability and cell death. FA is manifested clinically by progressive pancytopenia, variable physical anomalies, and predisposition to malignancy. Four complementation groups have been identified, termed A, B, C, and D. The gene for the FA complementation group C, FACC, has been cloned. Expression of the FACC cDNA corrects the phenotypic defect of FA(C) cells, resulting in normalized cell growth in the presence of DNA cross-linking agents such as mitomycin C (MMC). Gene transfer of the FACC gene should provide a survival advantage to transduced hematopoietic cells, suggesting that FA might be an ideal candidate for gene therapy. We demonstrated efficient transduction, expression, and phenotypic correction in lymphoblastoid cell lines derived from FA(C) patients using a recombinant adeno-associated virus (rAAV) vector containing the FACC gene. Molecular characterization of the transduced FACC gene showed an intact unrearranged proviral genome with expression sufficient to normalize cell growth, cell cycle kinetics and chromosomal breakage in the presence of MMC. These observations were extended by testing rAAV transduction in hematopoietic progenitor cells. Peripheral blood CD34+ cells isolated from a FA(C) patient and transduced with rAAV/FACC virus yielded 5–10-fold more progenitor colonies than mock-infected cells, consistent with genetic "rescue" of corrected cells. This is the first demonstration of rAAV gene correction in primary human hematopoietic progenitor cells and has important implications for gene therapy of hematopoietic disorders, specifically FA. (*J. Clin. Invest.* 1994. 94:1440–1448.) Key words: gene therapy • transduction • DNA repair • hematopoiesis

Introduction

Fanconi anemia (FA)[1] is an autosomal recessive disorder characterized by pancytopenia, physical anomalies, and susceptibility to malignancy (1). Most patients are diagnosed in the first decade of life and die as young adults, usually from complications of severe bone marrow failure or, more rarely, from the development of acute leukemia or solid tumors. Therapy is currently limited to allogeneic bone marrow transplantation from a histocompatible sibling, but most patients do not have an appropriate marrow donor (2).

Although the biochemical defect in FA has not been delineated, several lines of evidence implicate a defect of DNA repair. Cells derived from FA patients exhibit a marked increase in the number of spontaneous chromosomal aberrations compared to cells from normal individuals (3, 4). Chromosomal breakage is enhanced when FA cells are incubated in the presence of the DNA cross-linking agents mitomycin C (MMC) and diepoxybutane (DEB) (5, 6). Hypersensitivity to these agents is also reflected by delayed transit through the G2 phase of the cell cycle (7) and by accelerated cell death (8). Chromosomal breakage, abnormal cellular sensitivity to DNA damage, and aberrant cell cycle kinetics are features which link FA nosologically with other DNA repair disorders such as xeroderma pigmentosum, ataxia telangiectasia, and Bloom's syndrome.

Somatic cell fusion methods have established that at least four different genes can cause FA (9). A novel gene termed FACC (Fanconi anemia C complementing) has been identified by functional complementation cloning (10). This gene, which maps to chromosome 9q, shares no homology to any known gene. The FACC protein has a predicted molecular weight of 63 kD. FACC mutations have been identified in ~ 15% of all FA patients (11, 12). In tissue culture, transfected FACC cDNA corrects the phenotypic defect, resulting in normalized cell growth in the presence of MMC or DEB (10). Because FA cells proliferate poorly, transfer of the FACC gene should provide a survival advantage to the gene-corrected FA cells, making this disease an ideal candidate for human gene therapy.

Correction of the Fanconi anemia phenotype provides a unique paradigm to test the novel recombinant adeno-associated virus (rAAV) gene transfer system. The adeno-associated virus (AAV) is a single-stranded DNA parvovirus which requires a helper virus, such as adenovirus, for replication and viral production in permissive cells (for reviews see references 13–15). In the absence of helper virus, AAV can persist as an integrated provirus in susceptible cells. Unlike other viruses, wild-type AAV is unique in that it integrates preferentially at a specific locus on chromosome 19q (16–18). Virtually any mammalian cell line can be productively or latently infected. Despite its broad host range, no disease has been associated with AAV in human or animal populations suggesting that AAV would be an attractive alternative to other established viral vectors.

We previously demonstrated the utility of rAAV as a gene transfer vector for the human gamma globin gene into the eryth-

Address correspondence to Christopher E. Walsh, Hematology Branch, NHLBI, National Institutes of Health, Bethesda, MD 20892.

Received for publication 11 March 1994 and in revised form 2 June 1994.

1. *Abbreviations used in this paper*: AAV, adeno-associated virus; rAAV, recombinant adeno-associated virus; DEB, diepoxybutane; FA, Fanconi anemia; FACC Fanconi anemia C complementing; MMC, mitomycin C.

PAGE 53/77 * RCVD AT 8/29/2005 7:17:05 PM [Eastern Daylight Time] * SVR:USPTO-EFXRF-6/26 * DNIS:2738300 * CSID:6504936811 * DURATION (mm-ss):60-28

roleukemia cell line, K562 (19). Further studies have used this vector to characterize *cis*-acting elements required for globin expression (20). Suppression of HIV-1 gene expression and replication has been documented in lymphoid cell lines using a rAAV vector carrying HIV-1 antisense sequences (21). In addition, rAAV transduction of primary hematopoietic progenitors has been demonstrated using marker genes (22, 22a). The self-selecting growth advantage that the FACC gene confers allows for a functional assay to test gene transduction in FA(C) hematopoietic progenitor cells. We report the first demonstration of rAAV vector transduction of human FA(C) hematopoietic cells and correction of the FACC phenotype.

Methods

Viruses and cells. Human adenovirus type 5 was obtained from the American Type Culture Collection (Rockville, MD). Epstein–Barr virus (EBV) transformed lymphoblast cell lines were generous gifts from Dr. Christopher Mathew (UMDS Guy's Hospital, London, UK) (BD0215) and Dr. Manuel Buchwald (Hospital for Sick Children, Toronto, Canada) (HSC536). All lymphoblasts were grown as previously described (10). Detroit 6 (D6) and 293 cells were maintained as previously described (19).

Plasmids and DNA. Plasmids pAAV/Ad, psub 201, and pUC008/Neo^R have been previously described (19, 23). The plasmid pFAC3 was kindly provided by Dr. Manuel Buchwald. This plasmid contains the FACC cDNA within a pREP4 backbone. pREP4 (Invitrogen, San Diego, CA) contains an expression cassette containing the Rous sarcoma virus (RSV) 3′ LTR and Simian Virus (SV)40 polyadenylation sequences.

Construction of rAAV plasmids. The FACC cDNA was excised from the plasmid pFAC3 after digestion with SalI. This fragment was then subcloned into the SalI site of pUC19 (New England Biolabs, Beverly, MA). To remove the FACC 3′ untranslated region, the pUC19 intermediate was digested with restriction enzymes XbaI (located at the stop codon of the FACC coding region) and NheI. These fragment ends were religated within the pREP4 polylinker, with the trimmed FACC lying between the RSV promoter and the SV40 polyadenylation site. The trimmed version of the FACC cDNA within the expression cassette derived from pREP4 was then subcloned into the SalI site of pUC008/Neo^R. The RSV-driven FACC cDNA and the TK-driven neomycin phosphotransferase gene were then excised from pUC008/Neo^R with NheI and inserted into the XbaI site of psub201 to create pAAV/FACC/Neo^R.

Generation of rAAV. Recombinant AAV were generated as previously described (19). Dishes (10 cm^2) containing 60–80% confluent 293 cells were infected with adenovirus type 5. rAAV virions were generated by subsequent calcium phosphate cotransfection of 10 μg of plasmid pAAV/FACC/Neo^R and 10 μg of helper plasmid (pAAV/Ad). Cells were harvested 40 h posttransfection, frozen, and thawed four times, heat-treated (56°C, 1 h) to inactivate adenovirus, and centrifuged to remove cellular debris.

Cell lysates were titered on D6 cells in the presence of 0.5 mg/ml Geneticin (GIBCO BRL, Grand Island, NY). Drug resistant colonies were isolated at 10–14 d. The rAAV titer was calculated from the number of resistant colonies and averaged 10^4–10^5 Neo^R infectious particles per milliliter.

rAAV Infection of EBV-transformed lymphoblasts. Lymphoblasts (1×10^5) were infected with cell lysate (3×10^4 Neo^R infectious particles). Cells were harvested after 2 d and grown in 15% fetal calf serum/RPMI with glutamine and antibiotics. Cells were passaged for 10 d and then resuspended at 2×10^5 cells per ml in the presence of active G418 (0.2–0.6 mg/ml). Noninfected lymphoblasts yielded no viable cells following drug selection. Drug-resistant cells were maintained in media containing G418 for 3–4 wk after infection.

Lymphoblast mitomycin C (MMC) sensitivity. Cellular sensitivity to mitomycin C (Calbiochem-Behring Corp., San Diego, CA) was assayed by plating cells at a density of 2×10^5 per ml in 24-well plates. Increasing concentrations of MMC were added, and after a 5-d incubation, cellular viability was assayed via Trypan blue exclusion. Each sample was performed in quadruplicate.

Cytogenetic analysis of transduced lymphoblasts. Lymphoblast cultures were analyzed for cytogenetic breakage and radial formation by exposure to MMC (40 ng/ml final) for 2 d in the dark. Cultures were harvested after a 1-h exposure to 0.25 μg/ml colcemid. After a 10 min treatment with 0.075 M KCl, the cells were fixed with a 3:1 mixture of methanol: acetic acid. Slides were prepared using wet slides, air dried, and stained with Wright's stain. 50 metaphase figures from each culture were scored for obvious breaks, gaps larger than a chromatid width, and for radial formations.

Cell cycle analysis of transduced lymphoblasts. Lymphoblasts were plated at 2×10^5/ml and grown overnight. Either phosphate-buffered saline (PBS) or MMC (100 nM final concentration) was added and cells incubated for 24 h. A total of 1×10^6 cells were resuspended in 1.0 ml PBS with 2.0 ml cold 70% ethanol and incubated on ice for 30 min. Cells were centrifuged and cell pellet incubated with propidium iodide (20 μg/ml)/RNase A (0.04 mg/ml) solution for 20 min at room temperature before analysis on an Epics Elite (Coulter Electronics Inc., Hialeah, FL) flow cytometer. Data was analyzed using the Multicycle software program based on the polynomial S-phase algorithm (Phoenix Flow Systems, San Diego, CA).

Southern blot analysis of genomic DNA. Genomic DNA digestion and Southern transfer was performed using ammonium acetate buffer (24) and Hybond N+ (Amersham Corp., Arlington Heights, IL) nylon filters. Blots were probed with a PstI (197 bp) P^{32}-labeled fragment of the neomycin phosphotransferase gene, Neo^R (Stratagene, La Jolla, CA). Filters were washed to a final stringency of 2× SSC at 65°C for 1 h.

Analysis of lymphoblast FACC expression. RNA was extracted from transduced lymphoblasts as described (19). 1.0 μg of RNA was reverse transcribed using the RNA PCR reagent kit (Perkin-Elmer Corp., Norwalk, CT). The cDNA sample was amplified using standard conditions including P^{32}dCTP. Primers specific for the endogenous FACC gene were: 5′ CAC AGA CTA TGG TCC AGG TGA AGG 3′ and 5′ ACC AGG AGT ACC GAA GCT CAC TTG 3′. Primers specific for the transduced FACC gene were: 5′ AAT TAC TGA TGT CGG CAG CCG AAC 3′ and 5′ TTA TCA TGT CTG GAT CCG GCC TTG 3′. The amplification conditions used were: 95°C for 2 min followed by 30 cycles at 95°C for 30 s, 55°C for 30 s, 72°C for 1 min, and then a 72°C extension for 8 min. PCR products were separated on a 5% polyacrylamide gel, dried, and autoradiographed.

Metabolic labeling and immunoprecipitation. [^{35}S]Methionine (100 μCi, 1,000 Ci/mmol) (Amersham Corp.) labeling of lymphoblasts (1×10^7 cells) was performed over 3 h and cells extracted in phosphate buffered saline, pH 7.5, containing 1% (vol/vol) Triton-X-100, aprotinin (1 μg/ml, ICN Biomedicals, Inc., Aurora, OH), leupeptin (1 μg/ml, ICN Biomedicals, Inc.), and AEBSF (10 μg/ml, ICN Biomedicals, Inc.). The extract was mixed with rabbit antiserum (1:200 dilution) raised against a glutathione S-transferase (GST)-FACC fusion protein (kindly provided by Dr. A. D'Andrea, Dana Farber Cancer Center). Immune complexes bound to protein A sepharose CL-4B (Pharmacia, Piscataway, NJ) were washed twice with 1% Triton X-100 and 0.1% SDS, and electrophoresed on a 10% SDS/polyacrylamide gel.

Isolation of CD34+ hematopoietic cells. Apheresis was performed after obtaining written informed consent from patients enrolled on a protocol approved by the National Heart, Lung, and Blood Institute Institutional Review Board. Peripheral blood (PB) cells were collected on a Fenwall CS3000 Blood Cell Separator. Mononuclear cells were obtained following Ficoll density gradient centrifugation and immunoselected on a Ceprate LC cell separation system (Cell Pro, Inc., Bothell, WA). Cells were incubated with a mouse IgM anti–human CD34, washed, and then incubated with a biotinylated goat anti–mouse IgM antibody. Cells were filtered through an avidin column and adsorbed cells eluted.

Cell purity was assessed by flow cytometric analysis. A total of 2–4 $\times 10^4$ cells were incubated at 4°C for 30 min in 1% BSA with 10

PAGE 54/77 * RCVD AT 8/29/2005 7:17:05 PM [Eastern Daylight Time] * SVR:USPTO-EFXRF-6/26 * DNIS:2738300 * CSID:6504936811 * DURATION (mm-ss):60-28

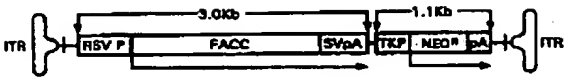

Figure 1. Construction of the rAAV/FACC/Neo^R plasmid. The FACC cDNA coding sequence was inserted into an expression cassette and linked to the Neo^R gene. These transcription units were then subcloned into psub201. The orientation and size (kb) of each gene are indicated.

μl phycoerythrin-conjugated anti-CD34 antibody (mouse anti-human HPCA2; Becton Dickinson, Mountain View, CA). After they were washed, cells were analyzed on a Coulter Epics FACS. The percentage of cells staining for the CD34 antigen was compared with that of cells stained with an isotypic control (IgG 2a mouse anti-human antibody; Becton Dickinson).

rAAV CD34+ cell transduction and CFU-C assay. CD34+ immunoselected cells were cultured at a density of 6×10^4 or 6×10^5 per ml in IMDM, 15% fetal calf serum containing 20 ng/ml human interleukin-3 (IL-3, donated by Dr. Robert E. Donahue, Hematology Branch, NHLBI), 100 ng/ml human stem cell factor (SCF; Amgen Inc., Thousand Oaks, CA), and 50 ng/ml human interleukin 6 (IL-6, donated by Dr. Robert E. Donahue). rAAV lysate was added to maintain a multiplicity of infection of 0.1. Cells were incubated overnight, spun down and resuspended in fresh media and viral lysate. This protocol was repeated for 3 d. Mock-infected cells grown only in media and colony stimulating factors served as controls.

After infection, 1×10^5 cells were plated in 3.0 ml methylcellulose (Terry Fox Labs, Vancouver, Canada) supplemented with SCF (100 ng/ml), IL-3 (20 ng/ml), IL-6 (50 ng/ml), and recombinant human erythropoietin (3 U/ml). Of this 3.0 ml mixture, 1.0 ml was plated in colony culture petri dishes (Nunc). MMC was added directly to methylcellulose cultures to final concentrations of 1–10 nM. Cultures were grown in a humidified atmosphere at 37°C and 5% CO_2. Colonies were counted at day 15.

Reverse transcriptase–polymerase chain reaction analysis of CFU-C. Individual progenitor colonies containing 50–500 cells were harvested from methylcellulose into 50 μl of RNA Stat-60 (Tel-Test B Inc., Friendswood, TX) containing 10 μg transfer RNA and immediately frozen at −70°C. The RNA was isolated after chloroform extraction and precipitation with isopropanol. The sample was washed with ethanol, air dried, and resuspended in RNase-free water. An aliquot of each sample was reverse transcribed using the RNA PCR reagent kit (Perkin-Elmer Corp.) for 30 min at 42°C. Identical reactions without reverse transcriptase were performed. 20 μl of the cDNA generated was amplified using the manufacturer's recommended conditions and included P^{32}dCTP (800 Ci/mmol, Amersham Corp.). Primers mentioned previously were used for amplification. The conditions for amplification included: 95°C for 2 min, followed by 35 cycles at 95°C for 1 min, 60°C for 1 min, and 72°C for 2 min, followed by extension at 72°C for 8 min. PCR-generated products were run on 5% polyacrylamide gels and autoradiographed.

Results

Phenotypic correction of FACC lymphoblasts by rAAV-mediated gene transfer. EBV-transformed lymphoblast cell lines derived from FA(C) patients were used to study in vitro gene complementation and functional correction of the FA defect. Two established cell lines from patients known to bear FACC mutant alleles were used to determine if a rAAV vector containing a copy of the normal FACC cDNA could correct the FA defect. The BD0215 lymphoblast cell line is homozygous for a nonsense mutation in exon 6 of the FACC coding sequence (25). The mutation causes a premature termination of translation at amino acid residue 185, producing a truncated nonfunctional FACC protein. Lymphoblast cell line HSC536 contains

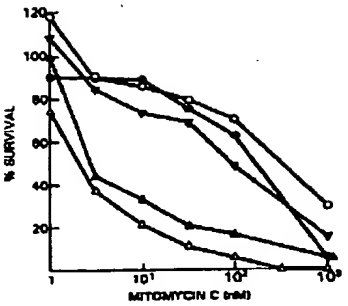

Figure 2. Analysis of rAAV/FACC-transduced lymphoblast mitomycin C sensitivity. Plot of cell viability of FA(C) lines, BD0215 (▲), HSC536 (△), normal lymphoblasts (○), rAAV/FACC-transduced BD0215 (▼), and rAAV/FACC-transduced HSC536 (●) after incubation for 5 d with varying concentrations of MMC.

a T to C transition leading to an amino acid substitution of leucine to proline (designated L554P). This mutation completely abolishes the activity of the FACC protein in functional assays (26). Recombinant AAV virus, carrying the FACC cDNA in an expression cassette linked to the selectable gene Neo^R (Fig. 1), was generated and used to infect FA(C) lymphoblast cell lines. G418-selected cells were used in functional complementation assays.

rAAV-mediated transfer and expression of the normal FACC gene corrected the defect in lymphoblast survival revealed by exposure to clastogenic agents such as MMC. Cells were incubated in the presence of varying concentrations of MMC for 5 d, and viable cells were counted. Parental cells were highly sensitive to DNA cross-linking agents with an EC_{50} of 1.0–5.0 nM MMC. As shown in Fig. 2, cells transduced with rAAV were phenotypically altered so that the resistance of these lymphoblasts to MMC was comparable with that of normal lymphoblasts. The EC_{50} of transduced cells was 100–500 nM, 100-fold higher than parental controls and comparable to the EC_{50} of normal cells.

Hypersensitivity of FA cells to DNA cross-linking agents is known to result in an increased frequency of chromosomal breakage. rAAV-transduced cells were analyzed for chromosomal breakage after incubation in MMC. As shown in Table I and Fig. 3, rAAV/HSC536 and rAAV/BD0215 cells had a significantly reduced number of chromosomal breaks and radials (< 5%) compared with mock-infected parental cells ~ 50% of which had multiple chromosomal breaks and radial formation. The transduced cell lines no longer met the diagnostic criteria for FA, defined cytogenetically as > 20% radial formation. Notably, these rAAV-transduced cells were routinely passaged without selection more than 50 times before use in the

Table I. Chromosomal Breakage Analysis of FA(C) Lymphoblasts

Cell line	Radials*‡
	%
HSC536	48.0
BD0215	36.0
HSC536/rAAV/FACC/Neo^R	6.0
BD0215/rAAV/FACC/Neo^R	1.0

* 50 cells from each cell line analyzed after a 2-day exposure to MMC (40 ng/ml). ‡ >20% of cells with radial formation are diagnostic for FA phenotype.

PAGE 55/77 * RCVD AT 8/29/2005 7:17:05 PM [Eastern Daylight Time] * SVR:USPTO-EFXRF-6/26 * DNIS:2738300 * CSID:6504936811 * DURATION (mm-ss):60-28

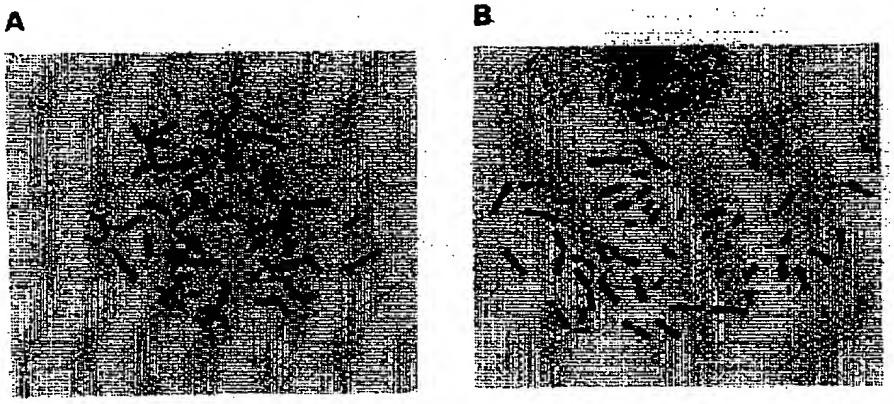

Figure 3. Cytogenetic analysis of rAAV-transduced lymphoblasts. (*A*) A representative metaphase spread from the cell line BD0215 after incubation with MMC (40 ng/ml). Chromatid breaks, gaps (→), and radials (⇢) are indicated. (*B*) Metaphase preparation of rAAV/FACC-transduced BD0215 cells after exposure to MMC.

cytogenetic assay. This implied that stable integration of the rAAV provirus had occurred.

FA cells in each phase of the cell cycle were analyzed by propidium iodide staining and flow cytometry (Fig. 4, Table II). The percentage of cells in the G2 phase is increased in FA patients as compared with normal individuals; this has been

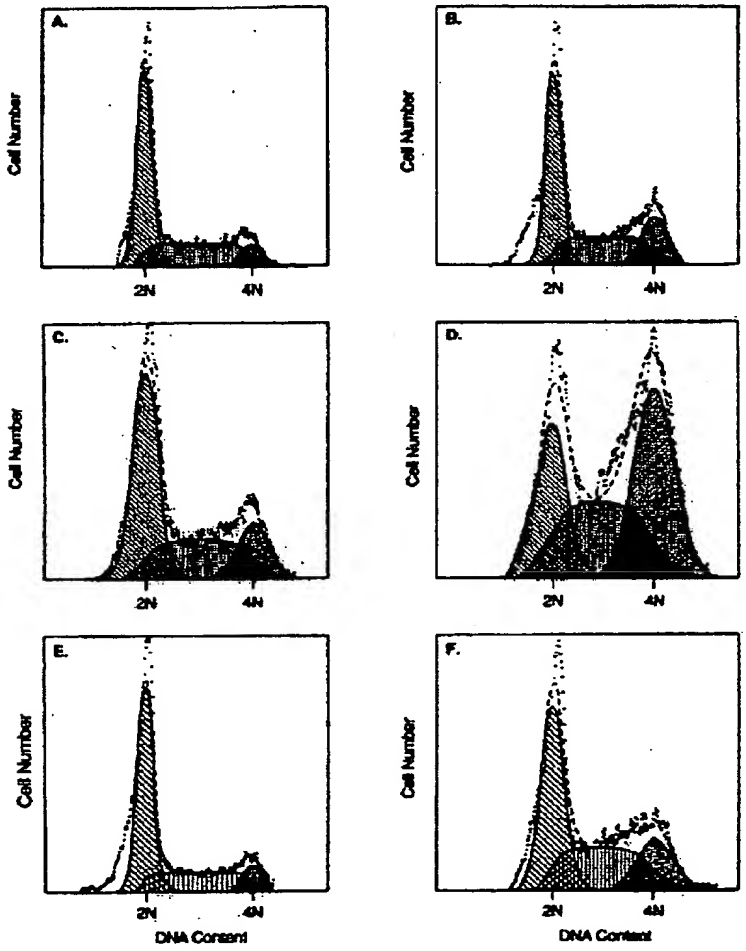

Figure 4. Effect of mitomycin C on DNA flow cytometry histograms of rAAV-transduced lymphoblasts. The rAAV-transduced FA lymphoblast cell line (BD0215) was compared to the parental and normal lymphoblast cell lines. Cells were harvested, stained with propidium iodide, and DNA histograms were obtained 24 h after cells were exposed to 100 nM MMC (*B, D,* and *F*). *A, C,* and *E* are untreated cells. Lymphoblasts from a normal individual: *A* and *B;* FA lymphoblasts (BD0215): *C* and *D;* rAAV-transduced lymphoblasts: *E* and *F.* Data is expressed as number of cells (*ordinate*) versus DNA content. Raw data are shown with data smoothed by MULTIPLIER. Areas under the curve for G1, S, and G2 are shown.

PAGE 56/77 * RCVD AT 8/29/2005 7:17:05 PM [Eastern Daylight Time] * SVR:USPTO-EFXRF-6/26 * DNIS:2738300 * CSID:6504936811 * DURATION (mm-ss):60-28

Table II. Cell Cycle Analysis of rAAV Transduced Lymphoblasts

Cell type	Condition	Cell number %		
		G1	S	G2
Normal lymphoblast	−MMC	58.8	32.5	8.7
Normal lymphoblast	+MMC	46.1	36.8	17.8
BD0215 lymphoblast	−MMC	51.4	32.2	16.4
BD0215 lymphoblast	+MMC	24.3	34.4	41.3
BD0215/rAAV	−MMC	59.6	31.4	9.1
BD0215/rAAV	+MMC	45.9	34.9	19.2

* Refers to the percentage of cells in the G1, S, and G2 phases of the cell cycle in the absence or presence of 100 nM MMC. Results are from duplicate samples from two experiments.

used diagnostically for evaluation of patients (27, 28). The major effect of MMC on DNA flow histograms was the expected increase in the number of cells in G2 (see Fig. 4). Cell cycle analysis of lymphoblasts derived from a normal individual in the absence and presence of MMC (100 nM) indicated only a modest increase (8%) in the number of cells delayed in G2 phase (Fig. 4, *A* and *B*, and Table II). A marked delay in G2 transit was observed when the parental lymphoblast cell line BD0215 was incubated with MMC (Fig. 4, *C* and *D*). The percentage of cells in G2 increased from 16 to 41% (Table II). In marked contrast, cells from the rAAV-transduced FA line showed normalized cycle kinetics in both the absence or presence of MMC (Fig. 4, *E* and *F*, and Table II). No significant change in the number of cells in S phase was observed at the concentration of MMC tested (shown in Table II).

Structure and expression of the FACC gene in rAAV transduced lymphoblasts. rAAV-transduced cells selected in G418 were pooled and characterized by Southern blot analysis of genomic DNA. Shown in Fig. 5 are Southern analyses of DNAs from rAAV/FACC/Neo^R transduced cells hybridized with a probe recognizing a fragment of the neomycin phosphotransferase gene. Digestion with SnaBI, which cuts within the termini, resulted in a single DNA band of predicted length, consistent with unrearranged integration of the provirus.

A reverse transcription (RT)-PCR assay was performed to determine the relative level of expression from both the transduced and endogenous FACC coding sequences. PCR primers, specific for the 3′ untranslated sequences of the proviral and native FACC mRNAs, were designed to generate a 602-bp or a 486-bp product from the endogenous or transduced FACC gene, respectively. Total RNA isolated from lymphoblasts was reverse transcribed and the cDNA used for the PCR amplification (Fig. 6). An mRNA signal for the endogenous FACC product was obtained from mock-infected HSC536 cells. As expected, no mRNA signal was observed using primers for the transduced FACC gene. However, both the endogenous and proviral mRNAs were amplified from lymphoblasts transduced with rAAV/FACC/Neo^R.

FACC protein expression in normal, parental BD0215, and transduced BD0215/rAAV lymphoblasts was analyzed by immunoprecipitation (Fig. 7). The rabbit polyclonal antiserum used was generated from an epitope of a glutathione S-transferase (GST)-FACC fusion protein directed to the carboxy terminus of FACC (amino acids 281–558). The predicted 63-kD FACC protein was detected in both normal and transduced cell

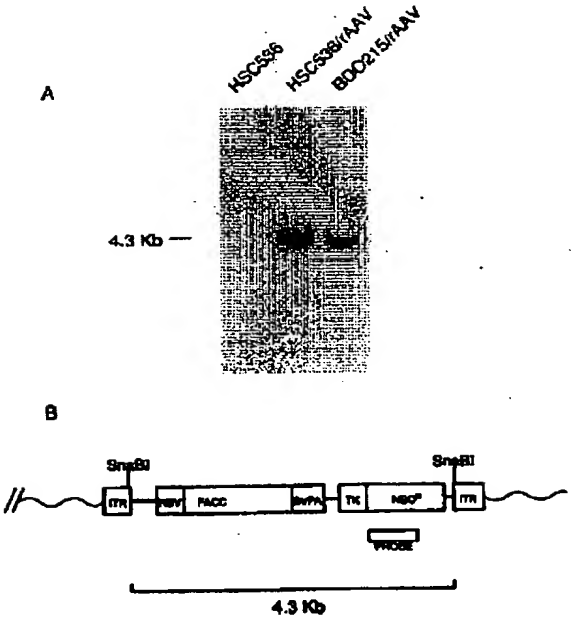

Figure 5. Southern blot analysis of FA(C) lymphoblasts infected with rAAV/FACC virus. (*A*) SnaBI digestion of genomic DNA isolated from rAAV/FACC-transduced BD0215, rAAV/FACC-transduced HSC536, and HSC536 cell lines. The expected 4.3-kb band represents an intact, unrearranged rAAV proviral form. HSC536 mock-infected cells served as a control DNA. (*B*) Schematic diagram of the integrated rAAV proviral form. The SnaBI restriction site located within each of the ITRs is indicated. A 197-bp Neo^R fragment was used as probe.

lines. As expected, no protein was detected from the parental line with a predicted truncated protein of 185 amino acids.

AAV-mediated gene transfer and expression into CD34+ hematopoietic progenitor cells. After the successful phenotypic correction of rAAV-transduced FACC lymphoblasts, we approached the problem of correcting the FACC defect in primary hematopoietic cells derived from a FA(C) patient. CD34+ cells contain an enriched population of self-renewing stem cells, capable of sustaining long-term bone marrow reconstitution (29, 30). Peripheral blood mononuclear cells were obtained by apheresis from a FA(C) patient documented to have a splice mutation at FACC intron 4 (A to T) yielding a nonfunctional protein. Selected cells were isolated using a column containing an avidin-coated matrix that absorbs the human CD34-biotin–conjugated antibody. Flow cytometric analysis of the isolated cells revealed that 92% of the cells were CD34+ after immunopurification. Cells were incubated with rAAV/FACC/Neo^R at a multiplicity of infection (moi) of 0.1 for 3 d, washed, and 3×10^4 cells suspended in methylcellulose, as described in Methods. After a 15-d culture period, hematopoietic colonies derived from CD34-enriched cells were counted (shown in Fig. 8). Compared with mock-infected CD34+ cells, cells incubated with virus yielded a fourfold increased number of colonies. Cells plated in media containing MMC (1.0 nM) yielded nearly an 8–10-fold increased number of measurable colonies, compared to nontransduced control cells incubated in MMC. Mor-

PAGE 57/77 * RCVD AT 8/29/2005 7:17:05 PM [Eastern Daylight Time] * SVR:USPTO-EFXRF-6/26 * DNIS:2738300 * CSID:6504936811 * DURATION (mm-ss):60-28

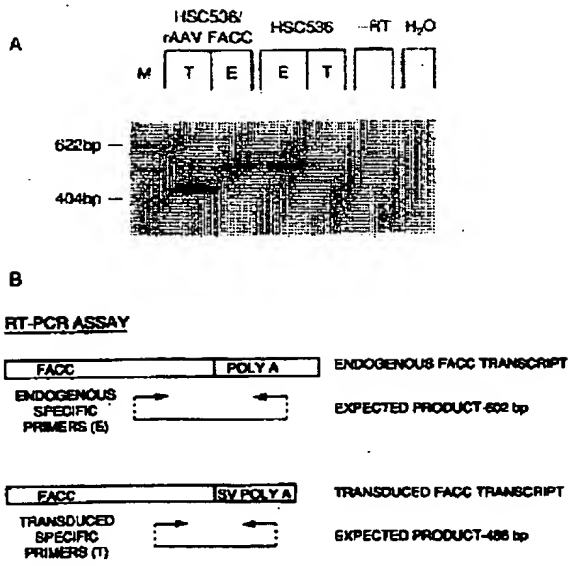

Figure 6. Expression of FACC mRNA in FA(C) lymphoblasts measured by the polymerase chain reaction. (*A*) Total RNAs isolated from rAAV-infected HSC536 and mock-infected HSC536 were analyzed for both endogenous and transduced FACC transcription. Primers specific for the endogenous FACC transcript (E) and the transduced FACC transcript (T) are indicated. RNA processed identically without reverse transcriptase (RT) and samples without RNA (labeled H_2O) served as negative controls. (*B*) The expected 602- or 486-bp products generated using reverse-transcribed RNA from the endogenous FACC gene and the transduced FACC gene, respectively.

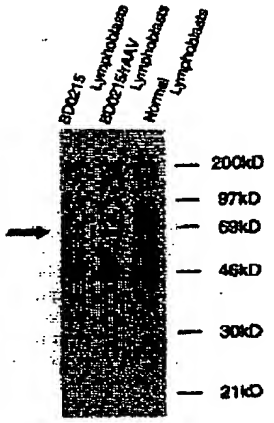

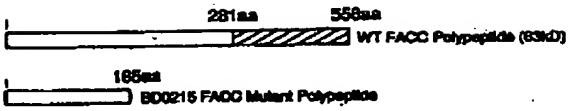

Figure 7. Immunoprecipitation analysis of normal, mutant (BD0215), and rAAV/transduced BD0215 lymphoblasts. Cells were labelled with [^{35}S]methionine and radiolabeled proteins immunoprecipitated with anti-FACC antiserum. Proteins were resolved on a 10% SDS/polyacrylamide gel. Arrow indicates the predicted molecular weight of the wild-type FACC polypeptide. The expected sizes of the wild-type and mutant FACC proteins are shown schematically below. A GST-FACC fusion protein containing FACC amino acid sequence 281–558, indicated by the hatched region, was used to generate rabbit antiserum. Molecular weight markers are indicated at the right.

phologically, the majority of colonies were of the myeloid/macrophage lineage (CFU-GM).

RT-PCR analysis was used to verify that the MMC progenitor colonies were transduced by rAAV. Apparent MMC-resistant colonies were isolated; total RNA was obtained and analyzed by RT-PCR using conditions described in Methods. The autoradiograph in Fig. 9 demonstrated the appropriate 486-bp size fragment in 6 of 9 colonies assayed. RNA not reverse transcribed generated no signal and ruled out the possibility of DNA contamination. Analysis of additional colonies demonstrated that 60% of colonies yielded the expected 486-bp signal without detectable contaminating DNA (data not shown). Although the majority of colonies scored positive for rAAC/FACC expression, some colonies did not express FACC as determined by our RT-PCR assay. RT-PCR results using β-actin primers generated the appropriate signal in all of the FA(C) colonies analyzed (data not shown).

Discussion

We have shown that a recombinant AAV vector can transfer a functioning copy of the normal FACC gene to FA(C) lymphoblasts and CD34+ hematopoietic progenitors, correcting the phenotypic defect of these cells. Phenotypic correction was determined by resistance of cells to MMC-induced cell death and insusceptibility to chromosomal breakage in lymphoblastoid cell lines. Corrected cell lines represented two distinct FACC mutations known to result in the disease phenotype. Using PCR analysis, the level of rAAV/FACC expression appeared to be equivalent to that of the endogenous gene. Transduced lymphoblasts maintained a corrected phenotype over more than 50 cell passages without selection, consistent with stable proviral integration. Of importance to the application of

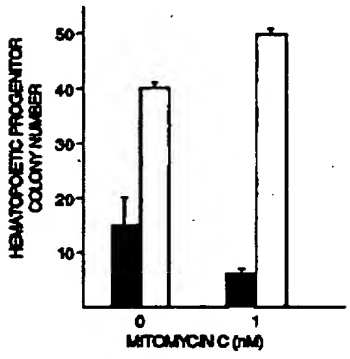

Figure 8. Analysis of hematopoietic progenitor colony growth following rAAV/FACC infection of CD34+ cells isolated from a FA(C) patient. The number of progenitor colonies (> 50 cells/colony) measured at day 15 in methylcellulose culture following rAAV/FACC virus (□) or mock infection (■) are shown. Cells were grown in either the absence or presence of 1 nM MMC. Results are expressed as mean colony number ± SEM.

PAGE 58/77 * RCVD AT 8/29/2005 7:17:05 PM [Eastern Daylight Time] * SVR:USPTO-EFXRF-6/26 * DNIS:2738300 * CSID:6504936811 * DURATION (mm-ss):60-28

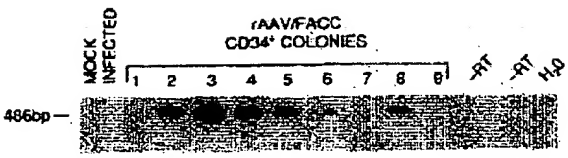

Figure 9. RT-PCR analysis of rAAV/FACC-transduced mRNA expression in hematopoietic progenitor colonies. Total RNAs obtained from apparent MMC-resistant bone marrow colonies were analyzed for rAAV/FACC-specific transcription. RNA isolated from a pool of mock-infected colonies was processed identically to serve as control. Primers specific for the detection of rAAV/FACC transduced expression, the predicted 486-bp fragment, were used. Data from isolated progenitor colonies are shown. RNA from clones processed without reverse transcriptase (RT) and samples without RNA were employed as negative controls.

rAAV vectors to the gene therapy of Fanconi anemia, we also demonstrated rAAV transduction of primary hematopoietic cells by both functional and molecular studies. CD34+ immunoselected hematopoietic progenitors from an FA(C) patient transduced with rAAV demonstrated increased colony formation both in the absence and presence of MMC. Furthermore, RT-PCR analysis confirmed rAAV/FACC expression.

Recombinant AAV gene transfer to hematopoietic cells. Testing the utility of the recombinant AAV vector system for gene transfer in hematopoietic progenitor cells was one of the main objectives of this study. The first report of transduction of murine hematopoietic progenitors described the use of a rAAV vector bearing a neo^R gene with a transduction efficiency of only 1.5% (31). Transduction was determined solely from the number of geneticin-resistant bone marrow colonies. These early generation rAAV preparations were contaminated with wild type AAV virions which decreased rAAV transduction efficiency (13).

We have focused on the use of packaging systems which generate rAAV stocks devoid of wild type virions (23). We have used these helper-free rAAV vectors to transfer the β-galactosidase gene into primate CD34+ hematopoietic progenitor cells (22a). Enzyme expression was documented in 60–70% of the infected cells. A more recent report claimed 80% transduction of unpurified murine progenitors when scored by neomycin-selected bone marrow progenitor assays (22). DNA PCR data from individual bone marrow colonies grown in G418 demonstrated rAAV infection and presumed proviral integration. However, work in our laboratory has suggested that DNA PCR analysis of bone marrow colonies must be interpreted cautiously. Both unintegrated virus and vector plasmid forms which may be associated with cells will be detected by PCR (J. L. Miller, unpublished results). For this reason, we used RT-PCR as a method to determine rAAV-transduced FACC expression in both human lymphoblasts and CD34+ primary hematopoietic progenitors.

It should be noted that > 90% of the FA(C) immunoaffinity-purified cells were CD34 antigen positive, suggesting that primitive populations of hematopoietic cells can be transduced with rAAV. Unfortunately, the efficiency of rAAV transduction is difficult to accurately assess, particularly when the moi is quite low. We presume that colonies arose from transduced pluripotential cells but we have no way to ascertain what fraction of the CD34+ population contain these cells. While the spectrum of cell types targeted by rAAV vectors needs to be defined, it seems reasonable to conclude that rAAV vectors may be useful in gene transduction of hematopoietic progenitors and stem cells, especially if conventional vector systems prove inadequate or inefficient.

Role of FACC in hematopoiesis. In vitro culture assays of hematopoiesis in FA patients have consistently shown a reduction or absence of colony forming progenitor cells (CFU-C) of all hematopoietic lineages (32, 33). Long-term bone marrow culture experiments, which require the development of an adherent stromal cell layer for the maintenance of progenitor growth, have also revealed a significant reduction in the number of CFU-C (34). Although defects of the bone marrow stromal elements cannot be totally excluded, fibroblasts (a major cell constituent of the stroma) from FA patients seem to express the appropriate repertoire of hematopoietic growth factors (35). Available evidence suggests, therefore, that FA is a disorder of a primitive hematopoietic stem cell. We have been able to show that CD34+ progenitors from a FA(C) patient retain the hypersensitivity to MMC which characterizes cultured FA cells.

In this study, we utilized the unique characteristics of the FACC gene to serve as a biological marker for rAAV/FACC gene transfer. As we demonstrated with rAAV-transduced FA(C) lymphoblasts, expression of the FACC gene in FACC-deficient cells promotes cell growth in the presence of MMC. The self-selecting growth advantage conferred by expression of the FACC gene was also evident from the results obtained following the incubation of virally transduced FA(C) progenitor cells with low dose MMC (1 nM), a dose which has no effect on colony growth of CD34+ cells from normal individuals. The increased colony growth reflects genetic rescue of CD34+ progenitor cells after rAAV/FACC transduction. FACC gene expression detected from the majority of progenitor cell colonies provides presumptive evidence that the growth advantage was due to expression of the normal gene in cells bearing defective FACC alleles. Notably, even in the absence of MMC, rAAV transduced CD34+ cells yielded a fourfold greater number of viable progenitor colonies compared with mock-infected controls. Conversely, normal hematopoiesis is inhibited when the FACC gene is repressed using antisense oligonucleotides incubated with normal bone marrow cells (36). We suggest that the FACC gene may therefore be involved in the maintenance of hematopoietic cell growth in addition to its role in the cellular response to DNA damage induced by agents such as MMC.

FACC biological function. The exact biochemical function of the FACC gene is not known, but recent data indicate that the gene product is expressed ubiquitously and conserved phylogenetically (37). Conflicting data exist concerning the subcellular location of the FACC protein (38, 39). Current hypotheses suggest that the FA defect involves DNA repair. Circumstantial evidence for aberrant repair processes is based upon the marked cellular hypersensitivity to bifunctional DNA cross-linking agents coupled with spontaneous and chemical-induced chromosomal instability. In our experiments, FACC gene-transduced lymphoblasts (as compared with parental controls) exhibited a markedly reduced susceptibility to chromosomal breakage after treatment with MMC. Radial formation is thought to result from chromatid exchange and was used diagnostically to score for aberrations in our experiments. Thus, FACC may be implicated in a primary or secondary pathway involved in the repair of DNA. One implication of our work is that the FACC gene may function at an early stage in the re-

PAGE 59/77 * RCVD AT 8/29/2005 7:17:05 PM [Eastern Daylight Time] * SVR:USPTO-EFXRF-6/26 * DNIS:2738300 * CSID:6504936811 * DURATION (mm-ss):60-28

sponse of the cell to DNA damage, since complementation alters both chromosomal stability and (subsequently) cell survival.

FA cells are markedly retarded during progression through the G2 phase of the cell cycle (7, 40). rAAV-transduced FA lymphoblasts were phenotypically corrected not only in terms of MMC-induced cell survival and chromosomal aberrations but also demonstrated normalized cell cycle kinetics. At least two periods in the cell cycle are regulated in response to DNA damage, the G1-S and G2-M transitions. These "checkpoints" function as surveillance mechanisms which delay cell cycle progression and allow for the repair of damaged DNA. Both G1 and G2 checkpoints are known to be under genetic control (41). Many eukaryotic cells delay in the G2 phase of the cell cycle after DNA damage induced by a variety of chemical agents, γ-irradiation, or by inactivation of DNA replication or repair enzymes. The delay in the G2 phase provides the cell with additional time to complete DNA repair before mitosis; prevention of G2 arrest by chemical treatment (caffeine) or genetic mutation (*Rad 9* mutants in *S. cerevisiae*) results in increased cytogenetic damage and cell death (42, 43). Caffeine treatment of FA cells shortens the duration of G2 phase but does not lead to rapid death of cells exposed to MMC (44, 45); chromosomal breakage is dramatically increased (46), due possibly to loss of the G2 checkpoint. In contrast, we have shown that rAAV/FACC-transduced FA(C) cells exhibit normal cell cycle kinetics and normal cytogenetics when treated with MMC. By implication, the FACC gene product may function as a DNA repair enzyme, a surveillance protein, or as a factor coupling the two activities.

In summary, our experiments may shed light on the nature of the specific FA cellular defect as well as suggest new strategies for the treatment of patients. FA cells suffer from an increased generation time and from an increased rate of cell death. We have shown that the FACC gene product can alter (and normalize) both of these phenotypes in mutant cell lines and hematopoietic progenitor cells derived from a FA(C) patient. One interpretation of these data is that relief of G2 phase checkpoint arrest may enable improved cell survival. However, those cells not only survive MMC treatment but also exhibit fewer cytogenetic abnormalities. Thus, we infer that the FACC gene is able to correct some aspect of DNA damage which accumulates prior to the G2 phase. From the standpoint of therapeutic strategies for FA(C) patients, we believe that transfer of the FACC gene into appropriate hematopoietic target cells could allow for hematopoietic reconstitution with a genetically normalized pool of stem cells. Our data indicate that rAAV vectors can transduce primitive hematopoietic progenitor cells and correct an inherited defect and suggests that in vivo studies of rAAV gene therapy are warranted.

Acknowledgments

We thank Stacie Anderson for excellent technical assistance, Dr. M. Buchwald for the plasmid pFAC3 and cell line HSC536, Dr. C. Mathew for the cell line BD0215, Dr. M. Grompe, Dr. E. Magenis, and the Fanconi Anemia Research Fund. We also thank Drs. A. D'Andrea and T. Yamashita for providing the rabbit anti-FACC antiserum.

References

1. Alter, B., and N. S. Young. 1993. The bone marrow failure syndromes. *In* Hematology of Infancy and Childhood. D. G. Nathan, and F. A. Oski, editors. W. B. Saunders, Philadelphia, PA. 216–316.

2. Gluckman, E., A. Devergie, and J. Dutreix. 1989. Bone marrow transplantation for Fanconi anemia. *In* Fanconi Anemia. T. M. Schroeder-Kurth, A. D. Auerbach, and G. Obe, editors. Springer-Verlag, New York. 60–70.

3. Schroeder, T. M., F. Anschutz, and A. Knopp. 1964. Spontane Chromosomenaberrationen bei familiarer Panmyelopathie. *Humangenetik.* 1:194–196.

4. German, J., and C. L. Pugliatta. 1966. Chromosomal breakage in diploid cell lines from Bloom's syndrome and Fanconi's anemia. *Ann. Genet.* 9:143–154.

5. Sasaki, M. S., and A. Tonomura. 1973. A high susceptibility of Fanconi's anemia to chromosome breakage by DNA cross-linking agents. *Cancer Res.* 33:1829–1836.

6. Auerbach, A. D., A. Rogatko, and T. M. Schroeder-Kurth. 1989. International Fanconi Anemia Registry: relation of clinical symptoms to diepoxybutane sensitivity. *Blood.* 73:391–396.

7. Kubbies, M., D. Schindler, H. Hoehn, and P. S. Rabinovitch. 1985. Endogenous blockage and delay of the chromosome cycle despite normal recruitment and growth phase explain poor proliferation and frequent edomitosis in Fanconi anemia cells. *Am. J. Hum. Genet.* 37:1022–1030.

8. Ishida, R., and M. Buchwald. 1982. Susceptibility of Fanconi's anemia lymphoblasts to DNA cross-linking and alkylating agents. *Cancer Res.* 42:4000–4006.

9. Strathdee, C. A., A. M. V. Duncan, and M. Buchwald. 1992. Evidence for at least four Fanconi anaemia genes including FACC on chromosome 9. *Nature Genetics.* 1:196–198.

10. Strathdee, C. A., H. Gavish, W. R. Shannon, M. Buchwald. 1992. Cloning of cDNAs for Fanconi's anaemia by functional complementation. *Nature (Lond.).* 356:763–776.

11. Verlander, P. C., J. D. Lin, M. U. Udoso, R. A. Gibson, C. G. Mathew, S. L. Sherman, and A. D. Auerbach. 1993. Mutation and linkage analysis of the Fanconi anemia gene FACC. *Hum. Genet.* 53(suppl.):11a.

12. Whitney, M. A., H. Saito, P. M. Jakobs, R. A. Gibson, R. E. Moses, and M. Grompe. 1993. A common mutation in the FACC gene causes Fanconi anaemia in Ashkenazi jews. *Nature Genetics.* 4:202–205.

13. Muzyczka, N. 1992. Use of adeno-associated virus as a general transduction vector for mammalian cells. *Curr. Top. Microbiol. Immunol.* 158:97–129.

14. Nienhuis, A. W., C. E. Walsh, and J. Liu. 1993. Viruses as therapeutic gene transfer vectors. *In* Viruses and Bone Marrow Young. N. S. Young, editor. Marcel Dekker, New York. 353–414.

15. Walsh, C. E., J. M. Liu, J. L. Miller, A. W. Nienhuis, and R. J. Samulski. 1993. Gene therapy for human hemoglobinopathies. *Proc. Soc. Exp. Biol. Med.* 204:289–300.

16. Kotin, R. M., R. Siniscalco, R. J. Samulski, X. Zhu, L. Hunter, C. A. Laughlin, S. McLaughlin, N. Muzyczka, M. Rocchi, and K. Berns. 1990. Site-specific integration by adeno-associated virus. *Proc. Natl. Acad. Sci. USA.* 87:2211–2215.

17. Samulski, R. J., X. Zhu, X. Xiao, J. D. Brook, D. E. Housman, N. Epstein, and L. A. Hunter. 1991. Targeted integration of adeno-associated virus (AAV) into human chromosome 19. *EMBO (Eur. Mol. Biol. Organ.) J.* 10:3941–3950.

18. Samulski, R. J. 1993. Adeno-associated virus: integration at a specific chromosomal locus. *Current Opinion in Genetics and Development.* 3:74–80.

19. Walsh, C. E., J. M. Liu, X. Xiao, N. S. Young, A. W. Nienhuis, and R. J. Samulski. 1992. Regulated high level expression of a human γ-globin gene introduced into erythroid cells by an adeno-associated virus vector. *Proc. natl. Acad. Sci. USA.* 89:7257–7261.

20. Miller, J. L., C. E. Walsh, P. A. Ney, R. J. Samulski, and A. W. Nienhuis. 1993. Single-copy transduction and expression of the human γ-globin in K562 erythroleukemia cells using recombinant adeno-associated virus vectors: the effect of mutations in NF-E2 and GATA-1 binding motifs within the hypersensitivity site 2 enhancer. *Blood.* 82:1900–1906.

21. Chatterjee, S., P. R. Johnson, and K. K. Wong. 1992. Dual target inhibition of HIV-1 in vitro by means of an adeno-associated virus antisense vector. *Science (Wash. DC).* 258:1485–1488.

22. Zhou, S. Z., H. B. Broxmeyer, S. Cooper, M. A. Harrington, and A. Srivastava. 1993. Adeno-associated virus 2-mediated gene transfer in murine hematopoietic progenitor cells. *Exp. Hematol. (NY).* 21:928–933.

22a. Goodman, S., X. Xiao, R. E. Donahue, A. Moulton, J. Miller, C. Walsh, N. S. Young, R. J. Samulski, and A. W. Nienhuis. 1994. Recombinant adeno-associated virus-mediated gene transfer into hematopoietic progenitor cells. *Blood.* In press.

23. Samulski, R. J., L. S. Chang, and T. Shenk. 1989. Helper-free stocks of recombinant adeno-associated viruses: normal integration does not require viral gene expression. *J. Virol.* 63:3822–3828.

24. Rigaud, G., T. Grange, and R. Picet. 1987. The use of NaOH as transfer solution of DNA onto nylon membranes decreases the hybridization efficiency. *Nucleic Acids Res.* 15:857.

25. Gibson, R. A., A. Hafianpour, M. Murer-Orlando, M. Buchwald, and C. G. Mathew. 1993. A nonsense mutation and exon skipping in the Fanconi anemia group C gene. *Hum. Mol. Gen.* 2:797–799.

26. Gavish, H., C. C. dos Santos, and M. Buchwald. 1993. A leu_{554}-to-pro substitution completely abolishes the functional complementing activity of the Fanconi anemia (FACC) protein. *Hum. Mol. Gen.* 2:123–126.

27. Kaiser, T. N., A. Lojewski, C. Dougherty, L. Juergens, E. Sahar, and S. A.

PAGE 60/77 * RCVD AT 8/29/2005 7:17:05 PM [Eastern Daylight Time] * SVR:USPTO-EFXRF-6/26 * DNIS:2738300 * CSID:6504936811 * DURATION (mm-ss):60-28

Lat. 1982. Flow cytometry characterization of the response of Fanconi's anemia cells to mitomycin C treatment. *Cytometry*. 2:291–297.

28. Berger, R., M. LeConiast, and M-C Gendron. 1993. Fanconi anemia chromosome breakage and cell cycle studies. *Cancer Genet. Cytogenet.* 69:13–16.

29. Andrews, R. G., J. W. Singer, and I. D. Bernstein. 1990. Human hematopoietic precursors in long term culture: single CD34+ cells that lack detectable T cell, B cell, and myeloid cell antigen produce multipile colony-forming cells when cultured with marrow stroma. *J. Exp. Med.* 172:355–358.

30. Verfaillie, C., K. Blakolmer, and P. McGlave. 1990. Purified primitive human hematopoietic progenitor cells with long-term in vitro repopulating capacity adhere selectively to irradiated bone marrow stroma. *J. Exp. Med.* 172:509–520.

31. LaFace, D., P. Hermonat, and A. Peck. 1988. Gene transfer into hematopoietic progenitor cells mediated by an adeno-associated virus vector. *Virology*. 162:483–486.

32. Saunders, E. F., and M. H. Freedman. 1978. Constitutional aplastic anaemia: defective haematopoietic stem cell growth in vitro. *Br. J. Haematol.* 40:277–287.

33. Alter, B. P., M. E. Knobloch, L. Ho, A. P. Gillio, R. J. O'Reilly, L. K. Reilly, and R. S. Weinberg. 1992. Effect of stem cell factor on in vitro erythropoiesis in patients with bone marrow failure syndromes. *Blood.* 80:3000–3008.

34. Stark, R., D. Thierry, P. Richard, and E. Gluckman. 1993. Long-term bone marrow culture in Fanconi's anaemia. *Br. J. Haematol.* 83:554–559.

35. Bagby, G. C., G. M. Segal, A. D. Auerbach, T. Onega, W. Keeble, and M. C. Heinrich. 1993. Constitutive and induced expression of hematopoietic growth factor genes by fibroblasts from children with Fanconi anemia. *Exp. Hematol. (NY).* 21:1419–1426.

36. Segal, G. M., E. Magenis, M. Brown, T. D. Smith, W. Keeble, and G. C. Bagby. 1993. Repression of the Fanconi anemia complementation group C gene (FACC) inhibits normal hematopoiesis in vitro. *Clin. Res.* 41:276A.

37. Wevrick, R., C. A. Clarke, M. Buchwald. 1993. Cloning and analysis of the murine Fanconi anemia group C cDNA. *Hum. Mol. Gen.* 2:655–662.

38. Gavish, H., C. A. Clarke, W. R. Shannon, M. Buchwald. 1993. The Fanconi anemia (FACC) protein is primarily localized in the nucleus. *Hum. Genet.* 53(suppl):685a.

39. Youssoufian, H. 1993. Subcellular localization of Fanconi's anemia C protein by epitope-tagging. *Hum. Genet.* 53(suppl)656a.

40. Dutrillaux B., A. Aurias, A. M. Dutrillaux, D. Buriot, and M. Prieur. 1982. The cell cycle of lymphocytes in Fanconi anemia. *Hum. Genet.* 62:327–332.

41. Hartwell, L. H., and T. A. Weinert. 1989. Checkpoints: controls that ensure the order of cell cycle events. *Science (Wash. DC).* 246:629–634.

42. Lau, C. C., and A. B. Pardee. 1982. Mechanism by which caffeine potentiates lethality of nitrogen mustard. *Proc. Natl. Acad. Sci. USA.* 79:2942–2946.

43. Weinert, T. A., and L. H. Hartwell. 1988. The rad9 gene controls the cell cycle response to DNA damage in saccharomyces cerevisiae. *Science (Wash. DC).* 241:317–322.

44. Sabatier, L., and B. Dutrillaux. 1988. Effect of caffeine in Fanconi anemia. I. Restoration of a normal duration of G2 phase. *Hum. Genet.* 79:242–244.

45. Prazelle, J. H., J. S. Harris, and M. Swift. 1981. Response of Fanconi anemia fibroblasts to adenine and purine analogues. *Mutat. Res.* 80:373–380.

46. Pincheira, J., M. Bravo, and J. F. Lopez–Saez. 1988. Fanconi's anemia lymphocytes: effect of caffeine, adenosine and niacinamide during G2 prophase. *Mutat. Res.* 199:159–165.

PAGE 61/77 * RCVD AT 8/29/2005 7:17:05 PM [Eastern Daylight Time] * SVR:USPTO-EFXRF-6/26 * DNIS:2738300 * CSID:6504936811 * DURATION (mm-ss):60-28

Recombinant Adeno-Associated Virus-Mediated Gene Transfer Into Hematopoietic Progenitor Cells

By Stacey Goodman, Xiao Xiao, Robert E. Donahue, Austine Moulton, Jeffrey Miller, Christopher Walsh, Neal S. Young, Richard J. Samulski, and Arthur W. Nienhuis

Recombinant adeno-associated viruses (rAAV) containing only the inverted terminal repeats (ITR) from the wild-type virus are capable of stable integration into the host cell genome, and expression of inserted genes in cultured cells. We have now defined the ability of rAAV to introduce genes into primary hematopoietic progenitors. A vector was constructed containing the coding sequences for β-galactosidase (β-gal), including a nuclear localization signal, under the control of a strong viral promotor. Infectious vector particles were prepared by cotransfection of the vector plasmid with a second plasmid that contained the coding sequences for AAV proteins into adenovirus-infected human embryonic kidney cells. These vector preparations transferred and expressed the β-gal gene in human K562 erythroleukemia and Detroit 6 cells. Positive immunoselection yielded a population of enriched CD34⁺ cells that were transduced with the rAAV β-gal vector. Nuclear localized enzyme expression was documented in 60% to 70% of infected cells. Progenitor-derived colonies that developed after 2 weeks in clonogenic cultures were shown to have viral-associated DNA at an estimated copy number of 1 to 2 per cell using a semiquantitative polymerase chain reaction (PCR) method. Integration of AAV into hematopoietic progenitors was documented using wild-type virus, as its genome may integrate at a preferred site on chromosome 19. Our data suggest that rAAV will transfer and express genes in primitive hematopoietic progenitors with high frequency, and support the development of this vector system for therapeutic gene transfer.
© 1994 by The American Society of Hematology.

THE ABILITY TO transfer genes into repopulating hematopoietic stem cells and to achieve regulated gene expression in lymphoid or myeloid lineages would create many therapeutic opportunities.[1,2] Several genetic diseases affect one or more derivatives of the hematopoietic stem cell, including the red blood cell disorders—sickle cell anemia and thalassemia, chronic granulomatous disease affecting phagocytic cells, various platelet disorders, and immunodeficiency diseases affecting lymphoid cells. One proposed approach to the treatment of acquired immunodeficiency syndrome (AIDS) is to introduce a genetic element into hematopoietic stem cells that renders lymphoid cells in which this element is expressed resistant to human immunodeficiency virus (HIV) infection.[3] Targeting gene expression to individual hematopoietic lineages will undoubtedly depend on the use of tissue-specific, *cis*-active DNA elements, about which much is currently being learned.[4,5] A major barrier to stem-cell–targeted gene therapy in humans has been the difficulty of introducing new genetic information into the quiescent stem-cell population.[1,2,6]

During the past decade, murine models have been developed for stem-cell–targeted gene transfer using retroviral vectors.[1,6,7-11] Vector preparations devoid of replication competent virus are derived from engineered producer clones, in which the proteins required for retroviral particle formation result from expression of viral structural genes that are part of one or more transcriptional units.[2,12] A vector genome is introduced separately, and its expression generates the RNA genome needed for assembly of vector particles. Preparations containing 10^6 infectious particles/mL infect murine repopulating stem cells from animals pretreated with 5-fluorouracil given to activate the stem-cell population.[8,11] Stimulation of bone marrow cells in vitro with various cytokine combinations for 48 hours assures that some stem cells are in cell cycle when subsequently exposed to vector particles,[10,11] a condition necessary for integration of the retroviral vector genome.[13,14] Long-term reconstitution of recipient mice with genetically modified cells is regularly achieved, and gene expression has been documented for more than a year.[11,15-18] Unfortunately, the majority (60% to 70%) of murine bone marrow stem cells remain refractory to retroviral-mediated gene transfer with currently used protocols. Attempts have been made to apply lessons learned in the murine models in canine[19,20] or nonhuman primate models.[21,22] Persistent long-term gene expression has been documented in such large animal models, establishing the feasibility of this general approach, although the frequency of gene insertion into stem cells remains disappointingly low. Only 1% to 3% of primate stem cells are susceptible to retroviral-mediated gene transfer.[1,2]

Among the various approaches that are being explored to improve the efficiency of gene transfer into stem cells is the use of adeno-associated viral (AAV) vectors,[2,23] in hopes of developing a safe and efficient viral vector for human gene therapy. AAV is a dependent parvovirus; it requires coinfection with another virus (either adenovirus or certain members of the herpes virus group) for productive infection of cultured cells. In lytic infection, AAV DNA replicates as a 4.7-kilobase double-stranded molecule, and is packaged into virions as linear single strands of both polarities.[23] In the absence of coinfection with helper virus, the AAV genome integrates via its termini into the host genome in a site-specific manner, and remains latent until the cell is infected with helper virus[24-28] when the AAV DNA is rescued, replicates, and establishes a productive infection.[23] Several features of AAV make it an attractive vector: (1) the virus is ubiquitous in

From the Clinical Hematology Branch, National Heart, Lung and Blood Institute, Bethesda, MD; and the Department of Biology, University of Pittsburgh, Pittsburgh, PA.

Submitted December 8, 1993; accepted May 4, 1994.

Previously published in abstract form, Blood *80:167a, 1992.*

Address reprint requests to Arthur W. Nienhuis, MD, St Jude Children's Research Hospital, 332 N Lauderdale, Memphis, TN 38101.

The publication costs of this article were defrayed in part by page charge payment. This article must therefore be hereby marked "advertisement" in accordance with 18 U.S.C. section 1734 solely to indicate this fact.

© 1994 by The American Society of Hematology.

0006-4971/94/8405-0030$3.00/0

PAGE 62/77 * RCVD AT 8/29/2005 7:17:05 PM [Eastern Daylight Time] * SVR:USPTO-EFXRF-6/26 * DNIS:2738300 * CSID:6504936811 * DURATION (mm-ss):60-28

6504936811 8/29/2005 4:17 PM PAGE 63/077 Fax Server

humans, (2) AAV particles can be concentrated to titers exceeding 10^9 infectious units per milliliter, (3) AAV has a broad host range for infectivity (human, monkey, mouse, etc) when coinfected with the appropriate helper virus, and (4) it is a completely nonpathogenic integrating virus.

Current AAV vectors use an infectious recombinant clone in which 96% of the viral genome is replaced with the gene of choice, retaining only the viral terminal repeat sequences of 145 nucleotides[2,29,30] (X. Xiao and R.J. Samulski, unpublished observations). Packaging systems have been developed in which recombinant vector genomes generate vector preparations devoid of wild-type AAV.[29] These preparations, which require removal of the adenovirus helper, are thought to be capable of infecting quiescent cells.[23] Gene transfer and regulated expression has been achieved using a recombinant AAV (rAAV) vector to insert the human gamma-globin gene into human erythroleukemia cells.[31,32]

In working toward the ultimate goal of stem-cell–targeted gene transfer, we have now explored the ability of rAAV to achieve gene transfer into primate clonogenic hematopoietic progenitors. A rAAV containing the β-galactosidase (β-gal) gene was used, providing a convenient means to assay for transduction and gene expression in cell monolayers or in single-cell suspensions. Semiquantitative polymerase chain reaction (PCR) analysis was used to evaluate DNA from progenitor-derived colonies for evidence of gene transfer. Site-preferred integration into chromosome 19, a feature of latent infection with wild-type AAV, is not generally observed with rAAV. Therefore, in our experiments, we used wild-type AAV to evaluate integration in primary hematopoietic cells.

MATERIALS AND METHODS

Viruses and cells. Wild-type human adenovirus 5 (Ad5) was obtained from the American Type Culture Collection (ATCC), Rockville, MD. The human bladder carcinoma cell line, 5637, was also obtained from the ATCC. Detroit 6,[29] 293,[33] and 562 cells[34] were maintained in Dulbecco's modified Eagle's medium (DMEM) containing 10% fetal calf serum (FCS), 2 mmol/L glutamine, 100 U/mL penicillin, and 0.1 mg/mL streptomycin. A cell line containing a single integrated copy of the β-gal gene as part of a proviral genome (G1BgSVNa-clone 29), obtained from Genetic Therapy (Gaithersburg, MD), was maintained in the same medium. 5637 cells were maintained in RPMI 1640 containing 10% FCS, 2 mmol/L glutamine, 100 U/mL penicillin, and 0.1 mg/mL streptomycin. The cells were grown to confluence, transferred into DMEM containing 10% FCS, 2 mmol/L glutamine, 100 U/mL penicillin, and 0.1 mg/mL streptomycin, and the 5637 cell-conditioned media was harvested after 7 days.

Construction of the rAAV–β-Gal vector. The plasmid pnLacF containing the coding sequences for *LacZ* (β-gal), modified to incorporate a eukaryotic translation initiation codon, an N-terminal nuclear localization signal,[35] and the RNA-processing signals from the mouse protamine-1 (mP-1) gene,[36] was obtained from Jacques Pershon (Immunex Co, Seattle, WA). The CMV E1-A promoter within an *XhoI-PstI* fragment was inserted as a blunted fragment into a blunted *XbaI* site 5′ to the *LacZ* coding sequences. The entire cassette containing the CMV promoter, β-gal coding sequences, and mP-1 RNA-processing signals was inserted between the *NsiI-SnaBI* sites of pDX11[37] to create the plasmid pAB-11. pDX11 had been derived by subcloning the rAAV genome from pd113-94[37] into the *PstI* site of pGEM3A (Promega, Madison, WI).

Generation of AAV and rAAV vectors. AAV type 2 was obtained from ATCC, and maintained by infecting either 293 or HeLa cells; helper function was provided by Ad5 strain dl309 (a gift from T. Shenk, Princeton University), used at a multiplicity of infection (MOI) of 10. At 48 hours postinfection, the cells were collected with the medium, frozen, and thawed three times. After low-speed centrifugation, the cell lysate containing wild-type AAV was heated to 55°C for 1 hour to inactivate the adenovirus, aliquoted, and stored at −20°C for use. The titer of the AAV virus stock was determined indirectly either by immunostaining of infected cells with anticapsid antibodies or by quantitative Southern blot analysis. For preparation of rAAV, 60% to 80% confluent 293 cells were infected with adenovirus type 5 at an MOI of 5 to 10 as previously described.[29] rAAV viral stocks were generated by subsequent calcium phosphate cotransfection of 10 μg of plasmid pAB11 and 10 μg helper plasmid (pAAV/Ad), 2 to 4 hours after adenoviral infection. Cells were harvested 48 to 72 hours posttransfection, frozen and thawed four times, and centrifuged to remove debris. Inactivation of adenovirus was achieved by heating to 55°C for 30 minutes. Heating of the viral preparations eliminated infectious adenovirus, as no cytopathic effect was observed over 7 to 10 days after exposure of 293 or Detroit 6 cells to lysate diluted 1:1. For some preparations, in an effort to achieve a higher viral titer, the plasmid DNA was introduced by lipofection using liposomes prepared according to protocols provided by the vendor, GIBCO (Grand Island, NY). For these preparations, the cells were lysed by sonication in DMEM–10% FCS or phosphate-buffered saline (PBS), clarified by centrifugation, and stored at 4°C.

Histochemical staining for β-Gal activity. Aliquots of lysates (0.01 mL to 0.1 mL) were added to Detroit 6 cells at 60% to 80% confluency and allowed to incubate for 18 hours. Plates were washed, fixed with 2% formaldehyde and 0.2% glutaraldehyde for 5 minutes at 4°C, and stained for X-gal as previously described[38] for 36 hours. The cells were washed three times in PBS and the enzyme reaction developed in PBS containing 1 mg/mL of X-gal, 2 mmol/L $MgCl_2$, 5 mmol/L potassium ferrocyanide, and 5 mmol/L potassium ferricyanide at 37°C for 24 to 36 hours. The cells were then washed in PBS. Cytospin preparations of suspension cells were processed identically after fixation for some experiments. Individual blue nuclei were counted to estimate the viral titer. For processing of fresh cells, 150 μg of X-gal/mL was added to the culture medium and the incubation continued at 37°C in 5% CO_2 for 16 hours. Cytospin preparations were prepared using standard techniques.

Purification of human and rhesus bone marrow progenitors. Human bone marrow cells were obtained from normal volunteers after informed consent using a study protocol approved by the National Heart, Lung and Blood Institute Review Board. Bone marrow aspirates were obtained by standard clinical techniques. Low-density mononuclear cells were isolated by buoyant-density centrifugation (Ficoll-Hypaque), and $CD34^+$ cells were recovered by positive immunoselection using an avidin-biotin–conjugated column system (Ceprate LC) according to the manufacturer's instructions (Cell-Pro, Bothell, WA). Purity was estimated by flow cytometric analysis of the immunoselected $CD34^+$ cell population after restaining with an anti-CD34 antibody or mouse antihuman IgG2a (isotypic control) conjugated to phycoerythrin. Sixty percent to 90% of the recovered cells were $CD34^+$. In addition, the starting mononuclear cell population and immunoselected $CD34^+$ cells were plated in clonogenic cultures in methylcellulose using standard conditions (see below). A 57- to 90-fold enrichment in colony-forming progenitors was achieved.

Rhesus bone marrow cells were obtained by aspiration and a mononuclear cell preparation prepared by buoyant-density centrifu-

PAGE 63/77 * RCVD AT 8/29/2005 7:17:05 PM [Eastern Daylight Time] * SVR:USPTO-EFXRF-6/26 * DNIS:2738300 * CSID:6504936811 * DURATION (mm-ss):60-28

6504936811 8/29/2005 4:17 PM PAGE 64/077 Fax Server

gation; CD34 selection was performed using an antibody (K6.1) that reacts with rhesus CD34 antigen by techniques previously described.[39] A 12- to 94-fold enrichment was achieved, as reflected by the concentration of clonogenic progenitors in the starting mononuclear versus the immunoselected cell population.

Infection and culture of enriched progenitors. $CD34^+$ immunoselected cells were incubated in suspension culture containing DMEM with 10% to 15% FCS, 2 mmol/L glutamine, 100 U/mL penicillin, 0.1 mg/mL streptomycin, 10 ng/mL interleukin (IL)-3, 50 ng/mL IL-6, and 100 ng/mL stem-cell factor (SCF). These cultures were exposed to no virus, wild-type AAV, or rAAV for 1 to 96 hours, at which time cells were harvested, washed, and aliquoted for morphologic analysis (cytoprep), methylcellulose assay, and, in some instances, β-gal activity analysis.

Human bone marrow mononuclear cells (10^5/mL) and $CD34^+$ immunoselected cells (10^3/mL) were plated in Iscove's methylcellulose medium (Terry Fox Laboratories, Vancouver, Canada) consisting of Iscove's media, 0.8% methyl cellulose, 30% FCS, 1% bovine serum albumin, and 10^{-4} 2-mercaptoethanol, to which was added 10% 5637 cell-conditioned medium and 2 U/mL of erythropoietin. Cultures were maintained at 37°C in 5% CO_2 for 12 to 14 days. After scoring, colonies were processed individually or in pools for extraction of DNA. For certain experiments, IL-3 10 ng/mL, IL-6 50 ng/mL, and stem-cell factor (SCF) 100 ng/mL (provided by AMGEN, Thousand Oaks, California) were used in place of 5637 cell-conditioned medium. Culture of rhesus bone marrow cells before and after CD34 immunoselection in methylcellulose was as previously described.[39]

DNA isolation and analysis by the PCR methodology. For preparation of DNA from hematopoietic colonies, single colonies were plucked and placed into 50 μL of diethylpyrocarbonate-treated water. Mineral oil was layered over the aqueous phase, and the samples were heated at 100°C for 10 minutes and cooled to 4°C. Proteinase K (Pro-K) was added to a final concentration of 400 μg/mL, and the samples were incubated at 55°C for 90 minutes and then at 100°C for 5 minutes (to inactivate Pro-K) before cooling to 4°C. DNA, for use as controls, was isolated by standard techniques[40] from cultured cells or bone marrow mononuclear cells.

Standard PCR methodology for DNA analysis was performed using a kit provided by Perkin-Elmer/CETUS (Norwalk, CT) under the conditions specified by the manufacturer. Each 100-μL reaction contained 10 μL of the DNA preparation from individual or pooled colonies. [^{32}P]dCTP (800 Ci/mmol) (Amersham-Searle, Arlington Heights, IL) was added in the amount of 0.2 to 0.5 μL per reaction. Four hundred nanograms of each primer and 2.5 U of Taq DNA polymerase were also added to each 100-μL reaction. The PCR cycles for DNA analysis were preceded by incubation at 95°C for 2 minutes, and the final cycle was followed by elongation at 72°C for 7 minutes. Twenty-forty percent of each reaction mixture was analyzed on an 8% polyacrylamide gel that was processed for autoradiography as previously described.[39]

A set of primers based on the sequence of the mouse β-actin coding region were used to amplify the human β-actin sequences to yield a 232 bp fragment. The sequences were as follows: 5' primer, 5'-CATTGTGATGGACTCCGGAGACGG-3'; and 3' primer, 5'-CATCTCCTGCTCGAAGTCTAGAGC-3'. The PCR was conducted for 25 cycles under the following conditions: 95°C for 1 minute, 58°C for 1 minute, and 72°C for 1.5 minutes. The sequences of the primer pair used to amplify a 314 bp segment of the rhesus γ-globin gene are as follows: 5' primer, 5'-GTTGGGAGTGAAGAAACTGC-3'; and 3' primer, 5'-TAGCCTCAGACTCTGTTTGG-3'. The PCR was conducted for 30 cycles under the following conditions: 94°C for 1 minute, 55°C for 1 minute, and 72°C for 1 minute. Another primer pair was used to amplify a 247-bp segment of the β-Gal gene. The sequences are as follows: 5' primer, 5'CTACACCAACGTAACCTATCCC-3'; and 3' primer, 5'TTCTCCGGCGCGTAAAAATGCG-3'. The PCR was conducted for 30 cycles under the following conditions: 94°C for 1 minute, 55°C for 1 minute, and 72°C for 1 minute.

Integration site analysis. The wild-type AAV genome was detected using the primer pair, 5'GAACGCGCAGCCGCC and 5'GCGCATCAGAATTGGGATTC, that give a 635-bp amplification product derived from the 5' end of the AAV genome. PCR amplification was performed for 25 to 30 cycles under the conditions described below. AAV integration into chromosome 19 was detected by PCR using nested primer pairs that flank an AAV-chromosome 19 junction[24,25]: Jus2 (AAV) –5' AGTAGCATGGCGGGT and Jus3 (chromosome 19) –5' CGCGCATAAGCCAGTAGAGCC. PCR was for 25 cycles using previously described reaction conditions with the following parameters: 1 minute at 94°C, 1 minute at 55°C, and 2 minutes at 73°C. Two percent of the amplification product was diluted into a new reaction mixture containing a set of nested primers with the following sequences: TR-1 (AAV), 5'GGAATTCAGGAACCCCTAGTGATGG; and CR-2 (chromosome 19), –5'ACAATGGCCAGGGCCAGGCAG. The PCR parameters were the same as for the first amplification, and 25 cycles were completed. The products were resolved on a 1% agarose gel, transferred to Hybond N+ paper (Amersham), and probed with a previously cloned junction fragment[25] labeled by Amersham Megaprime DNA labeling system. For molecular cloning of amplified junction fragments, the two nested primers from the second amplification, TR-1 and CR-2, were modified by incorporation of an *Eco*RI or *Bam*HI restriction site, respectively. After amplification, the products were restricted with these enzymes, purified on a 1% agarose gel, and subcloned into plasmids, pUC18 and pUC19, by standard methods. Sequencing was performed by the chain-termination method using a kit obtained from Promega.

RESULTS

rAAV-mediated gene transfer and expression of the β-gal gene. An AAV vector carrying the β-gal reporter gene was constructed to assay rAAV's transduction efficiency in various cell types. Addition of vector preparations at an MOI of 1 or greater to subconfluent Detroit 6 cells resulted in expression of the β-gal gene in most cells within 18 hours (Fig 1A). The viral titers were estimated by adding serial dilutions to a fixed number of cells in each plate; individual preparations ranged from 10^4 to 10^6 infectious particles/mL. Similar results were obtained with vector lysates derived by $CaPO_4$-mediated gene transfer or by lipofection of the vector and helper (pAAV/Ad) plasmids; the titers of the two types of preparations did not vary in a consistent way. When the Detroit 6 cells were split twice and allowed to become confluent again, a much smaller proportion of cells expressed the β-gal gene. Expressing cells were clustered (Fig 1B), suggesting viral integration shortly after infection in a single cell that gave rise to a clone of expressing progeny. The disparity between the proportion of cells expressing the β-gal gene shortly after viral exposure, and the number exhibiting stable expression, suggest that viral uptake and initial gene expression may occur more efficiently than the integration step that leads to persistence of the rAAV genome. Retention of rAAV as an episome in the cluster of cells seems less likely, as most initially expressing cells had lost signal. Because the cells had been split twice before analysis, infection by an undispersed aggregate of virus seems unlikely, but cannot be completely ruled out. The frequency of positive

PAGE 64/77 * RCVD AT 8/29/2005 7:17:05 PM [Eastern Daylight Time] * SVR:USPTO-EFXRF-6/26 * DNIS:2738300 * CSID:6504936811 * DURATION (mm-ss):60-28

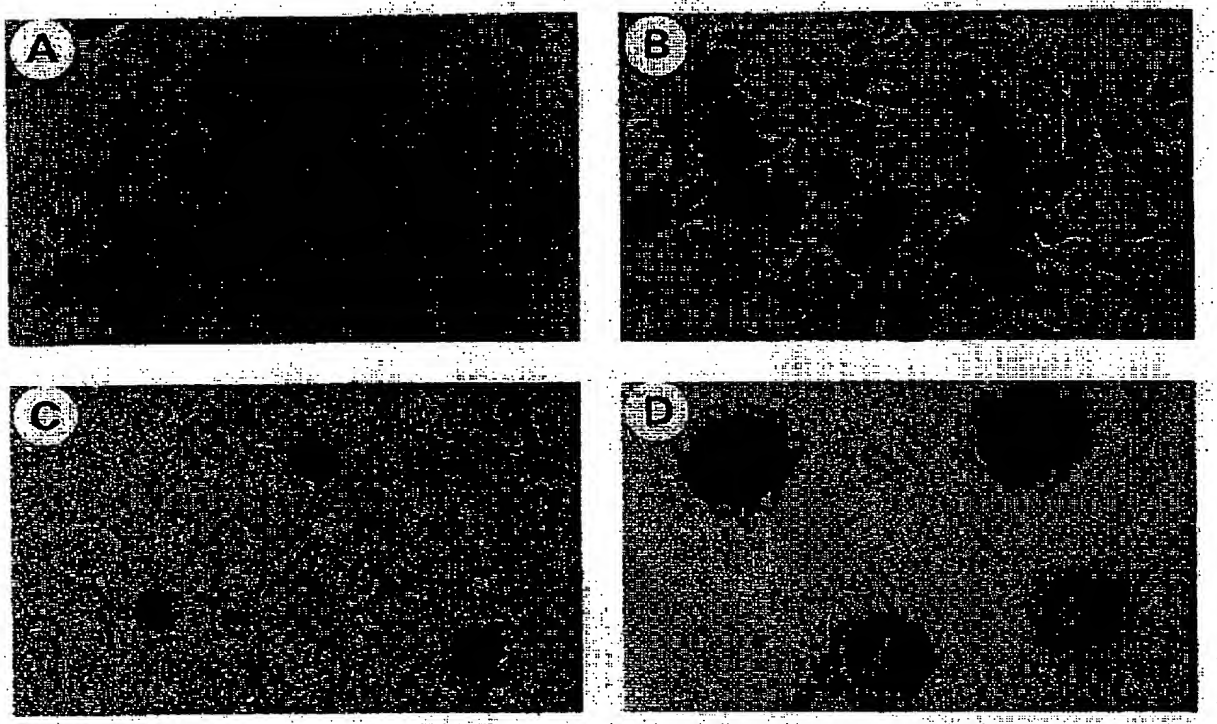

Fig 1. Expression of the β-gal gene after rAAV-mediated gene transfer. (A) Titering of viral preparations on Detroit 6 (D6) cells. D6 cells at 50% to 80% confluency in a 3.5-cm plate were infected by adding 100 μL of virus preparation to 1 mL of medium. After 16 hours, the cells were fixed, washed, and stained for 36 hours as described in Materials and Methods. (B) Persistent expression of the β-gal gene in D6 cells after rAAV-mediated gene transfer. D6 cells were infected by exposure to virus for 12 hours and passaged twice over a period of 7 days. Occasional foci of cells staining positively for β-gal were identified after in situ fixation and staining of the cells. (C) rAAV-mediated transfer of the β-gal gene into human erythroleukemia cells. K562 cells at a concentration of 2×10^5 cells/mL were incubated at a multiplicity of infection of approximately one with rAAV–β-Gal for 48 hours at 37°. The cells were washed and cultured in vitro for an additional 5 days. A cytospin preparation was made, fixed, and stained as described in Materials and Methods. (D) Transfer and expression of the β-gal gene in human $CD34^+$ progenitors. Progenitors were enriched 61-fold by CD34 immunoselection, as determined by clonogenic assay; 5×10^4 cells were incubated in 1 mL of bone marrow cell culture medium and 1 mL of virus preparation medium for 48 hours. Six hundred microliters of cell suspension was mixed with 200 μL of the X-gal stain and the culture continued for 16 hours. A cytospin preparation was then prepared.

clusters approximated the frequency with which we previously recovered G418 resistance colonies with vectors containing the neomycin phosphotransferase (neo^R) gene[32,33] supporting our interpretation that the rAAV β-gal genome has integrated in a small proportion of initially infected Detroit 6 cells (Fig 1B).

Transduction of human erythroleukemia cells was also achieved with the rAAV–β-gal vector. Approximately 2% to 3% of cells exposed briefly to the virus at an MOI of approximately 1 expressed the β-gal gene 5 days later (Fig 1C). Similarly, exposure of $CD34^+$ immunoselected human progenitor cells to the virus for 3 days at an MOI of 1 to 10 resulted in expression of the β-gal gene in 60% to 70% of the cells. Control K562 or $CD34^+$ selected cells showed no nuclear staining; low-level, nonspecific cytoplasmic staining was avoided by maintaining the pH of the washing buffer at greater than 7.5. These data established that viral uptake and rAAV-mediated gene expression could be achieved at high efficiency in hematopoietic cells.

rAAV–β-Gal–mediated gene transfer into primate clonogenic hematopoietic progenitors. Attempts to detect β-gal activity in intact mature colonies were confounded by the fact that nuclear and cytoplasmic activities could not be distinguished in intact colonies and background staining was variably high. Hence, we developed a quantitative PCR assay to detect the rAAV genome in individual colonies. A cell line having one integrated copy of the β-gal gene per cell was used as a control. Conditions were found for which the signal intensity generated with the β-gal primers was proportional to the concentration of the rAAV genome over a broad range of total DNA input (Fig 2). The β-actin amplification could be used to verify that DNA from individual colonies gave a readily detectable PCR product and, by comparing its intensity to that of the β-gal PCR product, we could estimate the copy number of the rAAV genome.

Shown in Fig 3 is the application of this assay to the analysis of colonies derived from human progenitors exposed to an rAAV virus preparation, after heat inactivation of adenovirus, at an MOI of approximately 1 for 24 hours. After the infection interval was completed, the cells were

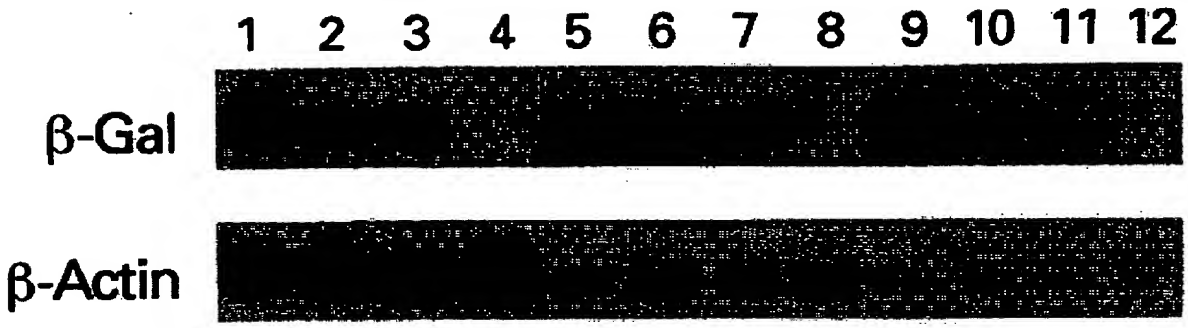

Fig 2. Calibration and sensitivity of the PCR reactions for detection of β-gal and β-actin coding sequences. Lanes 1 through 4 contain 1,000 ng of total DNA, lanes 5 through 8 contain 100 ng, and lanes 9 through 12 contain 10 ng. Each lane contains human DNA or mouse DNA from a cell line containing one integrated copy of the β-gal gene or mixtures thereof as follows: lane 1, 1,000 ng β-gal DNA; lane 2, 900 human DNA and 100 ng β-gal DNA; lane 3, 990 ng human DNA and 10 ng β-gal DNA; lane 4, 1,000 ng human DNA; lane 5, 100 ng β-gal DNA; lane 6, 90 ng human DNA and 10 ng β-gal DNA; lane 7, 99 ng human DNA and 1 ng β-gal DNA; lane 8, 100 ng human DNA; lane 9, 10 ng mouse β-gal DNA; lane 10, 9 ng human DNA and 1 ng β-gal DNA; lane 11, 9.9 ng human DNA and 0.1 ng β-gal DNA; lane 12, 10 ng human DNA. The β-actin coding sequences in mouse and human DNA amplified equivalently. The actin PCR product was generated with 25 cycles and visualized with a 20-minute exposure, whereas the β-gal–amplified PCR products were generated with 30 cycles and visualized with a 30-minute exposure.

plated in methylcellulose under standard conditions. Individual colonies were plucked when mature at 12 to 14 days. DNA from seven colonies gave an amplified β-gal signal of variable intensity, but in the range comparable to that of the β-actin control, suggesting that the viral genome was present at approximately single-copy equivalence in all cells of the colony. Four colonies were negative and one indeterminate (a β-actin signal was not generated from its DNA).

Shown in Fig 4 is an analogous experiment with CD34⁺ immunoselected rhesus hematopoietic progenitors infected with a vector preparation that had been heated for 1 hour at 55°C to inactivate the adenovirus. At a low MOI, heat inactivation of the adenovirus appeared to enhance the frequency of transfer of the rAAV genome (data not shown). Results are shown for 15 colonies. Five were negative, five gave a signal intensity approximately 50% of that of γ-globin, and the remaining five gave equivalent signal intensities with the two primer pairs. These data suggested that the proviral copy number may vary among colonies, and raised the possibility that integration occurs in only a proportion of the initial cells derived from a single progenitor.

Integration of wild-type AAV into chromosome 19 in hematopoietic progenitors. Wild-type[24-28] but not recombinant AAV[31] integrates into a preferred region on chromosome 19. To assess site-specific integration in primary hematopoietic progenitors, we exposed human CD34⁺ immunoselected cells to wild-type virus preparations at high MOI (100 to 1,000). After culture for 36 hours in the presence of virus, progenitors were plated in methylcellulose and the colonies allowed to mature over 12 to 14 days. DNA

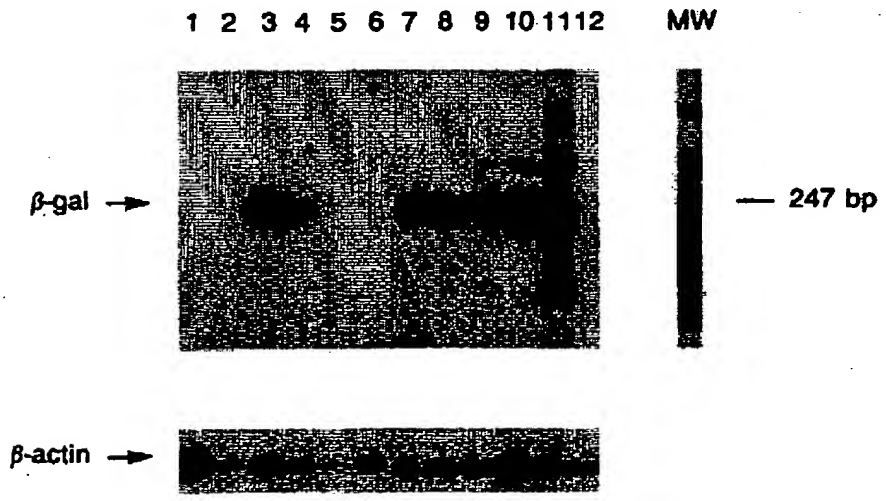

Fig 3. Detection of the rAAV–β-Gal genome in individual human hematopoietic progenitor-derived colonies. DNA from 12 separate colonies were analyzed by PCR with primers specific for the β-gal or the β-actin coding sequences. One colony (5) was indeterminant, as the β-actin signal was not detectable. Seven of the remaining 11 colonies contained β-gal coding sequences and four were scored as negative.

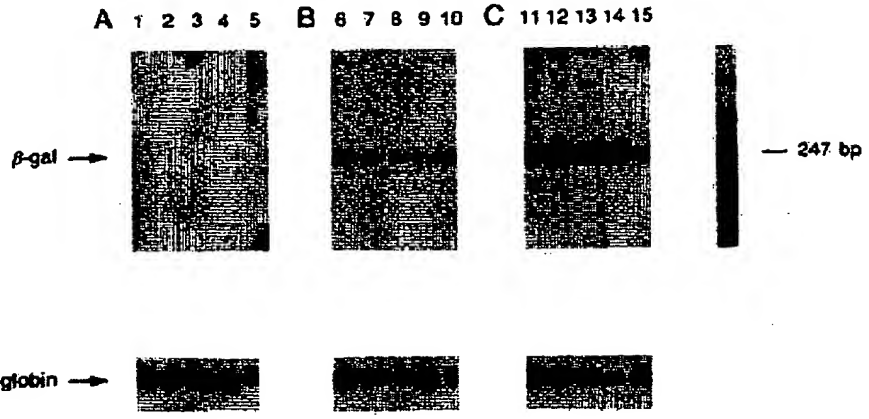

Fig 4. Detection of the rAAV-β-Gal genome in hematopoietic colonies derived from rhesus progenitors. Shown are the results from 15 colonies in which the control primer pair for the rhesus γ-globin gene gave equivalent signals. (A) Five colonies lacking the β-gal coding sequences. (B) DNA from five colonies that gave a β-gal signal of intermediate intensity. (C) Five colonies in which the β-gal signal was equivalent or greater than that derived from the γ-globin gene.

from the majority of colonies (70% to 80%) generated an amplification product with a primer pair specific for the AAV genome of intensity comparable to, or greater than, that achieved with the β-actin primers (Fig 5). Because of the high estimated MOI, the potential that residual virus contributed to the signal for some colonies cannot be excluded. All colonies were derived from a single donor; the negative colonies establish that this individual was not harboring a latent AAV infection in bone marrow.

DNA from pools of 40 to 80 colonies or DNA from individual colonies were analyzed using two sets of nested primers that span the potential junction between the AAV genome and chromosome 19 DNA sequences. The pools and all of the colonies gave positive signals when analyzed for wild-type AAV DNA sequences by PCR. Duplicate samples from one pool gave a positive signal on the integration site analyses (Fig 6). These PCR-amplified products were subcloned into a bacterial plasmid and the sequence determined. A novel junction was defined between the truncated inverted terminal repeat of AAV and chromosome 19 (Fig 7). DNA from four of 27 individual colonies, all of which were positive for wild-type AAV sequence, gave a junction amplification product that annealed to chromosome 19 and AAV genome probes. Three of these were also cloned and sequenced and shown to contain a novel junction between chromosome 19 and the AAV inverted terminal repeat (data not shown). These data suggested that association of wild-type viral DNA with progenitor-derived colonies occurs with high frequency, but that site-specific integration of the AAV genome into chromosome 19 is relatively rare.

DISCUSSION

These experiments were designed to evaluate the potential of rAAV to transcribe and express genes in primary hematopoietic progenitor cells. A high frequency of gene transfer and expression of the β-gal reporter gene was observed in progenitor cells, highly purified by positive immunoselection. A large proportion of colonies derived from these progenitors contained rAAV DNA at a concentration equivalent to one to two copies of the viral genome per cell. These data establish the potential of rAAV to infect human hematopoietic progenitors, but the efficiency of stable integration of the vector genome was not determined. Previous work has established that wild-type AAV will integrate into a preferred site on chromosome 19 in tissue culture cells.[25-28] To address the issue of AAV integration in hematopoietic progenitor cells, we tested wild-type AAV for targeted integration into chromosome 19 using a PCR-based assay. While we documented integration of the AAV genome into the preferred site on chromosome 19, this occurrence seemed to be a relatively rare event.

Because the AAV vector genome is packaged as a single-stranded DNA molecule, expression of the β-gal gene from the vector, as demonstrated in these experiments, argues for replication of the complementary strand after viral infection.[2,23] This step may not require cell division, since we

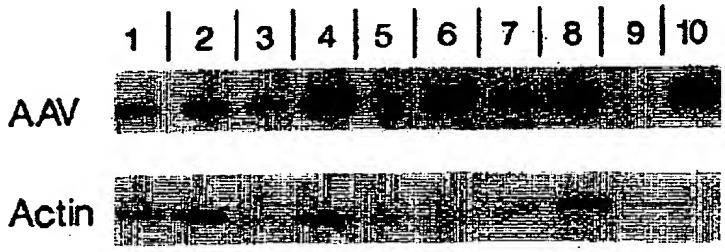

Fig 5. Integration of wild-type AAV into hematopoietic progenitors. DNA from 10 individual colonies was analyzed with primers specific for β-actin (control, below), and primers specific for the coding sequences of the AAV capsid protein. Eight colonies gave a positive signal, and two (5 and 9) were negative.

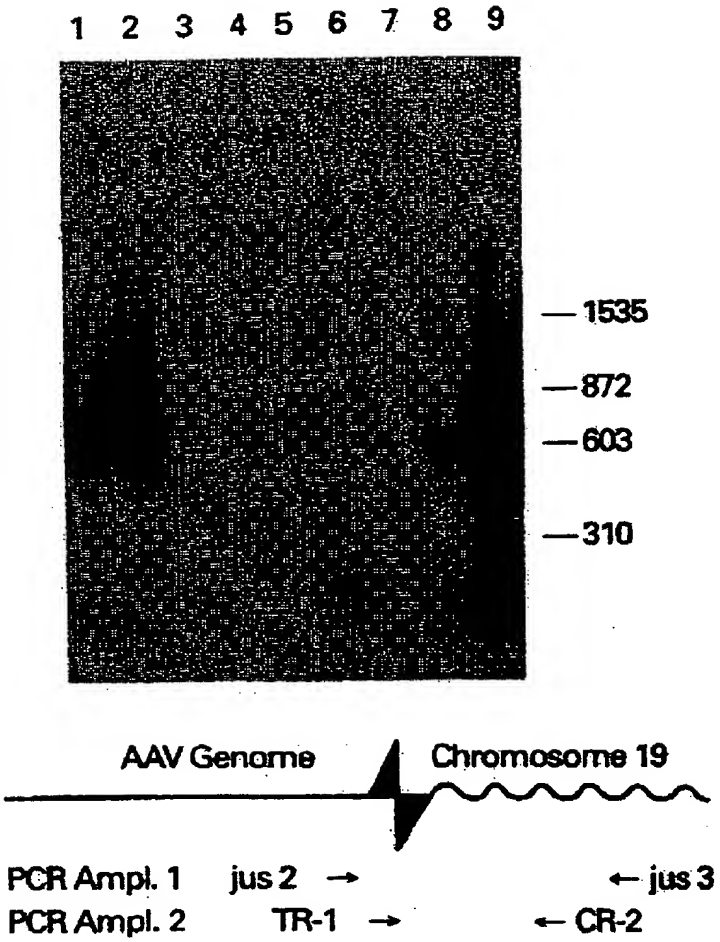

Fig 6. Integration site analysis of the wild-type AAV genome. DNA from pools of colonies or from single colonies was amplified using primer sets that span the potential junction between the AAV genome and the chromosome 19. Lanes 1, 2, 5, and 6 show DNA from pools of 40 to 80 individual colonies. Lanes 3 and 4 show DNA from single colonies. Lane 7 shows nonradioactive gel markers that gave the calibration lengths listed on the right. Lanes 8 and 9 show DNA from cell lines latently infected with the wild-type AAV genome. The multiple bands in lane 8 are thought to arise because the intact inverted terminal repeat present in this cell line causes formation of several discrete PCR products. Amplification was performed with nested primers that span the putative integration junction as shown in the diagram.

have recently observed transduction of β-gal in vivo in rat brain cells using AAV vectors (X. Xiao and R.J. Samulski, unpublished observation). Subsequent integration and, therefore, persistence of the AAV genome may not occur in all infected cells. Indeed, we found that most Detroit 6 cells expressed a reporter gene shortly after infection, but only a minority appeared to exhibit continued expression of the rAAV genome.

Very sensitive PCR assays can detect low levels of AAV DNA unassociated with cells in methylcellulose culture medium (unpublished observations), presumably because the virus particles to which the progenitors were exposed are stable during 10 to 14 days of incubation. These technical concerns distinguish analysis of rAAV from retroviral vectors where detection of proviral DNA can be equated with genome integration.[2] We scored colonies as positive only if the signal intensity was comparable to a cellular gene control (Fig 2). rAAV has recently been reported to infect murine clonogenic hematopoietic progenitors.[41] Neo^R colonies were observed and viral DNA was demonstrated in a proportion of these colonies by PCR analysis. Although these data are interesting and potentially important, there are a number of issues of concern. First, the ability of cells to grow for several days in G418 does not establish integration of the neo^R gene. Second, control amplification of a cellular gene was not performed, so that there was no calibration of the rAAV PCR-derived signal to verify that the genome was present in single-copy equivalence. In our experiments, we could not verify expression from the transduced rAAV genome using a reverse transcription-PCR (RT-PCR) because the spliced RNA species predicted by the small intron in the proviral genome (Fig 8) could not be detected (data not shown). In recent experiments, we have used a rAAV vector containing a mutationally marked human γ-globin gene, linked to elements from the β-globin gene cluster locus control region, to transduce human erythroid progenitors. Spliced globin mRNA derived from the rAAV-transduced gene was present at high levels in the majority of colonies (J. Miller and A. Nienhuis, unpublished observations), confirming the ability of rAAV to transduce human hematopoietic progenitors with high frequency.

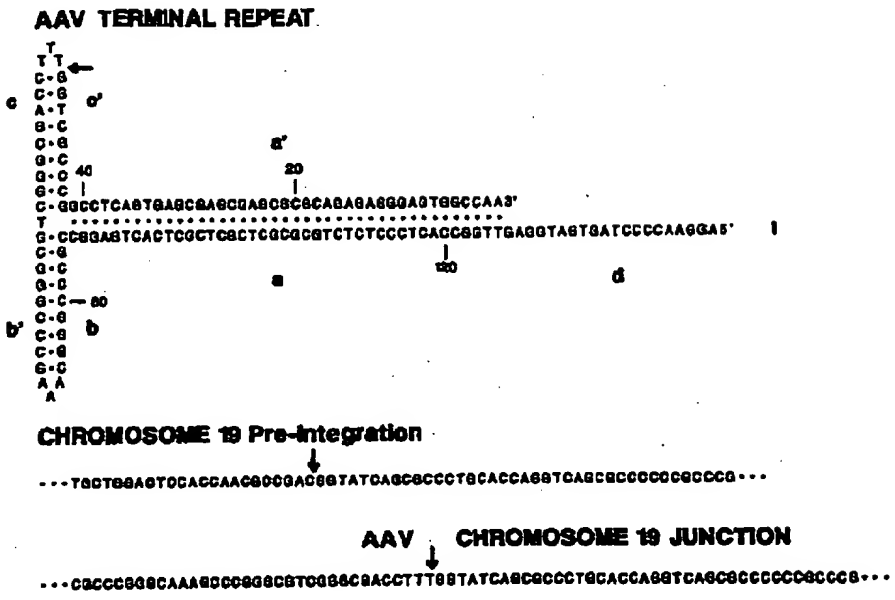

Fig 7. Sequence of a AAV-chromosome 19 junction generated by infection of a human hematopoietic progenitor with wild-type AAV. Shown is a sequence of the AAV terminal repeat; the horizontal arrow indicates the junction site. The sequence of chromosome 19 is shown[29,30] with the vertical arrow defining the junction position.

While data are accumulating supporting the use of this vector for hematopoietic gene delivery, preparation of rAAV vectors remains problematic. Viral preparations vary widely in titer, and are significantly contaminated with adenovirus. Needed are defined packaging lines that express the required helper functions of adenovirus and the packaging components of AAV. Conditional or inducible expression of the proteins may be needed because the rep function of AAV and the required adenovirus proteins may inhibit cell growth.[23]

Despite the remaining technical problems, rAAV appears to be a highly promising vector system. Previously, we had established that integration of one to two unrearranged genomes occurs in the majority of latently infected cells.[31,32] AAV's nonpathogenicity and potential for preferred chromosomal integration sites makes it a highly attractive vector system for gene therapy applications. Our demonstration that hematopoietic progenitors are infected with high efficiency supports future efforts to develop this vector system.

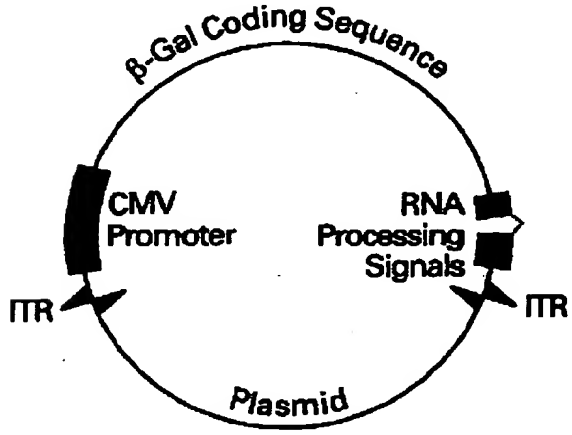

Fig 8. General organization of the β-gal vector in plasmid form. The CMV E1-A promoter was linked to the β-gal coding sequences followed by mP-1 RNA-processing signals. This entire cassette is flanked by the AAV inverted terminal repeats (ITR). This plasmid was constructed as described in Materials and Methods.

REFERENCES

1. Karlsson S: Treatment of genetic defects in hematopoietic cell function by gene transfer. Blood 78:2481, 1991

2. Nienhuis AW, Walsh CE, Liu J: Viruses as therapeutic gene transfer vectors, in Young NS (ed): Viruses in Bone Marrow. New York, NY, Dekker, 1993, p 353

3. Baltimore D: Gene therapy. Intracellular immunization. Nature 335:396, 1988

4. Abel T, Maniatis T: Mechanisms of eukaryotic gene regulation, in Stamatoyannopoulos G, Nienhuis AW, Majerus P, Varmus HE (eds): Molecular Basis of Blood Diseases (ed 2). Philadelphia, PA, Saunders, 1993, p 33

5. Stamatoyannopoulos G, Nienhuis AW: Hemoglobin switching, in Stamatoyannopoulos G, Nienhuis AW, Majerus P, Varmus HE (eds): Molecular Basis of Blood Diseases (ed 2). Philadelphia, PA, Saunders, 1993, p 107

6. Nienhuis AW, McDonaugh KT, Bodine DM: Gene transfer into hematopoietic stem cells. Cancer 67:2700, 1991

7. Williams DA, Lemischka IR, Nathan DG, Mulligan RC: Introduction of new genetic material into pluripotent haematopoietic stem cells of the mouse. Nature 310:476, 1984

8. Dick JE, Magli MC, Huszar D, Phillips RA, Bernstein A: Introduction of a selectable gene into primitive stem cells capable of long-term reconstitution of the hemopoietic system of W/Wv mice. Cell 42:71, 1985

9. Lemischka IR, Raulet DH, Mulligan RC: Developmental po-

tential and dynamic behavior of hematopoietic stem cells. Cell 45:917, 1986

10. Bodine DM, Karlsson S, Nienhuis AW: Combination of interleukins 3 and 6 preserves stem cell function in culture and enhances retrovirus-mediated gene transfer into hematopoietic stem cells. Proc Natl Acad Sci USA 86:9987, 1989

11. Bodine DM, McDonagh KT, Seidel NE, Nienhuis AW: Survival and retrovirus infection of murine hematopoietic stem cells in vitro: effects of 5-FU and method of infection. Exp Hematol 19:206, 1991

12. Miller AD: Retroviral vectors. Curr Top Microbiol Immunol 158:1, 1992

13. Miller DG, Adam MA, Miller AD: Gene transfer by retrovirus vectors occurs only in cells that are actively replicating at the time of infection. Mol Cell Biol 10:4239, 1990

14. Springett GM, Moen RC, Anderson S, Blaese RM, Anderson WF: Infection efficiency of T lymphocytes with amphotropic retroviral vectors is cell cycle dependent. J Virol 63:3865, 1989

15. Lim G, Apperley JF, Orkin SH, Williams DA: Long-term expression of human adenosine deaminase in mice transplanted with retrovirus-infected hematopoietic stem cells. Proc Natl Acad Sci USA 86:8892, 1989

16. Wilson JM, Danos O, Grossman M, Raulet DH, Mulligan RC: Expression of human adenosine deaminase in mice reconstituted with retrovirus-transduced hematopoietic stem cells. Proc Natl Acad Sci USA 87:439, 1990

17. Kaleko M, Garcia JV, Osborne WR, Miller AD: Expression of human adenosine deaminase in mice after transplantation of genetically-modified bone marrow. Blood 75:1733, 1990

18. Correll PH, Colilla S, Dave HP, Karlsson S: High levels of human glucocerebrosidase activity in macrophages of long-term reconstituted mice after retroviral infection of hematopoietic stem cells. Blood 80:331, 1992

19. Schuening FG, Kawahara K, Miller AD, To R, Goehle S, Stewart D, Mullally K, Fisher L, Graham TC, Appelbaum FR: Retrovirus-mediated gene transduction into long-term repopulating marrow cells of dogs. Blood 78:2568, 1991

20. Carter RF, Abrams-Ogg AC, Dick JE, Kruth SA, Valli VE, Kamel-Reid S, Dube ID: Autologous transplantation of canine long-term marrow culture cells genetically marked by retroviral vectors. Blood 79:356, 1992

21. van Beusechem VW, Kukler A, Heidt PJ, Valerio D: Long-term expression of human adenosine deaminase in rhesus monkeys transplanted with retrovirus-infected bone-marrow cells. Proc Natl Acad Sci USA 89:7640, 1992

22. Bodine DM, Moritz T, Donahue RE, Luskey BD, Kessler SW, Martin DIK, Orkin SH, Nienhuis AW, Williams DA: Long-term expression of a murine adenosine deaminase gene in Rhesus hematopoietic cells of multiple lineages following retroviral-mediated gene transfer into CD34$^+$ bone marrow cells. Blood 82:1975, 1993

23. Muzyczka N: Use of adeno-associated virus as a general transduction vector for mammalian cells. Curr Top Microbiol Immunol 158:97, 1992

24. Samulski RJ: Adeno-associated virus: Integration at a specific chromosomal locus. Curr Opin Genet Dev 3:74, 1993

25. Samulski RJ, Zhu X, Xiao X, Brook JD, Housman DE, Epstein N, Hunter LA: Targeted integration of adeno-associated virus (AAV) into human chromosome 19. EMBO J 10:3941, 1991

26. Kotin RM, Berns KI: Organization of adeno-associated virus DNA in latently infected Detroit 6 cells. Virology 170:460, 1989

27. Kotin RM, Siniscalco M, Samulski RJ, Zhu XD, Hunter L, Laughlin CA, McLaughlin S, Muzyczka N, Rocchi M, Berns KI: Site-specific integration by adeno-associated virus. Proc Natl Acad Sci USA 87:2211, 1990

28. Kotin RM, Menninger JC, Ward DC, Berns KI: Mapping and direct visualization of a region-specific viral DNA integration site on chromosome 19q13-qter. Genomics 10:831, 1991

29. Samulski RJ, Chang LS, Shenk T: Helper-free stocks of recombinant adeno-associated viruses: Normal integration does not require viral gene expression. J Virol 63:3822, 1989

30. Lebkowski JS, McNally MM, Okarma TB, Lerch LB: Adeno-associated virus: A vector system for efficient introduction and integration of DNA into a variety of mammalian cell types. Mol Cell Biol 8:3988, 1988

31. Walsh CE, Liu JM, Xiao X, Young NS, Nienhuis AW, Samulski RJ: Regulated high level expression of a human gamma-globin gene introduced into erythroid cells by an adeno-associated virus vector. Proc Natl Acad Sci USA 89:7257, 1992

32. Miller JL, Walsh CE, Ney PA, Samulski RJ, Nienhuis AW: Single copy transduction and expression of human gamma-globin in K562 erythroleukemia cells using recombinant adeno-associated virus ectors: The effect of mutations in NF-E2 and GATA-1 binding motifs within the HS2 enhancer. Blood 82:1900, 1993

33. Graham FL, Smiley J, Russell WC, Naiva R: Characteristics of a human cell line transformed by DNA from adenovirus type 5. J Gen Virol 36:50, 1977

34. Papayannopoulou T, Nakamoto B, Kurachi S, Tweeddale M, Messner H: Surface antigenic profile and globin phenotype of two new human erythroleukemia lines: Characterization and interpretations. Blood 72:1029, 1988

35. Lanford RE, White RG, Dunham RG, Kanda P: Effect of basic and nonbasic amino acid substitutions on transport induced by simian virus 40 T-antigen synthetic peptide nuclear transport signals. Mol Cell Biol 8:2722, 1988

36. Peschon JJ, Behringer RR, Brinster RL, Palmiter RD: Spermatid-specific expression of protamine 1 in transgenic mice. Proc Natl Acad Sci USA 84:5316, 1987

37. McLaughlin SK, Collis P, Hermonat PL, Muzyczka N: Adeno-associated virus general transduction vectors: Analysis of proviral structures. J Virol 62, 1963, 1988

38. Janes JR, Rubenstein JLR, Nicholas JF: Use of a recombinant retrovirus to study post-implantation cell lineage in mouse embryos. EMBO J 5:3133, 1986

39. Donahue RE, Kessler SW, Bodine D, McDonagh K, Dunbar C, Goodman S, Agricola B, Byrne E, Raffeld M, Moen R, Bacher J, Zsebo KM, Nienhuis AW: Helper virus induced T cell lymphoma in nonhuman primates after retroviral mediated gene transfer. J Exp Med 175:1125, 1992

40. Sorrentino B, Ney P, Bodine D, Nienhuis AW: A 46 base pair enhancer sequence within the locus activating region is required for induced expression of the gamma-globin gene during erythroid differentiation. Nucleic Acids Res 18:2721, 1990

41. Zhou SZ, Broxmeyer HE, Cooper S, Harrington MA, Srivastava A: Adeno-associated virus 2-mediated gene transfer in murine hematopoietic progenitor cells. Exp Hematol 21:928, 1993

Single-Copy Transduction and Expression of Human γ-Globin in K562 Erythroleukemia Cells Using Recombinant Adeno-Associated Virus Vectors: The Effect of Mutations in NF-E2 and GATA-1 Binding Motifs Within the Hypersensitivity Site 2 Enhancer

By Jeffery L. Miller, Christopher E. Walsh, Paul A. Ney, Richard Jude Samulski, and Arthur W. Nienhuis

The use of recombinant adeno-associated virus (rAAV) vectors provides a new strategy to investigate the role of specific regulatory elements and *trans*-acting factors in globin gene expression. We linked hypersensitivity site 2 (HS2) from the locus control region (LCR) to a $^{A}\gamma$-globin gene ($^{A}\gamma^{*}$) mutationally marked to allow its transcript to be distinguished from endogenous γ-globin mRNA. The vector also contains the phosphotransferase gene that confers resistance to neomycin (Neo^{R}). HS2 region mutations within the NF-E2 motifs prevented NF-E2 binding while preserving AP-1 binding. Another set in the GATA-1 motif prevented binding of the factor. Several Neo^{R} K562 clones containing a single unrearranged RAAV genome with the $^{A}\gamma^{*}$ gene linked to the native HS2 core fragment (WT), mutant NF-E2 HS2 (mut-NFE2), mutant GATA-1 HS2 (mut-GATA1), or no HS [(−)HS] were identified. In uninduced K562 cells, mut-NFE2 clones expressed $^{A}\gamma^{*}$ mRNA at the same level as the WT clones, compared with a lack of $^{A}\gamma^{*}$ signal in the (−)HS2 clones. However, hemin induction of mut-NFE2 clones did not result in an increase in the $^{A}\gamma^{*}$ signal above the level seen in uninduced cells. Mut-GATA1 clones expressed the $^{A}\gamma^{*}$ mRNA at the same level as WT clones in both uninduced and induced cells. Thus, GATA-1 binding to this site does not appear to be required for the enhancing function of HS2 in this context. This single-copy rAAV transduction model is useful for evaluating the effects of specific mutations in regulatory elements on the transcription of linked genes.

This is a US government work. There are no restrictions on its use.

THE HUMAN β-GLOBIN complex contains a 5′ locus control region (LCR) that confers high-level, position-independent expression on linked globin genes in transgenic mice.[1] This region is defined by a series of DNase I hypersensitive sites (HS1-5).[2] HS2 has been shown to contain a central core that is sufficient for its enhancing function in mouse erythroleukemia (MEL) cells and in transgenic mice.[3] Within this core are tandem NF-E2 binding motifs that are necessary[4-8] but not sufficient[3,9] for high-level expression of the linked genes. AP-1, which also binds to these sites, does not provide erythroid-specific enhancing activity. More of the HS2 core region or other hypersensitivity sites from the LCR[7,10,11] are needed to allow maximal enhancing activity of the NF-E2 motifs.

Adeno-associated virus (AAV) has a small single-stranded DNA genome flanked by inverted terminal repeats (ITR) that is packaged into a protein capsid.[12] The ITR contain *cis*-acting sequences required for encapsidation, replication, and integration,[13-15] but do not contain transcriptional control elements.[16] As implied by the name, AAV propagate in nature only in association with a helper adenovirus on which AAV depend for productive cellular infection.[17,18] Most humans have detectable serum antibodies to AAV, but the viruses are nonpathogenic.[19] In the absence of adenovirus, AAV may exist in a latent state, integrated in the host cell genome.[20]

From the Clinical Hematology Branch, National Heart, Lung and Blood Institute, National Institutes of Health, Bethesda, MD; and the Department of Biological Sciences, University of Pittsburgh, PA.

Submitted February 16, 1993; accepted May 24, 1993.

Address reprint requests to Arthur W. Nienhuis, MD, NIH, Bldg 10, Rm 7C103, Bethesda, MD 20892.

The publication costs of this article were defrayed in part by page charge payment. This article must therefore be hereby marked "advertisement" in accordance with 18 U.S.C. section 1734 solely to indicate this fact.

This is a US government work. There are no restrictions on its use.

0006-4971/93/8206-0026$0.00/0

Recombinant AAV (rAAV) have been shown to function as efficient gene transfer vectors.[21] Only the ITR are required for encapsidation of the vector genome.[13,22] The nonstructural and capsid proteins can be provided by a complementing helper genome from which the AAV ITR have been removed to prevent encapsidation. Cotransfection with plasmids containing the vector or helper genome and infection with wild-type adenovirus to provide its complementary functions results in release of rAAV and adenovirus. After heat-inactivation of the adenovirus, rAAV infect target cells efficiently and are integrated usually as 1 to 3 unrearranged tandem copies.[21] Recently, a rAAV vector transduction system has been shown to provide high level expression of the $^{A}\gamma^{*}$ globin gene in K562 erythroleukemia cells.[23] When linked to a wild-type HS2 enhancer core region, the $^{A}\gamma^{*}$ gene was transcriptionally active at levels of 40% to 110% of a single chromosomal γ-globin gene.

The goal of these experiments was to study the effects of mutations within the HS2 regulatory region on expression of the $^{A}\gamma^{*}$ gene using the rAAV vector transduction model to generate K562 erythroleukemia cell clones having a single unrearranged integrated vector genome. Previous analyses of HS function have generally relied on transfer methods that lead to multiple-copy integrants. With these methods, the effect of an individual regulatory element can only be inferred after correcting for gene copy number, and cooperative interactions between tandem gene copies are difficult to exclude. For example, in transgenic mice, single-copy versus multiple-copy transgenes appear to have separate requirements for LCR activity.[24] We have shown that the rAAV vector system can be used as a novel strategy for the functional study of regulatory elements present as single-copy integrants.

MATERIALS AND METHODS

Generation of mutant HS2 DNA. Polymerase chain reaction (PCR)-directed site-specific mutagenesis[25] was used to create the mutant *Hin*dIII-*Xba* I fragments shown in Fig 1. pUC 007/HS2[4] served as the template. Inside primers included the substituted

PAGE 71/77 * RCVD AT 8/29/2005 7:17:05 PM [Eastern Daylight Time] * SVR:USPTO-EFXRF-6/26 * DNIS:2738300 * CSID:6504936811 * DURATION (mm-ss):60-28

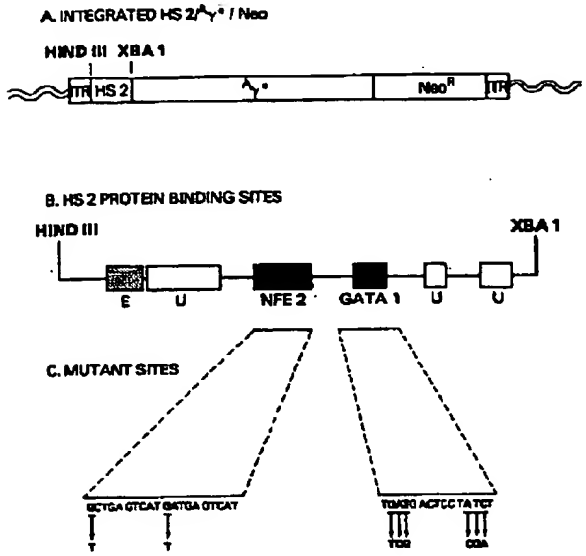

Fig 1. Mutant HS2 regions in integrated rAAV (HS2/$^{A}\gamma^{*}$/Neo^{R}). (A) Schematic representation of integrated rAAV (HS2/$^{A}\gamma^{*}$/Neo^{R}) containing the 374-bp core HS2 region. (B) Expanded view of the HS2 region extending from the *Hin*dIII (GeneBank 8486) to *Xba* I (GeneBank 8860) restriction sites of the human globin LCB. Protein binding regions including NF-E2 and GATA-1 motifs are indicated by boxes. Regions marked E and U denote protein binding from erythroid and ubiquitous cell extracts, respectively.[3] (C) Mutated NF-E2 and GATA-1 protein binding motifs within the HS2 region. Two single-base mutations in the NF-E2 binding motif and paired triple-base mutations in the GATA-1 motif were made, as shown with arrows. The selected mutations prevent their respective protein binding in gel-shift assays.[3,27]

bases and outside primers included the *Hin*dIII and *Xba* I sites. VENT Polymerase (NE Biolabs, Beverly, MA) was used in all PCR rounds (95°C for 1 minute, 55°C for 1 minutes, and 72°C for 1 minute, 30 cycles). Mutant fragments were then digested with *Hin*dIII and *Xba* I and subcloned into plasmid pSP72 (Promega, Madison, WI). Each mutant was then sequenced for structural confirmation using a USB Version 2.0 Kit (US Biochemicals, Cleveland, OH) before final construction of the pAAV/HS2/$^{A}\gamma^{*}$/Neo^{R} vectors.

rAAV. Construction of recombinant virions, infection of K562 erythroleukemia cells, and analysis of globin gene expression using reverse transcriptase-PCR (RT-PCR) has been described previously.[23] rAAV vectors containing wild-type HS2 (WT), no HS2 [(−)HS2], HS2 containing the mutant NF-E2 motif (mut-NFE2), and mutant GATA-1 motif (mut-GATA1) were assembled. All adenovirus and rAAV vector work was performed in a P-2 level laboratory.[24]

Nucleic acid analysis. Genome arrangement and copy number were determined by genomic DNA digestion and Southern blotting.[27] Genomic DNA was digested with *Hin*cII and transferred to Hybond N+ (Amersham, Arlington Heights, IL) after electrophoresis on an agarose gel. The membranes were then probed for γ-globin gene sequences, stripped with 1% sodium dodecyl sulfate (SDS), and reprobed for the Neo^{R} gene sequences.

RNA isolation and analysis using RT-PCR was performed using PCR conditions, primers, and input RNA amounts identical to those previously described.[10] The RT-PCR signals were used to calculate the level of $^{A}\gamma^{*}$ gene expression relative to endogenous γ-globin gene expression (Table 1). This method for quantitation of RNA expression from the transduced $^{A}\gamma^{*}$ gene has been shown to closely parallel values determined by RNase protection assays.[10,23] Comparison of the mRNA-derived signals from the endogenous and transduced γ-globin genes was made using the densitometry function of a Molecular Dynamics phosphor-imager (Molecular Dynamics, Sunnyvale, CA).

RESULTS

Southern blot analysis. Ten single neomycin resistant colonies from each rAAV construct were isolated and analyzed for the presence of an intact HS2/$^{A}\gamma^{*}$ gene region and for single-copy integration (Fig 2). The γ-globin probe was used to identify DNA from clones that had an rAAV-transferred globin gene of proper insert size. The Neo probe, used to identify DNA representing rAAV-host genome junction fragments, confirmed integration and provided an accurate assignment of copy number. The criteria used to identify colonies of transduced K562 cells containing a single integrated rAAV genome were as follows. γ-Probed lanes hav-

Table 1. Hemin-Induced $^{A}\gamma^{*}$ Globin Expression Relative to Endogenous γ-Globin Expression

Construct	Pools (%)*	Individual Clones (%)	
WT HS2	27 ± 6.3	Mean	66 ± 24.5†
		1.	75 ± 9.8‡
		2.	78 ± 9.9
		3.	29 ± 7.2
		4.	81 ± 8.2
No HS2	≤5	Mean	7 ± 2.1 (P = .02)§
		1.	9 ± 3.4
		2.	8 ± 2.3
		3.	≤5
Mut-NFE2	8 ± 1.2 (P = .006)	Mean	19 ± 6.0 (P = .04)
		1.	13 ± 4.2
		2.	15 ± 4.7
		3.	26 ± 3.2
		4.	22 ± 4.1
Mut-GATA1	40 ± 30.8 (NS)	Mean	97 ± 31.7 (NS)
		1.	62 ± 8.9
		2.	106 ± 13.0
		3.	123 ± 6.3

Abbreviation: NS, not significant.

* Percentages reflect mean transduced $^{A}\gamma^{*}$ RT-PCR signal from the samples shown in Fig. 3 expressed as a percentage of the signal from a single endogenous γ-globin gene. The percentages were calculated as follows:

$$\frac{^{A}\gamma^{*}\ \text{RNA}}{\gamma\ \text{RNA}} \times \frac{\text{Endogenous Gene Copy No.}}{^{A}\gamma^{*}\ \text{Gene Copy No.}} \times 100$$

Signals at or near background level were assigned a lower limit of ≤5%.

† Mean and standard deviation of all determinations on the individual clones.

‡ The assay was performed in triplicate on the individual clones.

§ Statistical analyses were performed using a Wilcoxon's rank sum test.[30] All P values reflect comparisons made with the WT HS2 group.

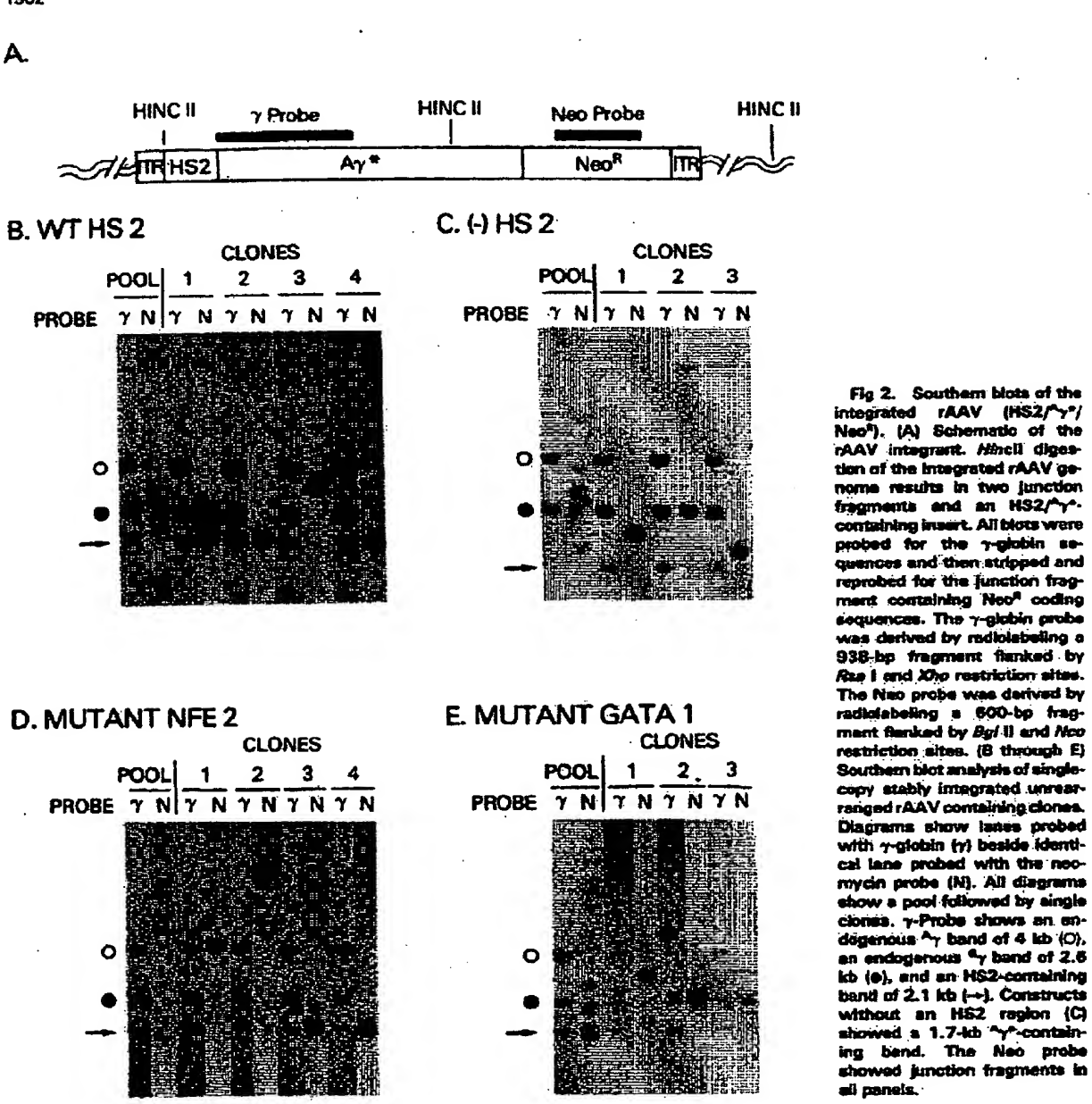

Fig 2. Southern blots of the integrated rAAV (HS2/$^{A}\gamma^{*}$/Neo^{R}). (A) Schematic of the rAAV integrant. *Hin*cII digestion of the integrated rAAV genome results in two junction fragments and an HS2/$^{A}\gamma^{*}$-containing insert. All blots were probed for the γ-globin sequences and then stripped and reprobed for the junction fragment containing Neo^{R} coding sequences. The γ-globin probe was derived by radiolabeling a 938-bp fragment flanked by *Rsa* I and *Xho* restriction sites. The Neo probe was derived by radiolabeling a 600-bp fragment flanked by *Bgl* II and *Nco* restriction sites. (B through E) Southern blot analysis of single-copy stably integrated unrearranged rAAV containing clones. Diagrams show lanes probed with γ-globin (γ) beside identical lane probed with the neomycin probe (N). All diagrams show a pool followed by single clones. γ-Probe shows an endogenous $^{A}\gamma$ band of 4 kb (○), an endogenous $^{G}\gamma$ band of 2.6 kb (●), and an HS2-containing band of 2.1 kb (→). Constructs without an HS2 region (C) showed a 1.7-kb $^{A}\gamma^{*}$-containing band. The Neo probe showed junction fragments in all panels.

ing an $^{A}\gamma^{*}$ band of correct size for the intact transferred $^{A}\gamma^{*}$ gene and intensity of approximately one-third that of the endogenous bands were selected. Neo-probed signals from the selected lanes were checked for the presence of a single band representing a single junction fragment. Lanes containing bands other than those described were felt to represent nonclonal populations versus clonal populations having rearranged or multiple-copy integrants.

Pooled K562 populations were derived from 15 individual colonies isolated and combined after 15 days under neomycin selection. The pools were then hemin induced for 3 days before nucleic acid extraction and analysis. Southern blotting showed an average copy number of less than three in 5 pools from each HS2-containing construct (data not shown). Multiple junction fragments seen in the pools (Fig 2) confirm the presence of multiple clones within each population.

DNA from 40 single colonies was analyzed, with 10 for each vector construct. *Hin*cII-digested fragments of duplex rAAV DNA that have not integrated contain a Neo-probed

band of 1.9 kb; no bands of this length were seen (data not shown). Thus, the rAAV genome that conferred neomycin resistance had integrated into the K562 cell genome. As previously reported, a high frequency of clones (6 of 10) derived with the vector lacking the HS2 fragment had a rearranged AAV genome, possibly because this rAAV genome is only 80% the length of the wild-type AAV genome. Of the remaining 30 colonies picked for the other vector constructs, 15 had a single unrearranged rAAV genome as determined by the criteria established above, 4 had 2 or more copies of a unrearranged genome, 2 had a single rearranged genome, 4 had a combination of unrearranged and rearranged genomes, and 5 appeared to be mixture of more than one clone and thus were indeterminate.

RNA expression of the transduced globin gene. Three or four clones with a single unrearranged rAAV vector genome for each construct were grown and studied for the expression of the transduced γ-globin gene. RT-PCR signals from matched, uninduced and hemin-induced populations are shown in Fig 3. RT-PCR signals from the endogenous γ genes were hemin inducible in all pools and clones studied. An estimate of expression relative to a single endogenous γ-globin gene was made by multiplying the ratio of $^{A}\gamma^{*}/\gamma$ by 6 to correct for the endogenous gene copy number. K562 cells are aneuploid for chromosome 11 (3 copies); hence, 6 endogenous γ-globin genes are present. Numerical expression data derived from the hemin-induced signals shown in Fig 3 are summarized in Table 1.

Analysis of RNA from mut-NFE2 clones grown without hemin induction showed a level of $^{A}\gamma^{*}$ expression comparable to the WT HS2 containing uninduced clones (Fig 3C). This level of expression is greater than that seen in the uninduced clones without an HS2 region (Fig 3B). Therefore, HS2 without the NF-E2 binding motif is sufficient for uninduced expression of the transferred gene. In marked contrast to the signal generated by mRNA from the endogenous γ genes of these mutant NF-E2 clones, no appreciable increase in $^{A}\gamma^{*}$ expression was found with hemin induction.

Clones containing the vector genome with the mut-GATA1 HS2 were also analyzed for $^{A}\gamma^{*}$ gene expression (Fig 3D). The pattern of expression mimicked that seen in the WT clones (Fig 3A). Therefore, mutation of a down-

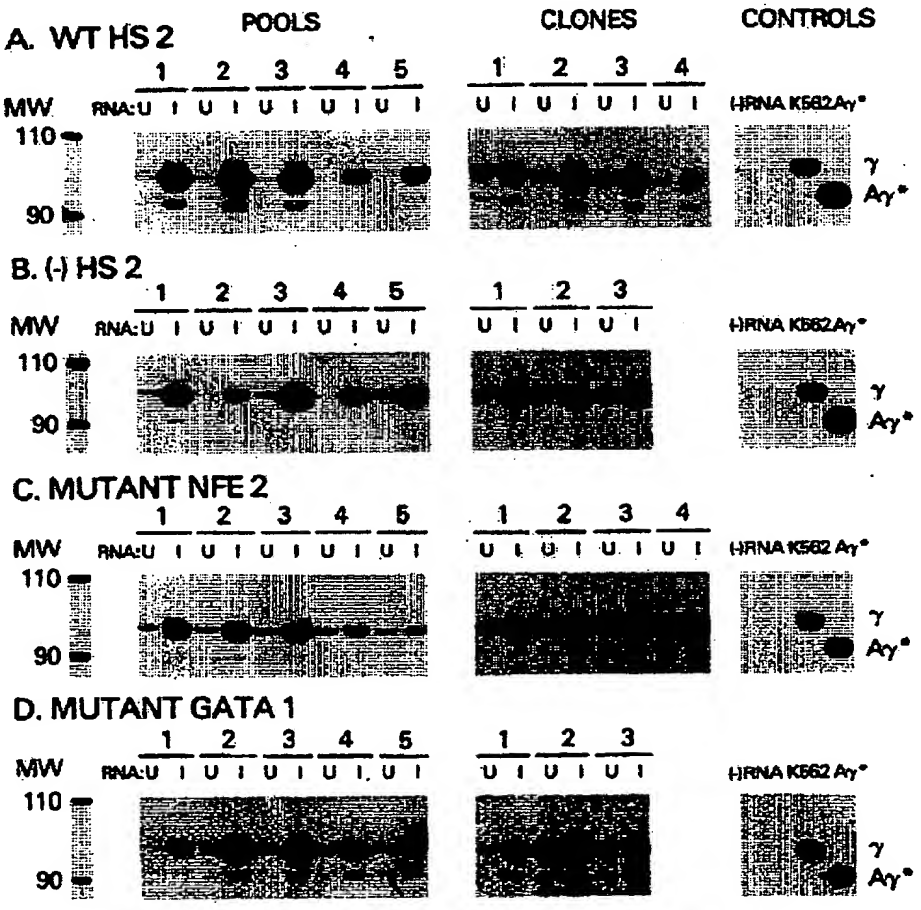

Fig 3. Detection and quantitation of $^{A}\gamma^{*}$ globin mRNA using RT-PCR. Molecular weight markers are shown on the left and controls on the far right. The RT-PCR product from the endogenous γ genes (γ) and the 6 nt shorter RT-PCR product from the transduced marked $^{A}\gamma$ genes ($^{A}\gamma^{*}$) were generated using ^{32}P-labeled dCTP in the PCR master mix. Five pools and three or four individual single-copy clones are shown for each construct. Individual panels (A through D) divide the results according to the HS2 region used in the rAAV constructs (see text for details). PCR products of RNA extracted from uninduced (U) and hemin-induced (I) K562 cells are shown in paired lanes. Matched (−) RT controls for all clones had no bands (data not shown).

6504936811 8/29/2005 4:17 PM PAGE 75/077 Fax Server

stream GATA-1 binding motif did not interfere with the ability of HS2 to enhance γ-globin gene expression using this system. The variability in the level of expression among the pools was greater, as reflected by a larger standard deviation for mut-GATA1 HS2 than for WT HS2 (Table 1), suggesting that the GATA-1 site may influence position-independent expression.

RT-PCR signals from the 20 pooled colonies described above are shown for comparison. The pattern of $^{A}\gamma^{*}$ gene expression seen in the pools was similar to that of the individual clones for each rAAV construct. The magnitude of hemin-induced $^{A}\gamma^{*}$ expression in the pools was approximately one-half that of individual clones (Table 1). Correction for differences in average copy number and endogenous γ signal between pools are reflected in the mean expression values shown.

DISCUSSION

The rAAV vector system provides a novel strategy for achieving integration of a single unrearranged gene with its transcriptional control elements. More than one-half of the K562 erythroleukemia cell clones derived by Neo^R selection contained a single intact copy of the γ-globin gene linked to the HS2 from the LCR. Using the system, we verified that NF-E2 binding to the tandem NF-E2/AP-1 sites in HS2 is necessary for hemin inducibility, and we showed that the consensus GATA-1 binding motif within the HS2 core enhancer fragment is not required for high-level expression.

Our prior studies suggested that the rAAV vector system might be useful to obtain clones containing a low copy number of the vector genome. These new data provide a more precise quantitative estimate; 60% of 25 evaluable clones transduced with an rAAV having a genome 90% the length of the wild-type virus had a single unrearranged copy and another 4 (16%) had 2 or more unrearranged copies. The other 7 evaluable Neo^R clones contained rearranged copies of the vector genome. Despite a modest difference in length between the vector lacking the HS2 fragment and the others, that vector gave a majority of Neo^R clones (6 of 10) having a rearranged genome and 2 of the pooled populations derived with this vector had an average genome copy number of less than 0.5 (data not shown). We conclude that the rAAV system can be used for deriving clones having single-copy integrants but that each vector and perhaps each cell type will require characterization with respect to this capacity.

The LCR of the β-globin cluster has a number of activities that together result in high-level, regulated globin gene expression in maturing erythroid cells.[28,29] Establishment of each individual site most likely represents the displacement of one or two nucleosomes by sequence-specific binding of both erythroid-restricted and ubiquitous transcriptional factors. The individual sites are thought to interact in forming the active chromatin domain that encompasses the entire β-globin gene cluster in erythroid cells. These two functions, site formation and domain establishment, seem most likely to be the basis for the ability of the LCR or components thereof to confer position-independent, copy number-dependent gene expression in transgenic animals. A third function, transcriptional enhancement, pertains specifically to the level of gene expression. In K562 erythroleukemia cells, the erythroid specific enhancer within HS2 has the greatest effect on the level of gene expression; whereas, in MEL cells and transgenic mice, HS3 and HS4 also confer high-level gene expression.[30,31] Our experiments were designed specifically to test the enhancing function of HS2. Individual clones were selected based on expression of the linked Neo^R gene; therefore, each integrated genome was likely to be in an active chromatin domain independent of HS2 function.

GATA-1 and NF-E2 motifs have been shown to be synergistic in creating a strong erythroid promoter when linked to a TATA box.[32] The human γ-globin promoters contain GATA-1 binding motifs, but lack the NF-E2 motif. When a 46-bp fragment containing the tandem NF-E2/AP-1 sites from HS2 was linked to the γ-globin promoter, repoter activity in hemin-induced K562 cells was increased significantly.[4,33] In contrast, when compared with the full HS2, the 46-bp fragment linked to the γ-globin promoter was not associated with high-level expression in stably transfected K562 cells.[8,9] In MEL cells or transgenic mice, an additional 200 bp of the HS2, which includes the GATA-1 motif mutated in this study, were required for high-level expression of a linked globin gene.[3,34]

The nature of DNA sequences within the additional HS2 region that participate in high-level globin gene expression remains complex. Mutations of the GATA-1 motif in a synthetic 215-bp core HS2 fragment resulted in no reduction in the expression of a linked human β-globin when present as multiple-copy integrants in transgenic mice.[24] The synthetic HS2 core did not function as a single copy in the transgenic mouse model. In pools of stably transfected MEL cells, a 38% reduction in β-globin expression was reported with the same GATA-1 mutated synthetic fragment. The effects of copy number on these pools was not reported. Also, independent of the GATA-1 mutation, the relative expression from those pools containing the wild-type synthetic HS2 was 75% less than the expression from those transfected with constructs having the *Hin*dIII-*Xba* I fragment of HS2. We were able to achieve high-level γ-globin expression from neomycin-resistant clones having a single copy of the rAAV genome that contained the full *Hin*dIII-*Xba* I fragment of HS2. Thus, the GATA-1 motif mutation was studied in clonal populations of K562 erythroleukemia cells independent of concatameric HS2 interactions. No mut-GATA1–related reduction in expression from the linked γ-globin was found using this model, although an influence on position-independent expression was suggested by the increased variability in expression level seen with the mut-GATA1 pools.

In vivo footprinting has been used to identify sites within HS2 occupied by proteins in intact K562 erythroleukemia cells.[35,36] This methodology shows protein-DNA interactions in vivo and may identify functionally relevant binding motifs. Both the tandem NF-E2/AP-1 and GATA-1 HS2 sites are occupied in K562 erythroleukemia cells and the

PAGE 75/77 * RCVD AT 8/29/2005 7:17:05 PM [Eastern Daylight Time] * SVR:USPTO-EFXRF-6/26 * DNIS:2738300 * CSID:6504936811 * DURATION (mm-ss):60-28

6504936811 8/29/2005 4:17 PM PAGE 76/077 Fax Server

pattern of protected nucleotides changes within each motif upon induction. NF-E2 appears to bind with induction, whereas GATA-1 may be released. Using the rAAV system to derive single-copy intergrants, we verified that the capacity for NF-E2 to bind to the tandem NF-E2/AP-1 sites is essential for the enhancing function of HS2. Binding of GATA-1, the only other erythroid-restricted transcriptional activator known to interact with this portion of HS2, did not appear to be required for inducible, high-level expression. These data are consistent with the results obtained by in vivo footprinting, and suggest the GATA-1 binding motif's role in HS2 function in vivo may relate to effects on chromatin structure rather than transcriptional enhancement.

ACKNOWLEDGMENT

We thank Dr Jonathan Hibbs for providing the PCR-directed site-specific mutagenesis protocols, Dr Johnson M. Liu for plasmids pUC 008 and pAAV/HS2/$^{A}\gamma^{*}$/Neo and for reading the manuscript, and Jean Johnson for secretarial help in preparing the manuscript.

REFERENCES

1. Grosveld F, van Assendelft GB, Greaves DR, Kollias G: Position-independent, high-level expression of the human β-globin gene in transgenic mice. Cell 51:975, 1988
2. Orkin SH: Globin gene regulation and switching: Circa 1990. Cell 63:665, 1990
3. Talbot D, Philipsen S, Fraser P, Grosveld F: Detailed analysis of the site 3 region of the human β-globin dominant control region. EMBO J 9:2169, 1990
4. Ney PA, Sorrentino BP, McDonagh KT, Nienhuis AW: Tandem AP-1–binding sites within the human β-globin dominant control region function as an inducible enhancer in erythroid cells. Genes Dev 4:993, 1990
5. Ney PA, Sorrentino BP, Lowrey CH, Nienhuis AW: Inducibility of the HS II enhancer depends on binding of an erythroid specific nuclear protein. Nucleic Acids Res 18:6011, 1990
6. Mignotte V, Eleouet JF, Raich N, Romeo PH: Cis- and trans-acting elements involved in the regulation of the erythroid promoter of the human porphobilinogen deaminase gene. Proc Natl Acad Sci USA 86:6548, 1989
7. Liu D, Chang JC, Moi P, Liu W, Kan YW, Curtin PT: Dissection of the enhancer activity of β-globin 5′ DNase I-hypersensitive site 2 in transgenic mice. Proc Natl Acad Sci USA 89:3899, 1992
8. Moon AM, Ley TJ: Functional properties of the β-globin locus control region in K562 erythroleukemia cells. Blood 77:2272, 1991
9. Sorrentino BP, Ney P, Nienhuis AW: A 46 base pair enhancer sequence within the locus activating region is required for induced expression of the gamma-globin gene during erythroid differentiation. Nucleic Acids Res 18:2721, 1990
10. Sorrentino BP, Ney PA, Nienhuis AW: Localization and characterization of the DNaseI-hypersensitive site II (HS II) enhancer: A critical regulatory element within the β-globin locus-activating region. Ann NY Acad Sci 612:141, 1990
11. Talbot D, Grosveld F: The 5′HS2 of the globin locus control region enhances transcription through the interaction of a multimeric complex binding at two functionally distinct NF-E2 binding sites. EMBO J 10:1391, 1991
12. Siegel G, Bates RC, Berns KI, Carter BJ, Kelly DC, Kurstak E, Tattersall P: Characteristics and taxonomy of Parvoviridae. Intervirology 23:61, 1985
13. McLaughlin SK, Collis P, Hermonat PL, Muzyczka N: Adeno-associated virus general transduction vectors: Analysis of proviral structures. J Virol 62:1963, 1988
14. Samulski RJ, Srivastava A, Berns KI, Muzyczka N: Rescue of adeno-associated virus from recombinant plasmids: Gene correction within the terminal repeats of AAV. Cell 33:135, 1983
15. Samulski RJ, Chang LS, Shenk T: A recombinant plasmid from which an infectious adeno-associated virus genome can be excised in vitro and its use to study viral replication. J Virol 61:3096, 1987
16. Tratschin J-D, Tal J, Carter BJ: Negative and positive regulation in trans of gene expression from adeno-associated virus vectors in mammalian cells by a viral Rep gene product. Mol Cell Biol 6:2884, 1986
17. Atchison RW, Casto BC, Hammond WMcD: Adenovirus-associated defective virus particles. Science 149:754, 1965
18. Buller RM, Janik JE, Sebring SE, Rose JA: Herpes simplex virus types 1 and 2 completely help adenovirus-associated virus replication. J Virol 40:241, 1981
19. Georg-Fries B, Biederlack S, Wolf J, zur Hausen H: Analysis of proteins, helper dependence, and seroepidemiology of a new human parvovirus. Virology 134:64, 1984
20. Cheung AK, Hoggan MD, Hauswirth WW, Berns KI: Integration of the adeno-associated virus genome into cellular DNA in latently infected human Detroit 6 cells. J Virol 33:739, 1980
21. Muzyczka N: Use of adeno-associated virus as a general transduction vector for mammalian cells. Curr Top Microbiol Immunol 158:97, 1992
22. Samulski RJ, Chang LS, Shenk T: Helper-free stocks of recombinant adeno-associated viruses: Normal integration does not require viral gene expression. J Virol 63:3822, 1989
23. Walsh CE, Liu JM, Xiao X, Young NS, Nienhuis AW, Samulski RJ: Regulated high level expression of a human γ-globin gene introduced into erythroid cells by an adeno-associated virus vector. Proc Natl Acad Sci USA 89:7257, 1992
24. Ellis J, Talbot D, Dillon N, Grosveld F: Synthetic human β-globin 5′HS2 constructs function as locus control regions only in multicopy transgene concatomers. EMBO J 12:127, 1993
25. Ho SN, Hunt HD, Horton RM, Pullen JK, Pease LR: Site-directed mutagenesis by overlap extension using the polymerase chain reaction. Gene 77:51, 1989
26. Richardson JH: Biosafety in Microbiological and Biomedical Laboratories. Washington, DC, US Government Printing Office, 1988
27. Sambrook J, Fritsch EF, Maniatis T (eds): Molecular Cloning: A Laboratory Manual (ed 2). Cold Spring Harbor, NY, Cold Spring Harbor Laboratory, 1989
28. Evans T, Felsenfeld G, Reitman M: Control of globin gene transcription. Annu Rev Cell Biol 6:95, 1990
29. Ney P, Sorrentino B, Purucker M, McDonagh K, Lowrey C, Feingold E, Lin H, Lee E, Westphal H, Nienhuis A: Distant and local regulatory elements in the human b-globin gene cluster, in Stamatoyannopoulos G, Nienhuis AW (eds): The Regulation of Hemoglobin Switching. Baltimore, MD, The Johns Hopkins University, 1991, p 69
30. Philipsen S, Talbot D, Fraser P, Grosveld F: The β-globin dominant control region: hypersensitive site 2. EMBO J 9:2159, 1990
31. Pruzina S, Hanscombe O, Whyatt D, Grosveld F, Sjaak P: Hypersensitivity site 4 of the human β globin locus control region. Nucleic Acids Res 19:1413, 1991

PAGE 76/77 * RCVD AT 8/29/2005 7:17:05 PM [Eastern Daylight Time] * SVR:USPTO-EFXRF-6/26 * DNIS:2738300 * CSID:6504936811 * DURATION (mm-ss):60-28

32. Walters MC, Martin DIK: Functional erythroid promoters created by interaction of the transcription factor GATA-1 with CACCC and AP-1/NFE-2 elements. Proc Natl Acad Sci USA 89:10444, 1992

33. Moi P, Kan YW: Synergistic enhancement of globin gene expression by activator protein-1–like proteins. Proc Natl Acad Sci USA 87:9000, 1990

34. Caterina JJ, Ryan TM, Pawlick KM, Palmiter RD, Brinster RL, Behringer RR, Townes TM: Human β-globin locus control region: Analysis of the 5'DNase I hypersensitive site HS 2 in transgenic mice. Proc Natl Acad Sci USA 88:1626, 1991

35. Ikuta T, Kan YW: In vivo protein-DNA interactions at the β-globin gene locus. Proc Natl Acad Sci USA 88:10188, 1991

36. Reddy PMS, Shen CJ: Protein-DNA interactions in vivo of an erythroid-specific, human β-globin locus enhancer. Proc Natl Acad Sci USA 88:8676, 1991

37. McDonagh KT, Lin HJ, Lowrey CH, Bodine DM, Nienhuis AW: The upstream region of the human γ-globin gene promoter: Identification and functional analysis of nuclear protein binding sites. J Biol Chem 266:11965, 1991

38. Armitag P, Berry G: Statistical Methods in Medical Research (ed 2). Oxford, UK, Blackwell Scientific, 1987

This Page is Inserted by IFW Indexing and Scanning Operations and is not part of the Official Record

BEST AVAILABLE IMAGES

Defective images within this document are accurate representations of the original documents submitted by the applicant.

Defects in the images include but are not limited to the items checked:

- ☐ BLACK BORDERS
- ☐ IMAGE CUT OFF AT TOP, BOTTOM OR SIDES
- ☐ FADED TEXT OR DRAWING
- ☐ BLURRED OR ILLEGIBLE TEXT OR DRAWING
- ☐ SKEWED/SLANTED IMAGES
- ☐ COLOR OR BLACK AND WHITE PHOTOGRAPHS
- ☒ GRAY SCALE DOCUMENTS
- ☐ LINES OR MARKS ON ORIGINAL DOCUMENT
- ☒ REFERENCE(S) OR EXHIBIT(S) SUBMITTED ARE POOR QUALITY
- ☐ OTHER: _____

IMAGES ARE BEST AVAILABLE COPY.
As rescanning these documents will not correct the image problems checked, please do not report these problems to the IFW Image Problem Mailbox.